Tensor Network States, an Introduction and Applications to Quantum Coherence Processes: I

Javier Prior

Universidad Politécnica de Cartagena

iCI Instituto Carlos I
Física teórica y computacional

TEDOPA: Time Evolving Density with Orthogonal Polynomial Algorithm

Javier Prior

Universidad Politécnica de Cartagena

iCI Instituto Carlos I
Física teórica y computacional

Spain, Murcia and Cartagena

Spain, Murcia and Cartagena

TEDOPA

PRL **105,** 050404 (2010) PHYSICAL REVIEW LETTERS week ending 30 JULY 2010

Efficient Simulation of Strong System-Environment Interactions

Javier Prior,[1,2] Alex W. Chin,[3] Susana F. Huelga,[3] and Martin B. Plenio[3,2]

[1]*Departamento de Física Aplicada, Universidad Politécnica de Cartagena, Cartagena 30202, Spain*
[2]*QOLS, The Blackett Laboratory, Prince Consort Road, Imperial College, London, SW7 2BW, United Kingdom*
[3]*Institut für Theoretische Physik, Albert-Einstein-Allee 11, Universität Ulm, D-89069 Ulm, Germany*

(Received 14 April 2010; revised manuscript received 1 July 2010; published 30 July 2010)

Multicomponent quantum systems in strong interaction with their environment are receiving increasing attention due to their importance in a variety of contexts, ranging from solid state quantum information processing to the quantum dynamics of biomolecular aggregates. Unfortunately, these systems are difficult to simulate as the system-bath interactions cannot be treated perturbatively and standard approaches are invalid or inefficient. Here we combine the time-dependent density matrix renormalization group with techniques from the theory of orthogonal polynomials to provide an efficient method for simulating open quantum systems, including spin-boson models and their generalizations to multicomponent systems.

DOI: 10.1103/PhysRevLett.105.050404 PACS numbers: 05.30.−d, 03.65.Yz, 03.67.−a, 05.60.Gg

TEDOPA

PHYSICAL REVIEW A **87**, 013428 (2013)

Quantum dynamics in photonic crystals

Javier Prior,[1] Inés de Vega,[2] Alex W. Chin,[2,3] Susana F. Huelga,[2] and Martin B. Plenio[2]
[1]*Departamento de Física Aplicada, Universidad Politécnica de Cartagena, Cartagena 30202, Spain*
[2]*Institut für Theoretische Physik, Albert-Einstein-Allee 11, Universität Ulm, D-89069 Ulm, Germany*
[3]*Theory of Condensed Matter Group, University of Cambridge, J J Thomson Avenue, Cambridge, CB3 0HE England, United Kingdom*
(Received 16 May 2012; revised manuscript received 3 August 2012; published 24 January 2013)

Employing a recently developed method that is numerically accurate within a model space simulating the real-time dynamics of few-body systems interacting with macroscopic environmental quantum fields, we analyze the full dynamics of an atomic system coupled to a continuum light field with a gapped spectral density. This is a situation encountered, for example, in the radiation field in a photonic crystal, whose analysis has so far been confined to limiting cases due to the lack of suitable numerical techniques. We show that both atomic population and coherence dynamics can drastically deviate from the results predicted when using the rotating-wave approximation, particularly in the strong-coupling regime. Experimental conditions required to observe these corrections are also discussed.

DOI: 10.1103/PhysRevA.87.013428 PACS number(s): 03.65.−w

TEDOPA

TEDOPA (Time Evolving Density matrix using Orthogonal Polynomials Algorithm) combines

- *Time adaptative DMRG*
- *Theory of Orthogonal Polynomials*

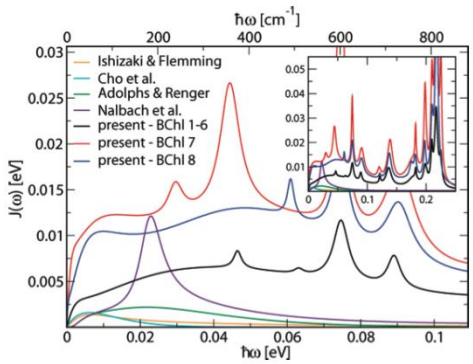

Olbrich et al. J. Phys. Chem Lett. 2. 2011

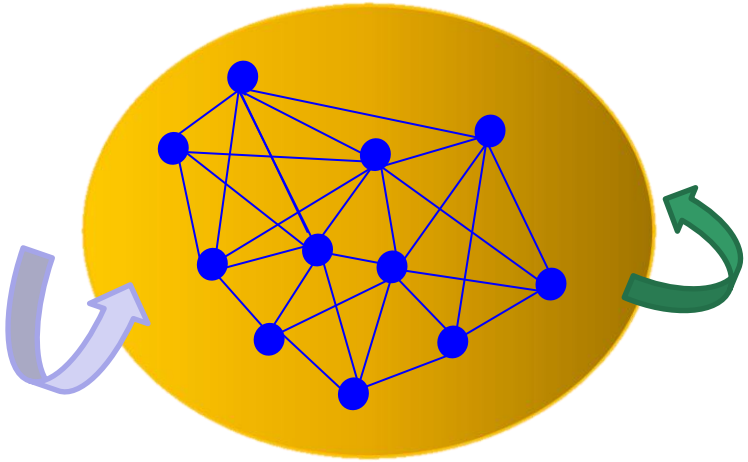

- *Handle richly structured enviromets used in pigment-protein complexes literatura.*
- *No restriction of the complexity of strength of the system-environment coupling.*
- *Provides complete information about the evolving state of the environment.*
- *Study system-bath correlations which give rise to long lasting coherences, entanglement, etc.*

TEDOPA

TEDOPA (Time Evolving Density matrix using Orthogonal Polynomials Algorithm) combines

- *Time adaptative DMRG*
- *Theory of Orthogonal Polynomials*

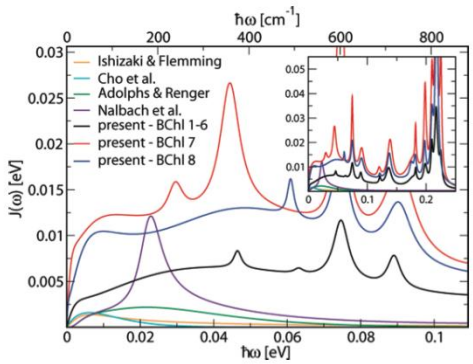

Olbrich et al. J. Phys. Chem Lett. 2. 2011

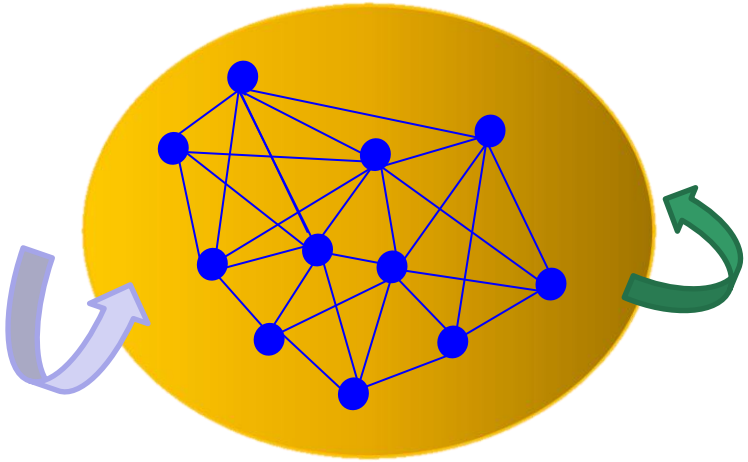

***General method*-Current applications include atoms in a photonic crystal, quantum impurities, superconduction qubits, NV centres, quantum biology ...**

Chain Mapping: Orthogonal polynomials

Total Hamiltonian $H = H_{\rm loc} + H_{\rm res} + V$

Dimer Hamiltonian

$$H_{\rm loc} = \epsilon_1 \sigma_z + \epsilon_2 \sigma_z + J\sigma_{1+}\sigma_{2-} + J\sigma_{2+}\sigma_{1-}$$

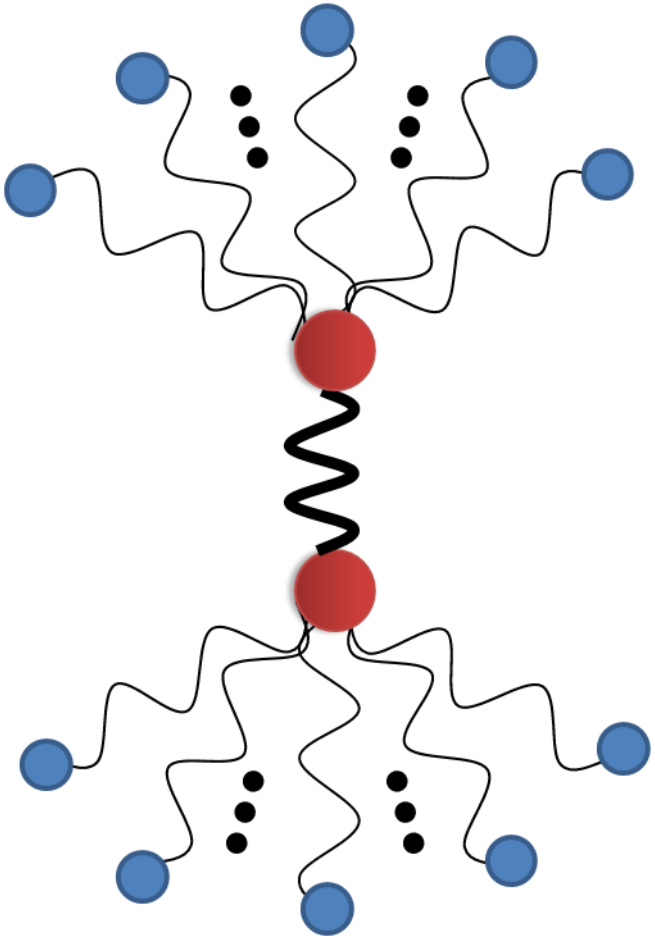

Chain Mapping: Orthogonal polynomials

Total Hamiltonian $H = H_{\rm loc} + H_{\rm res} + V$

Dimer Hamiltonian

$$H_{\rm loc} = \epsilon_1 \sigma_z + \epsilon_2 \sigma_z + J\sigma_{1+}\sigma_{2-} + J\sigma_{2+}\sigma_{1-}$$

Independent baths – continuum of bosons

$$H_{res} = \int dx\, g(x) a_x^\dagger a_x$$

$$V = \int dx\, h(x) \hat{A}(a_x^\dagger + a_x)$$

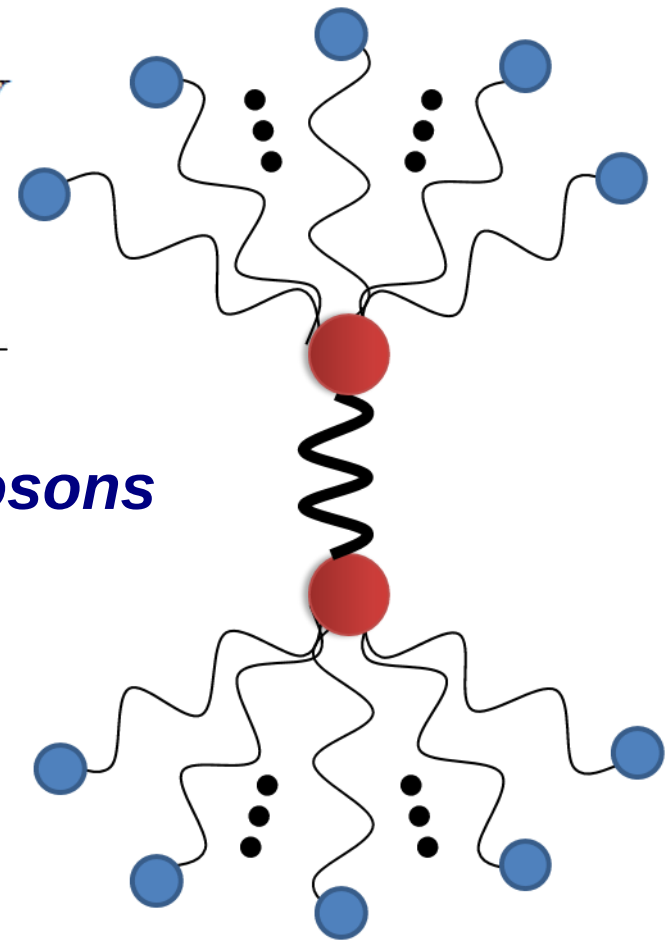

Chain Mapping: Orthogonal polynomials

Total Hamiltonian $H = H_{\rm loc} + H_{\rm res} + V$

Dimer Hamiltonian

$$H_{\rm loc} = \epsilon_1 \sigma_z + \epsilon_2 \sigma_z + J\sigma_{1+}\sigma_{2-} + J\sigma_{2+}\sigma_{1-}$$

Independent baths – continuum of bosons

$$H_{res} = \int dx\, g(x) a_x^\dagger a_x$$

$$V = \int dx\, h(x) \hat{A}(a_x^\dagger + a_x)$$

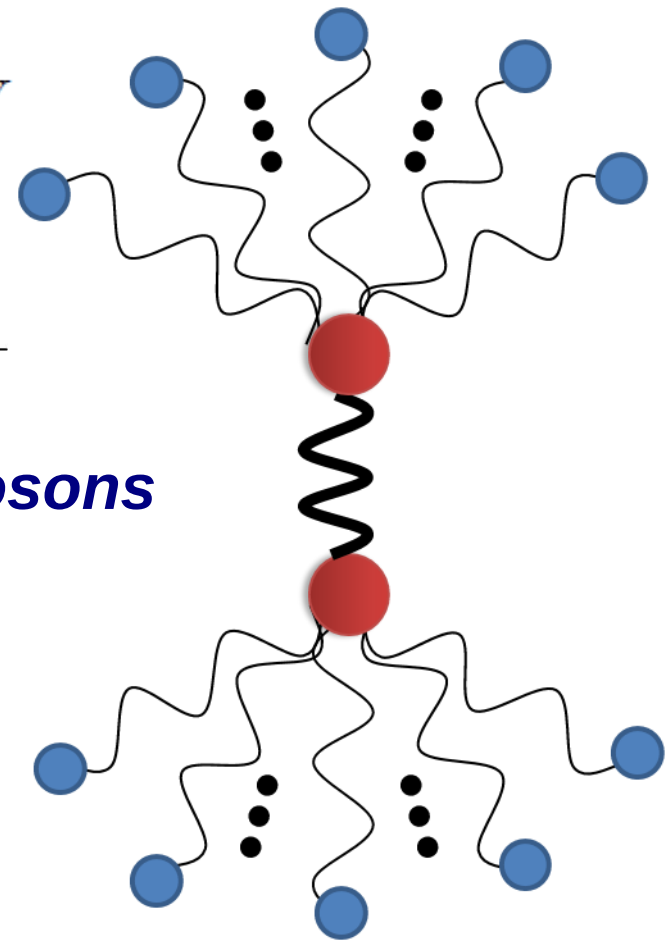

Spectral function $J(\omega) = \pi h^2(g^{-1}(\omega)) \dfrac{dg^{-1}(\omega)}{d\omega}$

Chain Mapping: Orthogonal polynomials

$$H_{res} = \int dx\, g(x) a_x^\dagger a_x \qquad V = \int dx\, h(x) \hat{A}(a_x^\dagger + a_x)$$

$$g(x) = gx$$

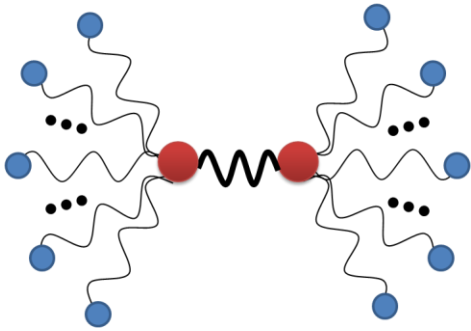

Goal:* *Find new modes

$$b_n^\dagger = \int dx\, U_n(x) a_x^\dagger \qquad a_x^\dagger = \sum_n U_n(x) b_n^\dagger$$

such that

$$c_0 \hat{A}(b_0 + b_0^\dagger) + \sum_{n=0}^{\infty} \omega_n b_n^\dagger b_n + t_n b_{n+1}^\dagger b_n + t_n b_n^\dagger b_{n+1}$$

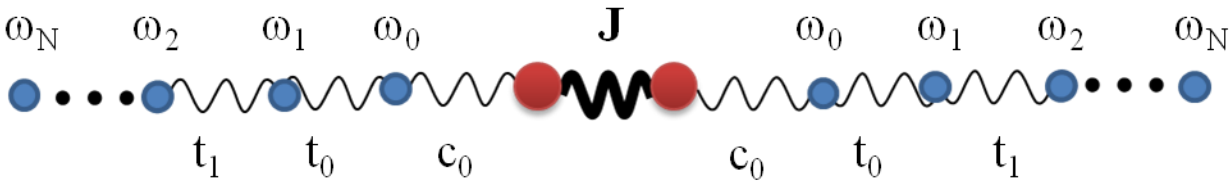

Chain Mapping: Orthogonal polynomials

$$a_x^\dagger = \sum_n U_n(x) b_n^\dagger$$

$$V = \int dx\, h(x) \hat{A}(a_x^\dagger + a_x)$$

$$U_n(x) = h(x)\tilde{p}_n(x)$$

$\tilde{p}_n(x)$ are some set of orthonormal polynomials with respect to the measure $d\mu(x) = h^2(x)dx$

Chain Mapping: Orthogonal polynomials

$$a_x^\dagger = \sum_n U_n(x) b_n^\dagger$$

$$V = \int dx\, h(x) \hat{A}(a_x^\dagger + a_x)$$

$$U_n(x) = h(x)\tilde{p}_n(x)$$

$\tilde{p}_n(x)$ are some set of orthonormal polynomials with respect to the measure $d\mu(x) = h^2(x)dx$

Orthonormality:

$$\int dx\, U_n(x) U_m^*(x) = \int dx\, h^2(x)\tilde{p}_n(x)\tilde{p}_m(x) = \delta_{nm}$$

Chain Mapping: Orthogonal polynomials

$$a_x^\dagger = \sum_n U_n(x) b_n^\dagger$$

$$V = \int dx\, h(x) \hat{A}(a_x^\dagger + a_x)$$

$$U_n(x) = h(x)\tilde{p}_n(x)$$

$\tilde{p}_n(x)$ are some set of orthonormal polynomials with respect to the measure $d\mu(x) = h^2(x)dx$

Orthonormality:

$$\int dx\, U_n(x) U_m^*(x) = \int dx\, h^2(x)\tilde{p}_n(x)\tilde{p}_m(x) = \delta_{nm}$$

Three terms recursion relation:

$$x\,\tilde{p}_n(x) = \frac{1}{C_n}\tilde{p}_{n+1}(x) + \frac{A_n}{C_n}\tilde{p}_n(x) + \frac{B_n}{C_n}\tilde{p}_{n-1}(x)$$

$$p_0(x) = 1$$

Chain Mapping: Orthogonal polynomials

$$a_x^\dagger = \sum_n U_n(x) b_n^\dagger$$

$$V = \int dx\, h(x) \hat{A}(a_x^\dagger + a_x)$$

$$U_n(x) = h(x)\tilde{p}_n(x)$$

$\tilde{p}_n(x)$ are some set of orthonormal polynomials with respect to the measure $d\mu(x) = h^2(x)dx$

$$V = \int dx\, h(x) \hat{A}(a_x^\dagger + a_x)$$

Chain Mapping: Orthogonal polynomials

$$a_x^\dagger = \sum_n U_n(x) b_n^\dagger$$

$$V = \int dx\, h(x) \hat{A}(a_x^\dagger + a_x)$$

$$U_n(x) = h(x)\tilde{p}_n(x)$$

$\tilde{p}_n(x)$ are some set of orthonormal polynomials with respect to the measure $d\mu(x) = h^2(x)dx$

$$V = \hat{A} \sum_n \int dx\, h(x) U_n(x)(b_n + b_n^\dagger)$$

Chain Mapping: Orthogonal polynomials

$$a_x^\dagger = \sum_n U_n(x) b_n^\dagger$$

$$V = \int dx\, h(x) \hat{A}(a_x^\dagger + a_x)$$

$$U_n(x) = h(x)\tilde{p}_n(x)$$

$\tilde{p}_n(x)$ are some set of orthonormal polynomials with respect to the measure $d\mu(x) = h^2(x)dx$

$$V = \hat{A} \sum_n \int dx\, h(x) U_n(x)(b_n + b_n^\dagger)$$

$$V = \hat{A} \sum_n \int dx\, h^2(x) \tilde{p}_n(x)(b_n + b_n^\dagger)$$

$$= c_0\, \hat{A}(b_0 + b_0^\dagger)$$

Chain Mapping: Orthogonal polynomials

$$a_x^\dagger = \sum_n U_n(x) b_n^\dagger$$

$$V = \int dx\, h(x) \hat{A}(a_x^\dagger + a_x)$$

$$U_n(x) = h(x)\tilde{p}_n(x)$$

$\tilde{p}_n(x)$ are some set of orthonormal polynomials with respect to the measure $d\mu(x) = h^2(x)dx$

$$H_{res} = \int dx\, g x a_x^\dagger a_x$$

Chain Mapping: Orthogonal polynomials

$$a_x^\dagger = \sum_n U_n(x) b_n^\dagger$$

$$V = \int dx\, h(x) \hat{A}(a_x^\dagger + a_x)$$

$$U_n(x) = h(x)\tilde{p}_n(x)$$

$\tilde{p}_n(x)$ are some set of orthonormal polynomials with respect to the measure $d\mu(x) = h^2(x)dx$

$$H_{res} = \sum_{n,m} \int dx\, gx U_n(x) U_m(x) b_n^\dagger b_m$$

$$= \sum_{n,m} \int dx\, gh^2(x) x \tilde{p}_n(x) \tilde{p}_m(x) b_n^\dagger b_m$$

Chain Mapping: Orthogonal polynomials

$$a_x^\dagger = \sum_n U_n(x) b_n^\dagger$$

$$V = \int dx\, h(x) \hat{A}(a_x^\dagger + a_x)$$

$$U_n(x) = h(x)\tilde{p}_n(x)$$

$\tilde{p}_n(x)$ are some set of orthonormal polynomials with respect to the measure $d\mu(x) = h^2(x)dx$

$$H_{res} = \sum_{n,m} \int dx\, g x U_n(x) U_m(x) b_n^\dagger b_m$$

$$= \sum_{n,m} \int dx\, g h^2(x) x \tilde{p}_n(x) \tilde{p}_m(x) b_n^\dagger b_m$$

Each $d\mu(x) = h^2(x)dx$ *defines orthonormal polynomials with recursion:*

$$x\,\tilde{p}_n(x) = \frac{1}{C_n}\tilde{p}_{n+1}(x) + \frac{A_n}{C_n}\tilde{p}_n(x) + \frac{B_n}{C_n}\tilde{p}_{n-1}(x)$$

Chain Mapping: Orthogonal polynomials

$$a_x^\dagger = \sum_n U_n(x) b_n^\dagger$$

$$V = \int dx\, h(x) \hat{A}(a_x^\dagger + a_x)$$

$$U_n(x) = h(x)\tilde{p}_n(x)$$

$\tilde{p}_n(x)$ are some set of orthonormal polynomials with respect to the measure $d\mu(x) = h^2(x)dx$

$$H_{res} = \sum_{n,m} \int dx\, g x U_n(x) U_m(x) b_n^\dagger b_m$$

$$= \sum_{n,m} \int dx\, g h^2(x) x \tilde{p}_n(x) \tilde{p}_m(x) b_n^\dagger b_m$$

$$= g \sum_{n,m} \int_0^{x_{\max}} dx h^2(x) \left[\frac{1}{C_n} \tilde{p}_{n+1}(x) + \frac{A_n}{C_n} \tilde{p}_n(x) + \frac{B_n}{C_n} \tilde{p}_{n-1}(x) \right] \tilde{p}_m(x) b_n^\dagger b_m$$

$$= g \sum_n \frac{1}{C_n} b_n^\dagger b_{n+1} + \frac{A_n}{C_n} b_n^\dagger b_n + \frac{B_{n+1}}{C_{n+1}} b_{n+1}^\dagger b_n$$

Numerical results: bound spectral function

$$J(\omega) = 2\pi\alpha\omega_c^{1-s}\omega^s\Theta(\omega_c - \omega) = \pi h^2(g^{-1}(\omega))\frac{dg^{-1}(\omega)}{d\omega}$$

$$g(x) = \omega_c x,$$
$$h(x) = \sqrt{2\alpha}\omega_c x^{s/2}$$

OPs are Jacobi Polynomials

Recurrence coefficients known analytically

$$\omega_n = \frac{\omega_c}{2}\left(1 + \frac{s^2}{(s+2n)(2+s+2n)}\right),$$

$$t_n = \frac{\omega_c(1+n)(1+s+n)}{(s+2+2n)(3+s+2n)}\sqrt{\frac{3+s+2n}{1+s+2n}}$$

Numerical results: bound spectral function

$$J(\omega) = 2\pi\alpha\omega_c^{1-s}\omega^s\Theta(\omega_c - \omega) = \pi h^2(g^{-1}(\omega))\frac{dg^{-1}(\omega)}{d\omega}$$

$$g(x) = \omega_c x,$$
$$h(x) = \sqrt{2\alpha}\omega_c x^{s/2}$$

OPs are Jacobi Polynomials

Recurrence coefficients known analytically

Formulae show that →

$$\lim_{n\to\infty} \epsilon_n \to \frac{\omega_c}{2}$$
$$\lim_{n\to\infty} t_n \to \frac{\omega_c}{4}$$

Numerical results: bound spectral function

Initial non-uniform part of the chain encodes spectral density

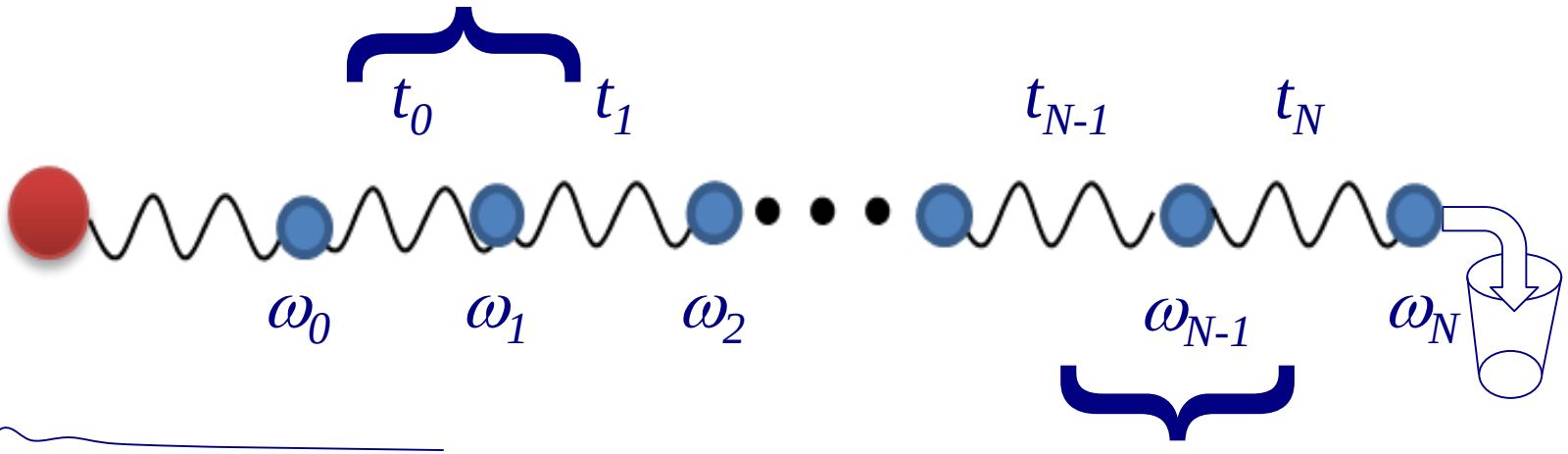

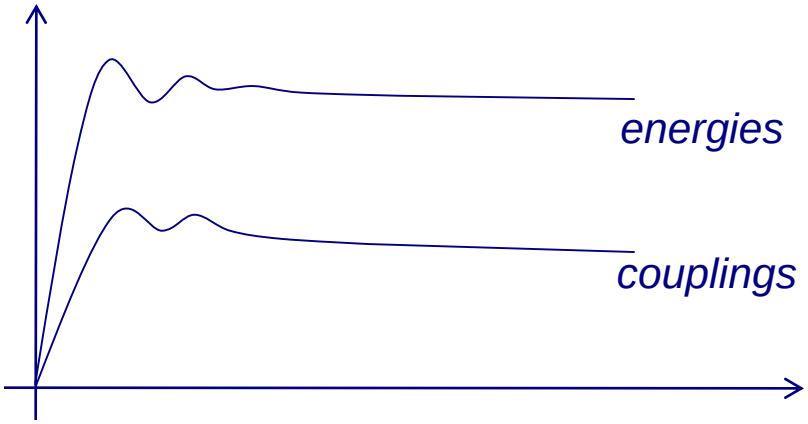

Uniform part of chain allows excitations to propagate away from system – Irreversibility.

Numerical results: bound spectral function

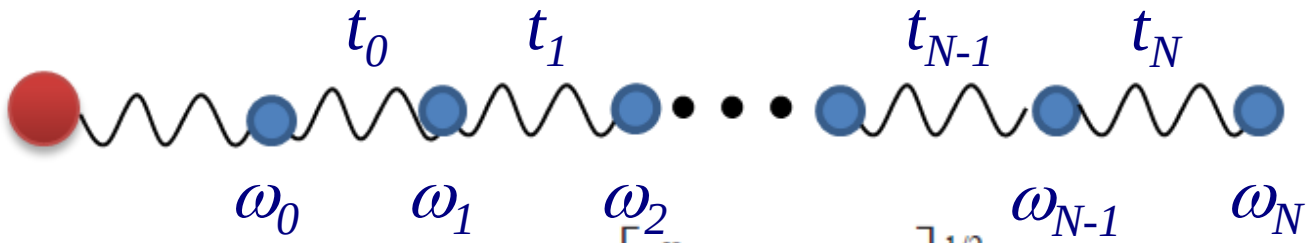

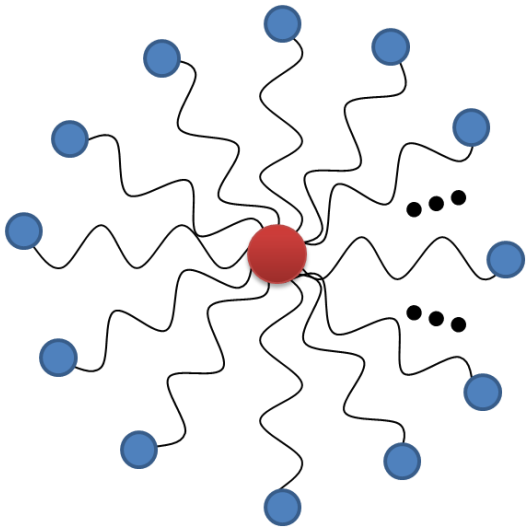

$$\epsilon_0 = \sum_{n=0} \xi_n U_{0n}^2 \qquad t_0 = \frac{1}{\sqrt{\eta_0}} \left[\sum_{n=0}^{\infty} (\xi_n - \epsilon_0)^2 \gamma_n^2 \right]^{1/2}$$

$$\epsilon_m = \sum_{n=0}^{\infty} \xi_n U_{mn}^2$$

$$U_{m+1n} = \frac{1}{t_m} \left[(\xi_n - \epsilon_m) U_{mn} - t_{m-1} U_{m-1n} \right]$$

$$t_m = \left[\sum_{n=0}^{\infty} \left[(\xi_n - \epsilon_m) U_{mn} - t_{m-1} U_{m-1n} \right]^2 \right]^{\frac{1}{2}}$$

$$\sum_{n=0} \xi_n a_n^\dagger a_n + \frac{\sigma_z}{2\sqrt{\pi}} \sum_{n=0} \gamma_n (a_n + a_n^\dagger)$$

Bulla, Tong & Vojta, Phys. Rev. Lett. 2003
Bulla, Lee, Tong, & Vojta, Phys. Rev. B 2005

Numerical results: bound spectral function

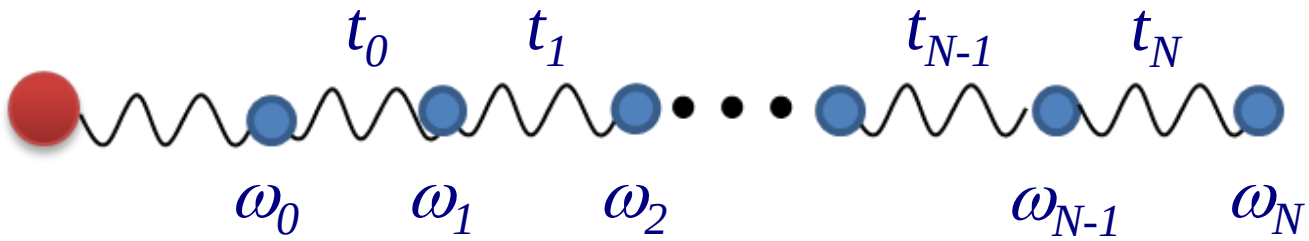

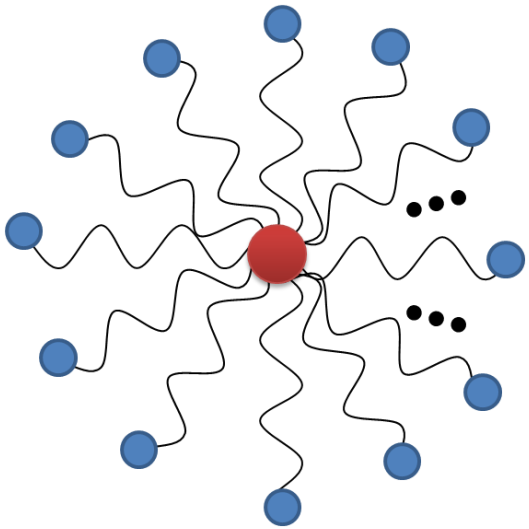

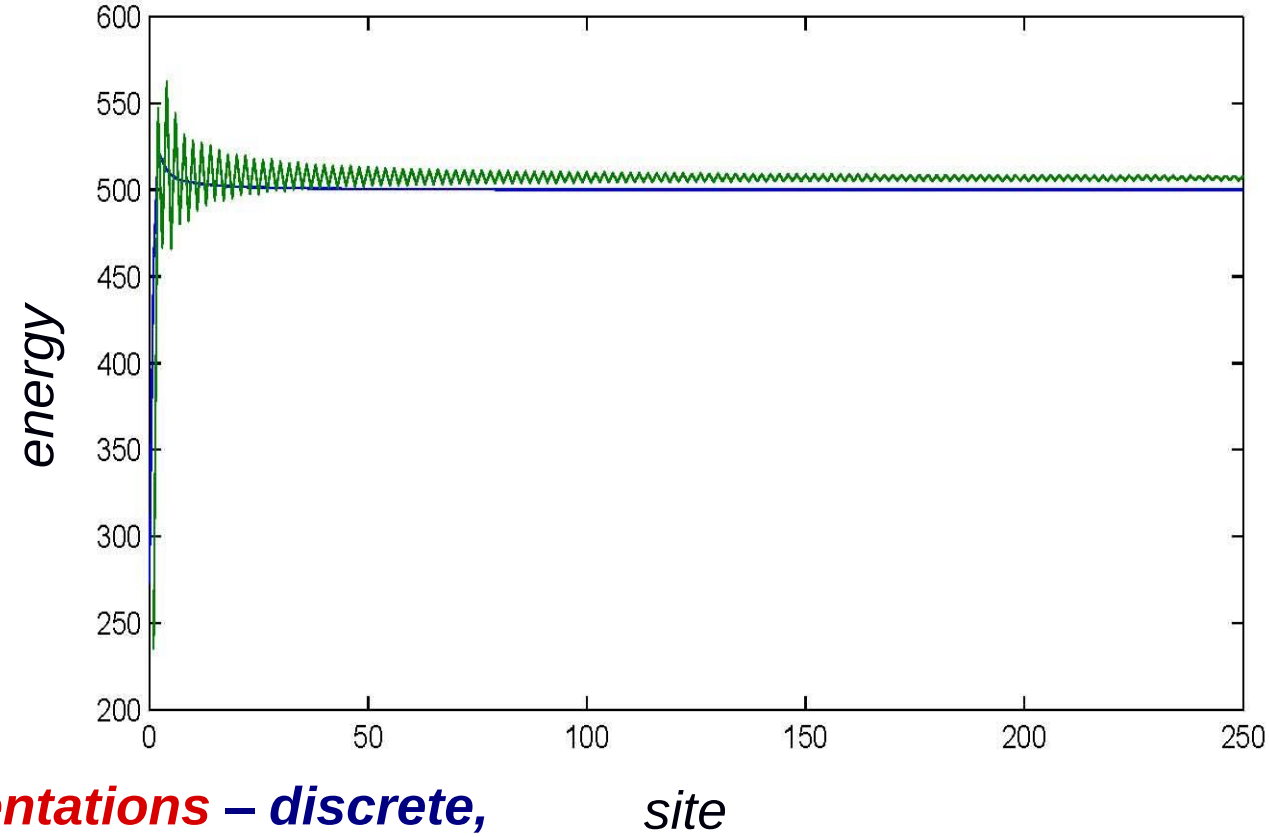

Previous implementations – discrete, numerically unstable.

Modeling system-environment interaction in the non- perturbative regime

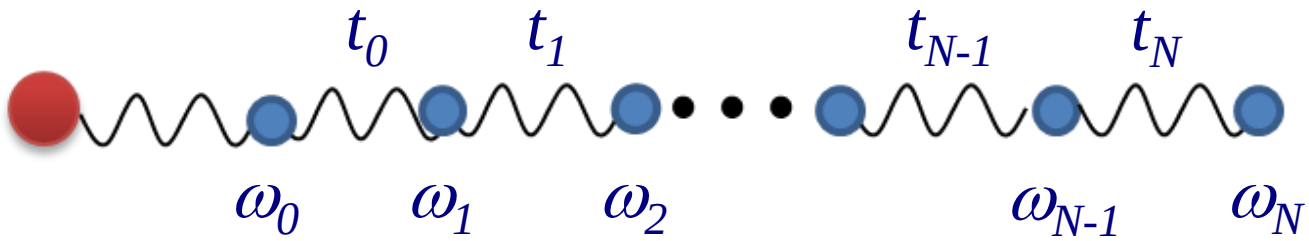

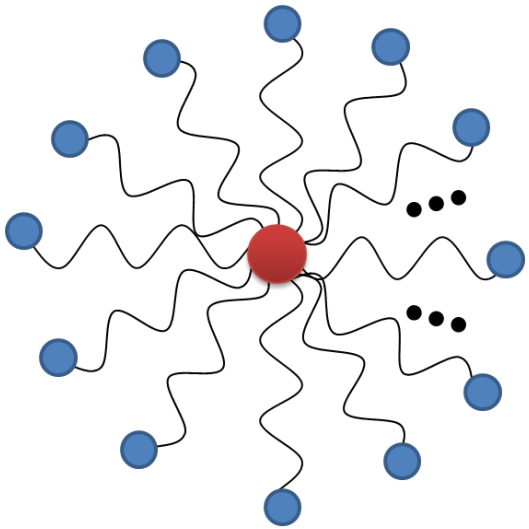

Modeling system-environment interaction in the non- perturbative regime

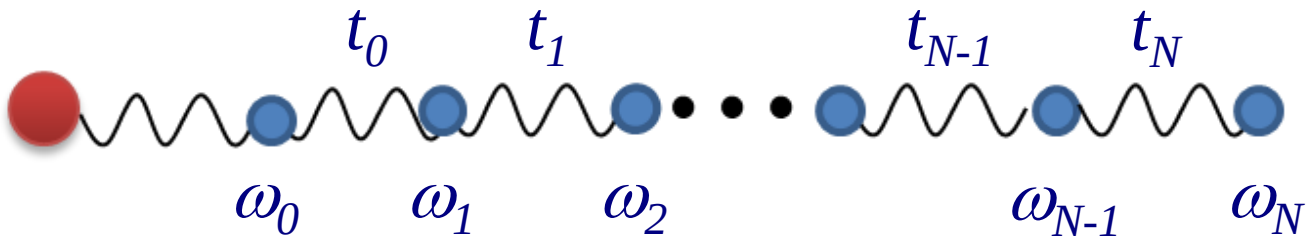

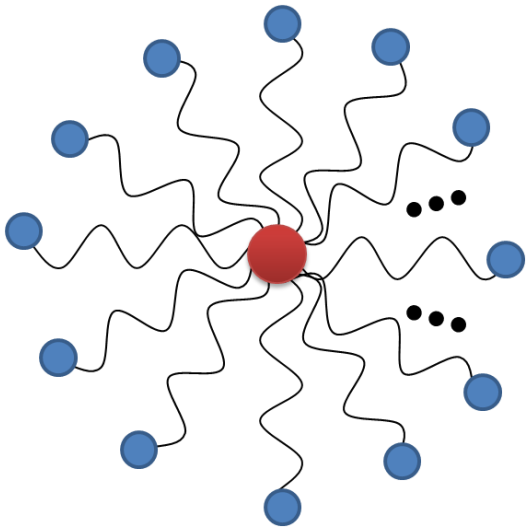

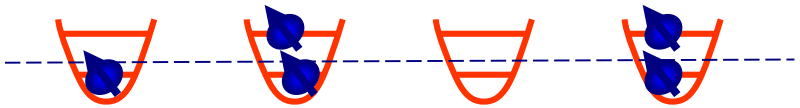

Hilbert Space dimension d^N=16

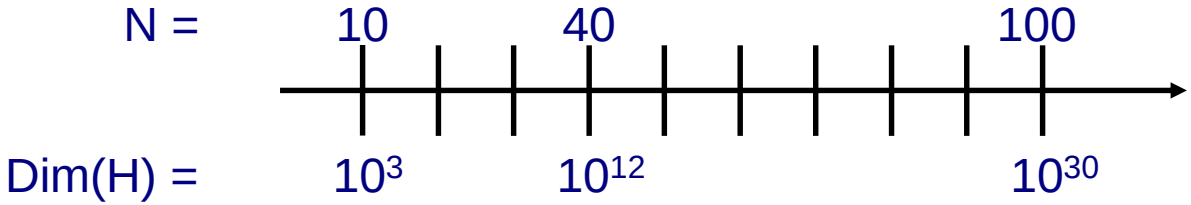

Matrix Product State (MPS)

$$|\Psi\rangle = \sum_{i_1,i_2,\ldots,i_N}^{d} C_{i_1,i_2,\ldots,i_N} \, |i_1,i_2,\ldots,i_N\rangle$$

$$|\Psi\rangle = \sum_{i_1,i_2,\ldots,i_N}^{d} tr\left[A_{i_1}^{(1)} A_{i_2}^{(2)} \ldots A_{i_N}^{(N)}\right] |i_1,i_2,\ldots,i_N\rangle$$

$|\psi\rangle =$

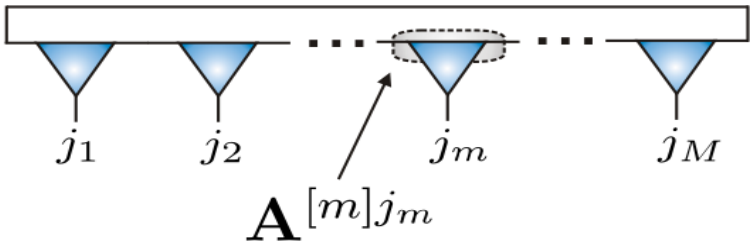

Example I: Product state

$$|\Psi\rangle = |01011\rangle$$

$C_{01011}=1$

others

$$C_{i_1 i_2 i_3 i_4 i_5} = 0$$

$$A_0^{(1)} = 1\,; \quad A_1^1 = 0$$

$$A_0^2 = 0\,; \quad A_1^2 = 1$$

$$A_0^3 = 1\,; \quad A_1^3 = 0$$

$$A_0^4 = 0\,; \quad A_1^4 = 1$$

$$A_0^5 = 0\,; \quad A_1^5 = 1$$

Example II: Greenberger-Horne-Zeilinger state

$$|\Psi\rangle = \frac{1}{\sqrt{2}}(|\uparrow\uparrow \cdots \uparrow\uparrow\rangle + |\downarrow\downarrow \cdots \downarrow\downarrow\rangle)$$

$$A^{j=\uparrow} = \frac{1}{2}(1+\sigma^z)\,; \quad A^{j=\downarrow} = \frac{1}{2}(1-\sigma^z)$$

Matrix Product State (MPS)

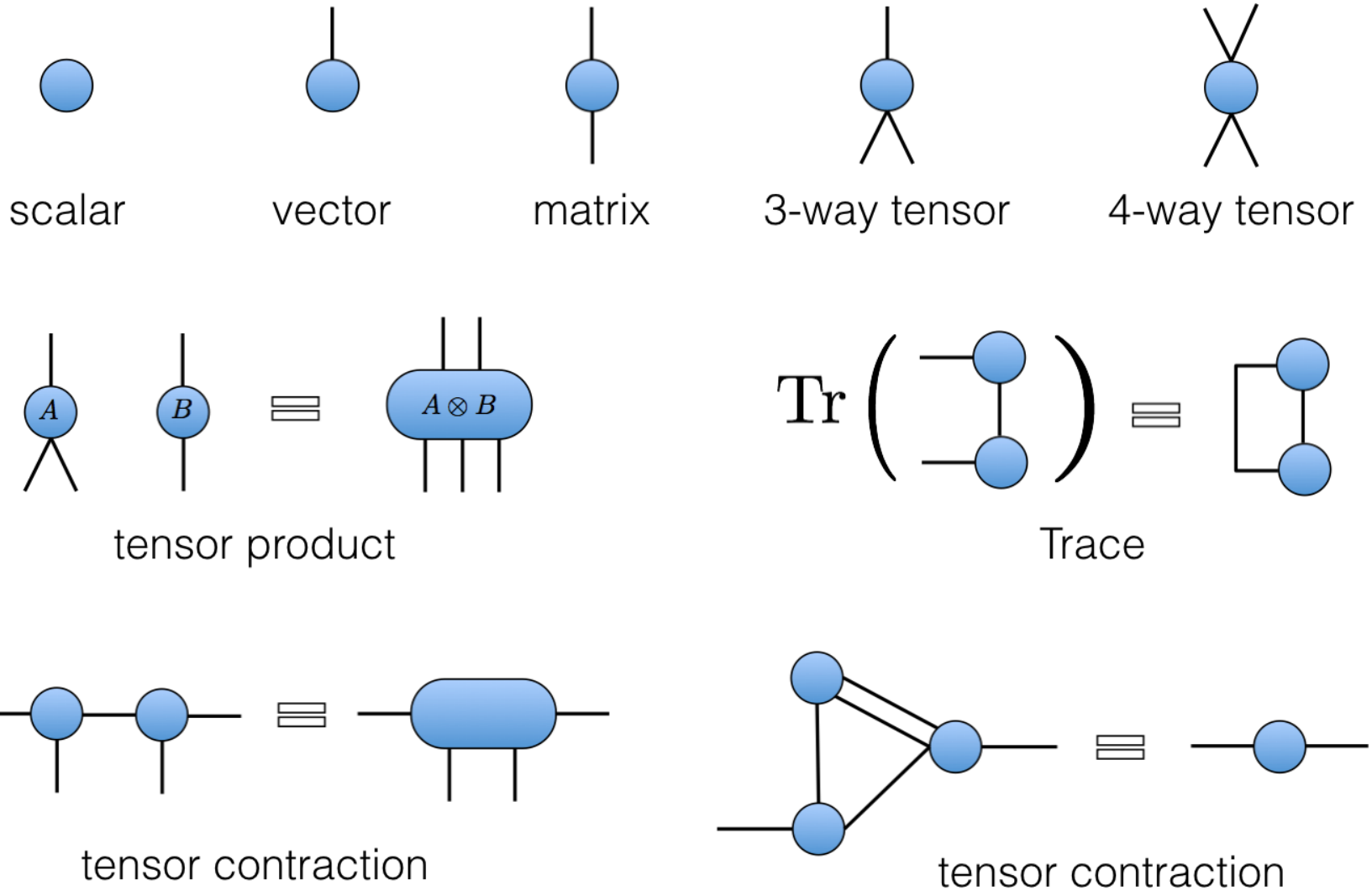

The role of entanglement

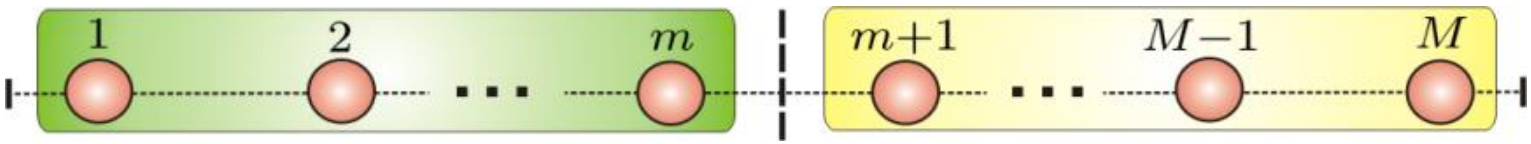

$$|\Psi\rangle = \sum_{i=1}^{d^m} \sum_{j=1}^{d^{M-m}} C_{ij} \, |i\,\rangle_A \otimes |j\,\rangle_B$$

$$|\Psi\rangle = \sum_{\alpha=1}^{\chi} \lambda_\alpha^2 \left(\sum_{i=1}^{d^m} U_{i\alpha} |i\,\rangle_A \right) \otimes \left(\sum_{i=1}^{d^m} V_{\alpha j} |j\,\rangle_B \right)$$

The role of entanglement

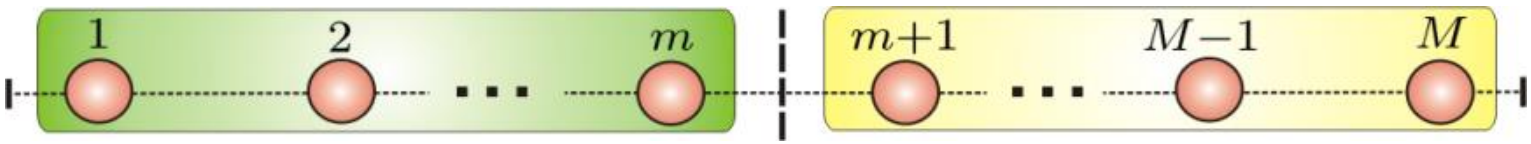

$$|\Psi\rangle = \sum_{\alpha=1}^{\chi} \lambda_\alpha^2 \left(\sum_{i=1}^{d^m} U_{i\alpha} |i\,\rangle_A \right) \otimes \left(\sum_{i=1}^{d^{M-m}} V_{\alpha j} |j\,\rangle_B \right)$$

$$|\Psi\rangle = \sum_{\alpha=1}^{\chi} \lambda_\alpha^2 \left| \phi_\alpha^{[A]} \right\rangle \otimes \left| \phi_\alpha^{[B]} \right\rangle$$

The role of entanglement

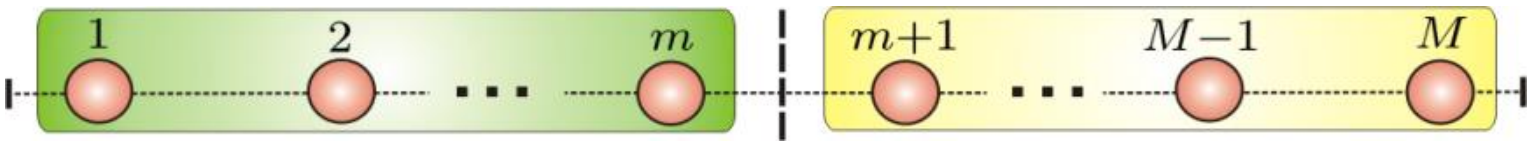

$$|\Psi\rangle = \sum_{\alpha=1}^{\chi} \lambda_\alpha^2 \, |\phi_\alpha^{[A]}\rangle \otimes |\phi_\alpha^{[B]}\rangle$$

The amount of entanglement (or quantum correlations) between the two blocks ***A*** and ***B*** is then quantified by the von Neumann entropy

$$S = -\sum_{\alpha=1}^{\chi} \lambda_\alpha^2 log_2(\lambda_\alpha^2)$$

Time evolving block decimation

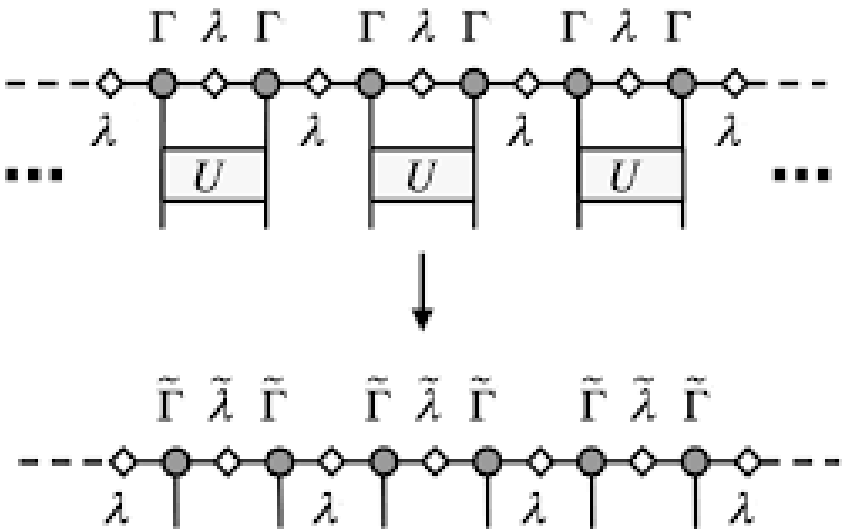

$$|\Psi\rangle = \sum_{\alpha_1,\alpha_2,\ldots,\alpha_N}^{\chi} tr\left[\Gamma_{\alpha_1}^{[1]i_1}\lambda_{\alpha_1}^{[1]}\Gamma_{\alpha_2}^{[2]i_2}\lambda_{\alpha_2}^{[2]}\ldots\Gamma_{\alpha_N}^{[N]i_N}\lambda_{\alpha_N}^{[N]}\right]|i_1,i_2,\ldots,i_N\rangle$$

Time evolving block decimation

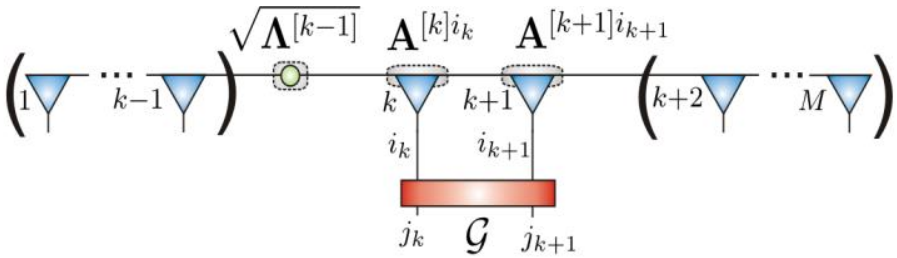

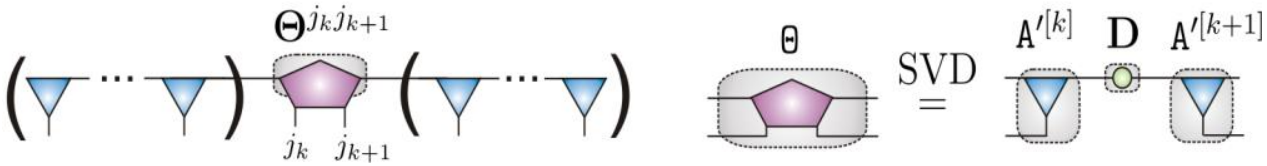

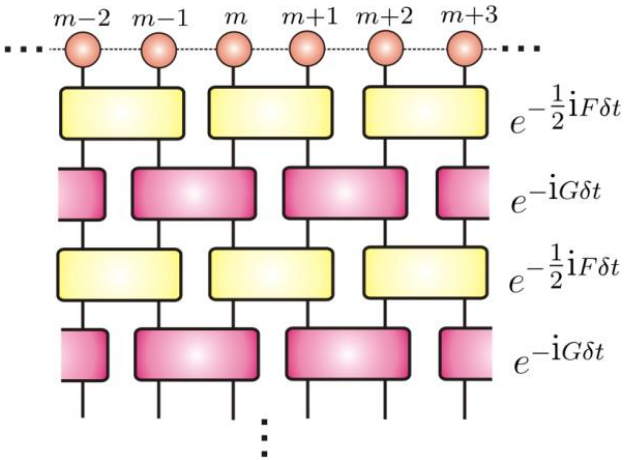

$$G_{i_k i_{k+1} j_k j_{k+1}} = e^{-iH_{i_k i_{k+1} j_k j_{k+1}} \delta t}$$

Time evolving block decimation

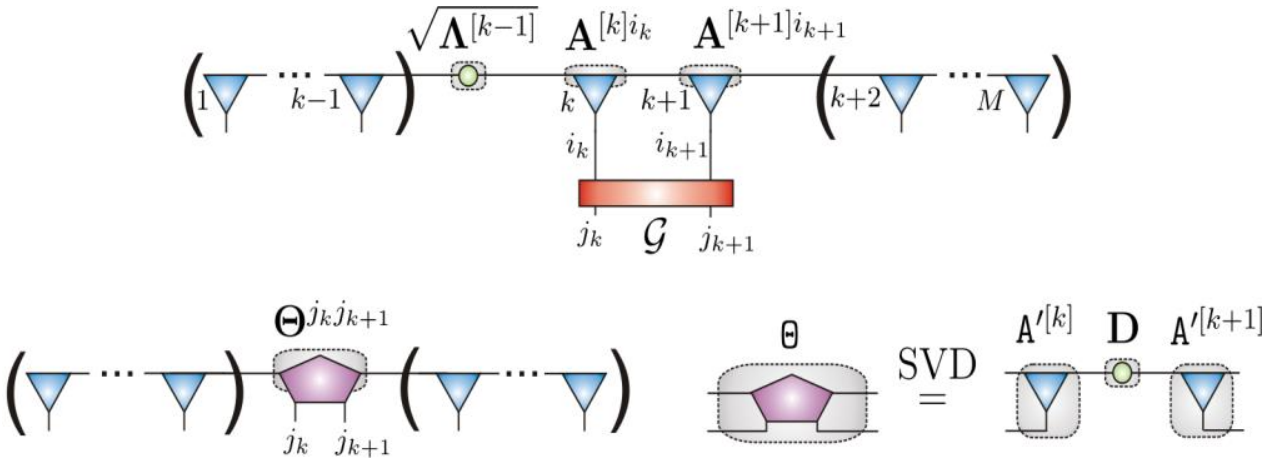

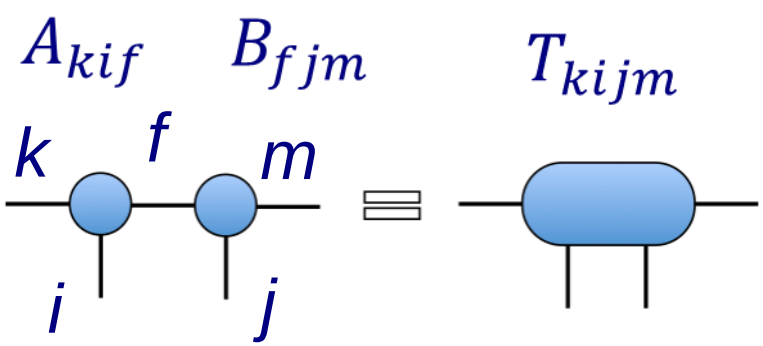

tensor contraction

$$T_{kijm} = \sum_{f=1}^{\chi} A_{kif} B_{fjm}$$

Time evolving block decimation

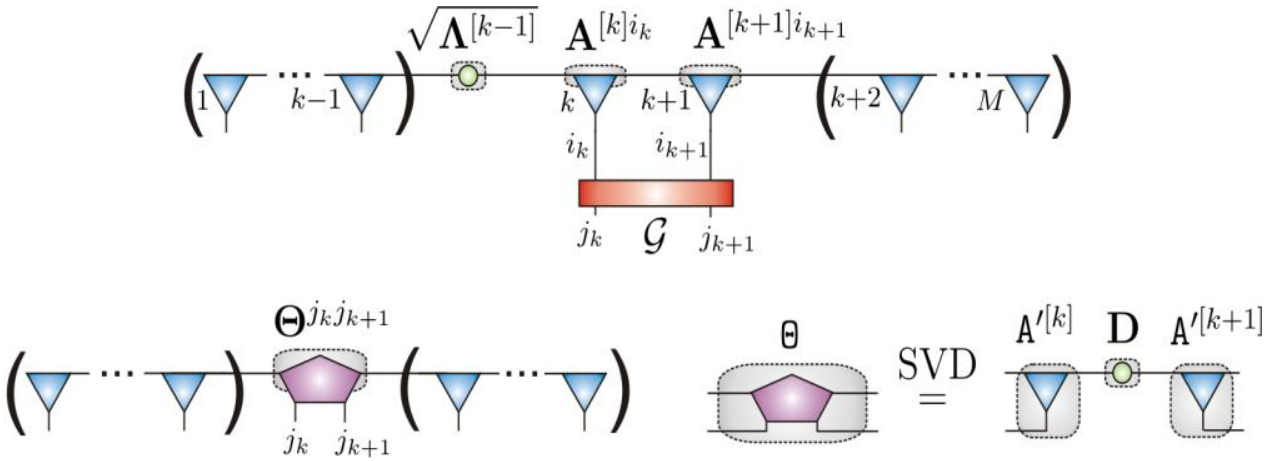

$$\Theta_{k,j_k,j_{k+1},m} = \sum_{f=1}^{\chi} \sum_{i_k=1}^{d} \sum_{i_{k+1}=1}^{d'} A_{k i_k f} B_{f i_{k+1} m} \, G_{i_k i_{k+1} j_k j_{k+1}}$$

Time evolving block decimation

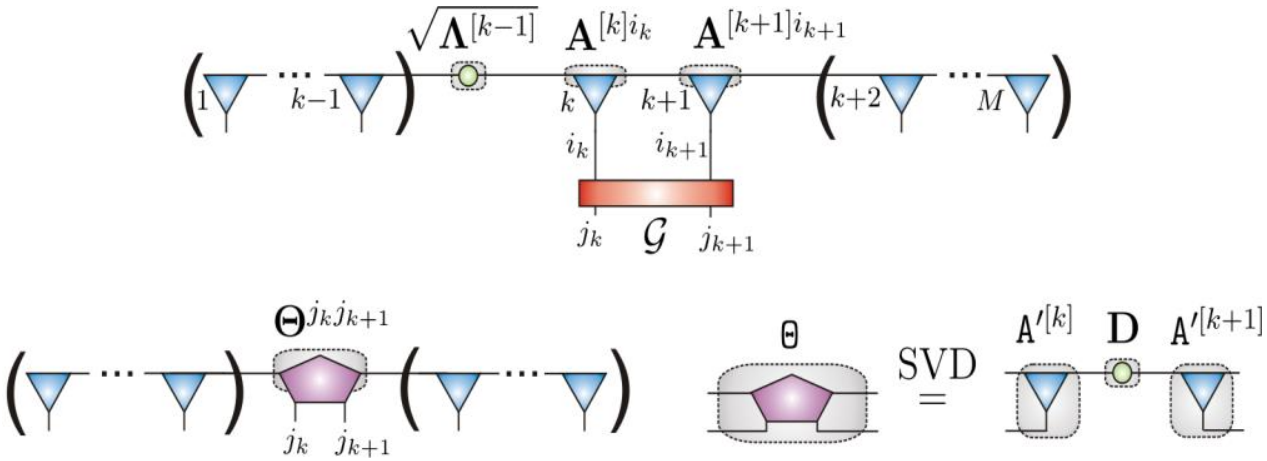

$$\Theta_{k j_k, j_{k+1} m} = \sum_{f=1}^{\chi} \sum_{i_k=1}^{d} \sum_{i_{k+1}=1}^{d'} A_{k i_k f} B_{f i_{k+1} m} \, G_{i_k i_{k+1} j_k j_{k+1}}$$

Time evolving block decimation

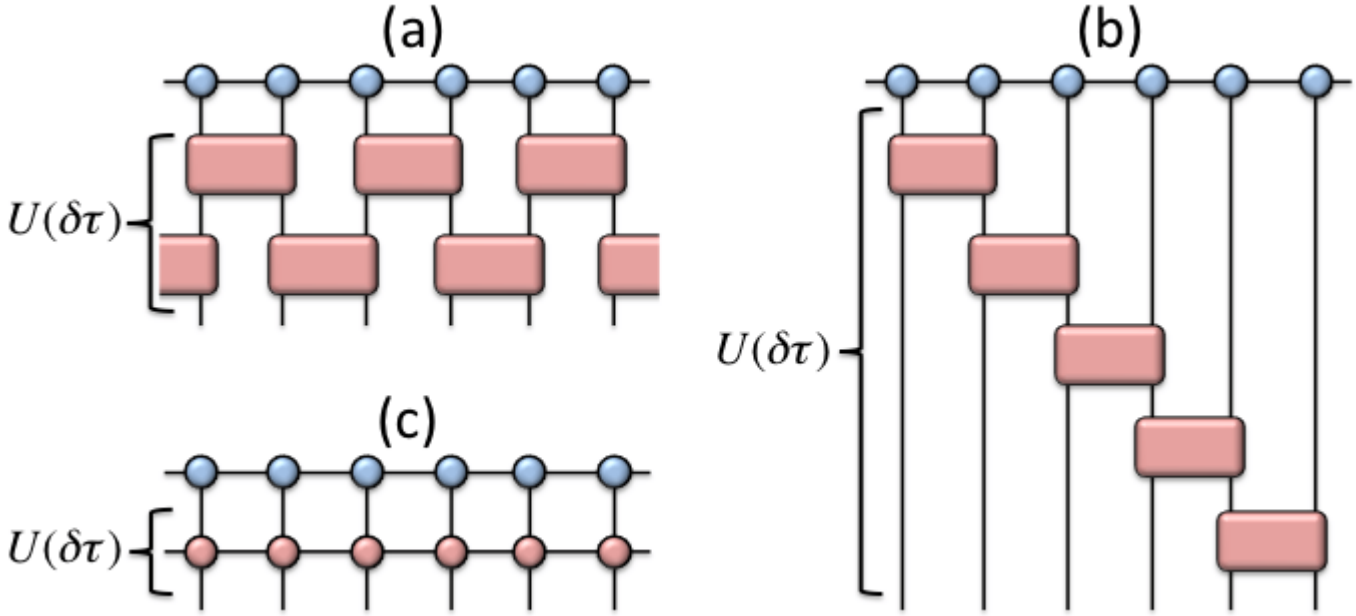

Time evolving block decimation

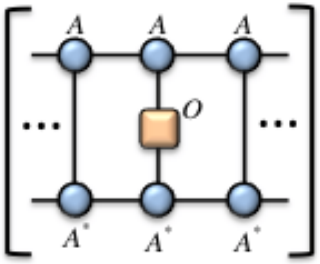

Time evolving block decimation

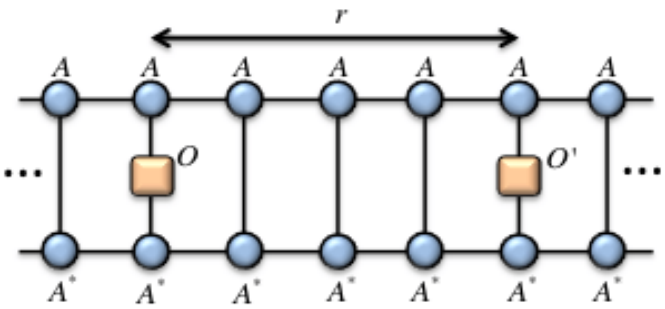

Time evolving block decimation

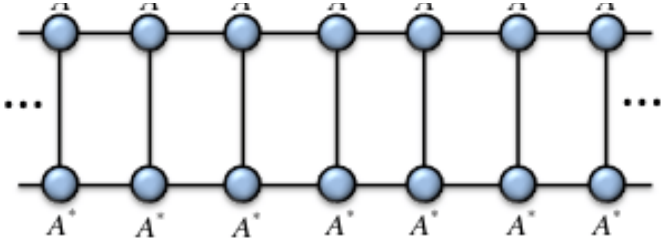

Modeling system-environment interaction in the non- perturbative regime

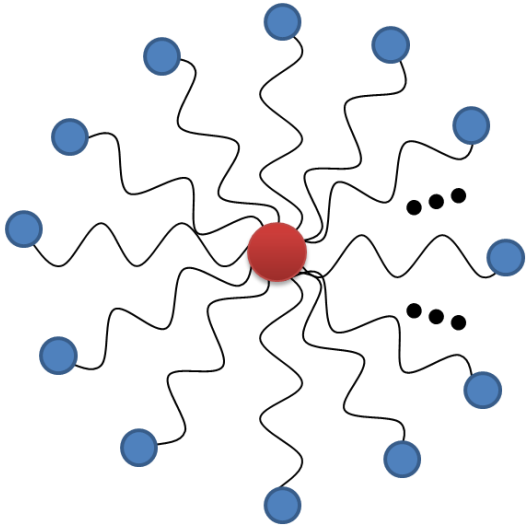

Modeling system-environment interaction in the non- perturbative regime

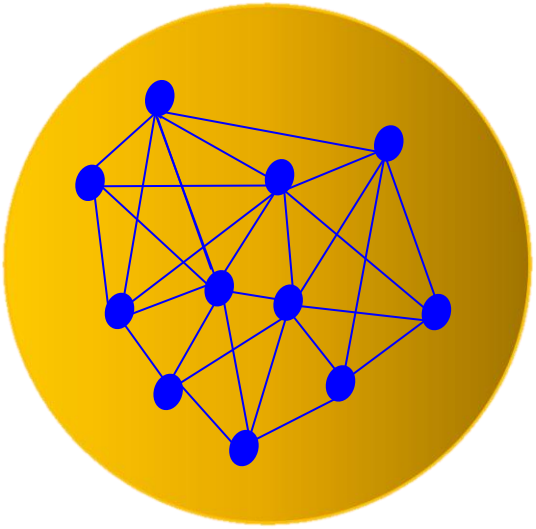

Modeling system-environment interaction in the non- perturbative regime

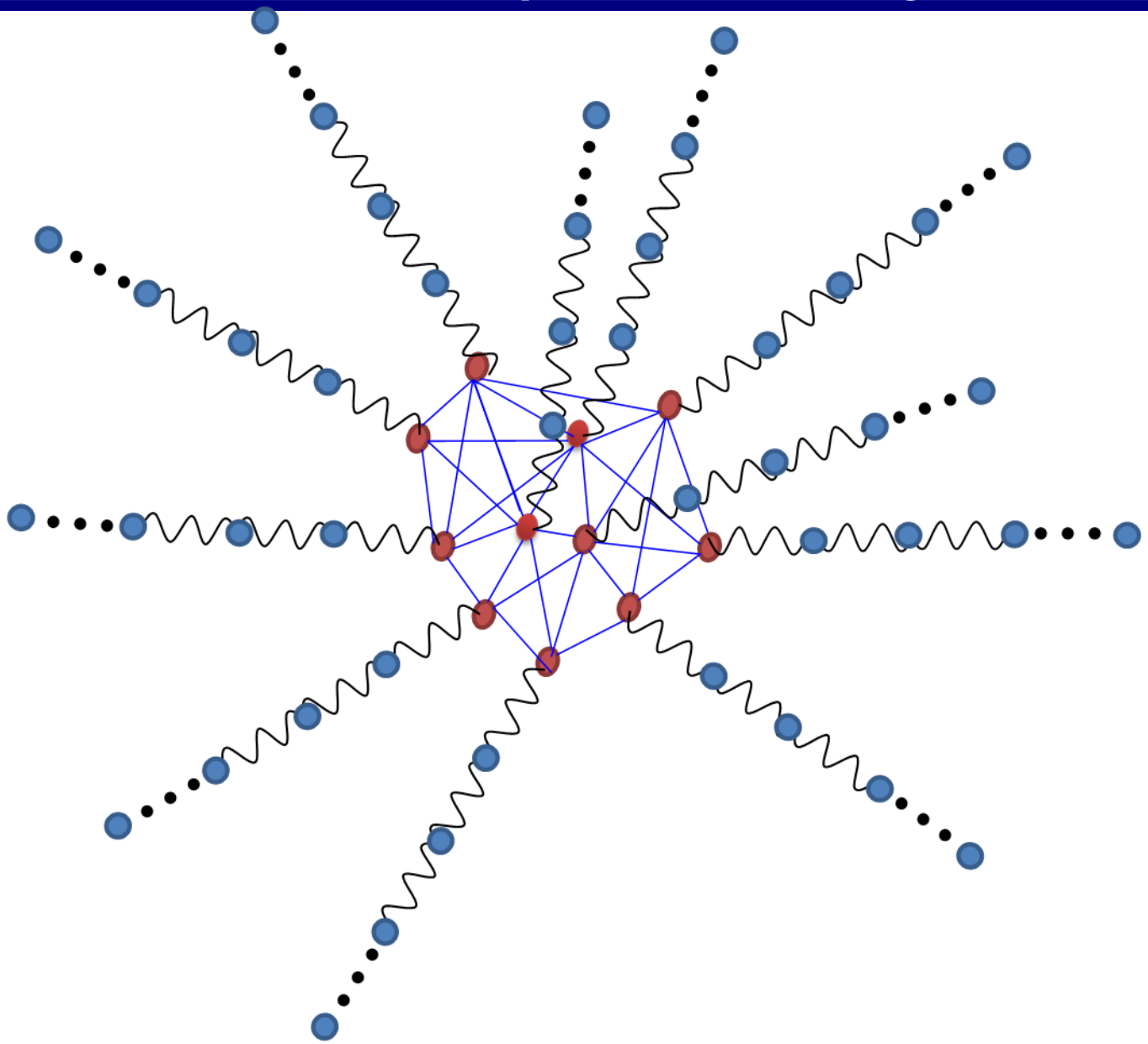

Modeling system-environment interaction in the non- perturbative regime

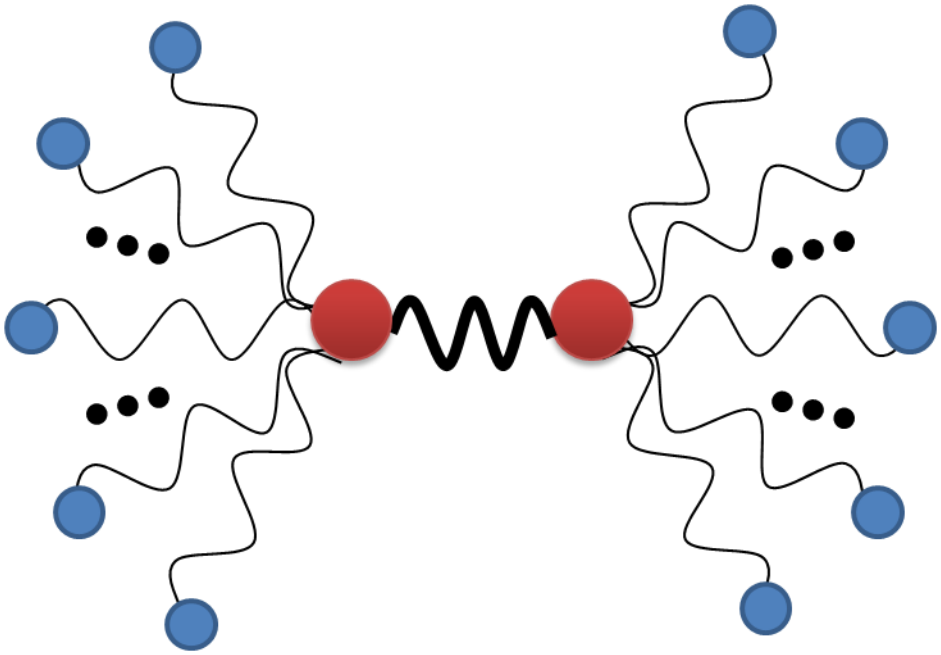

Modeling system-environment interaction in the non- perturbative regime

Modeling system-environment interaction in the non- perturbative regime

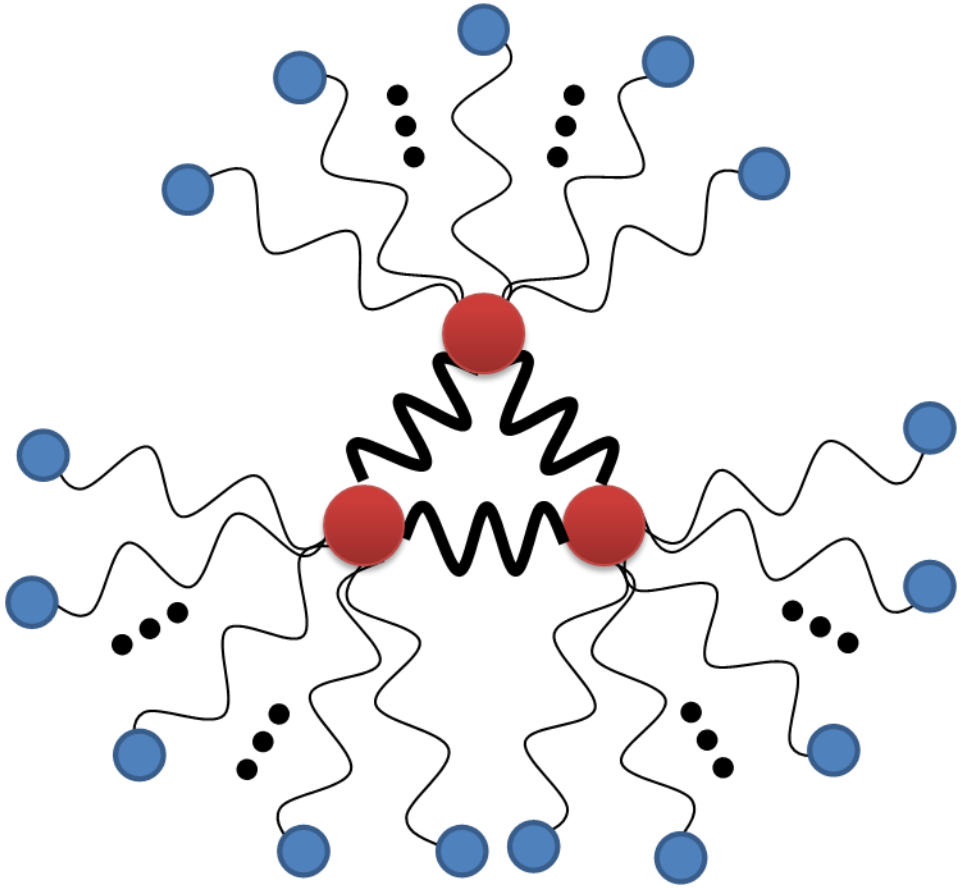

Modeling system-environment interaction in the non- perturbative regime

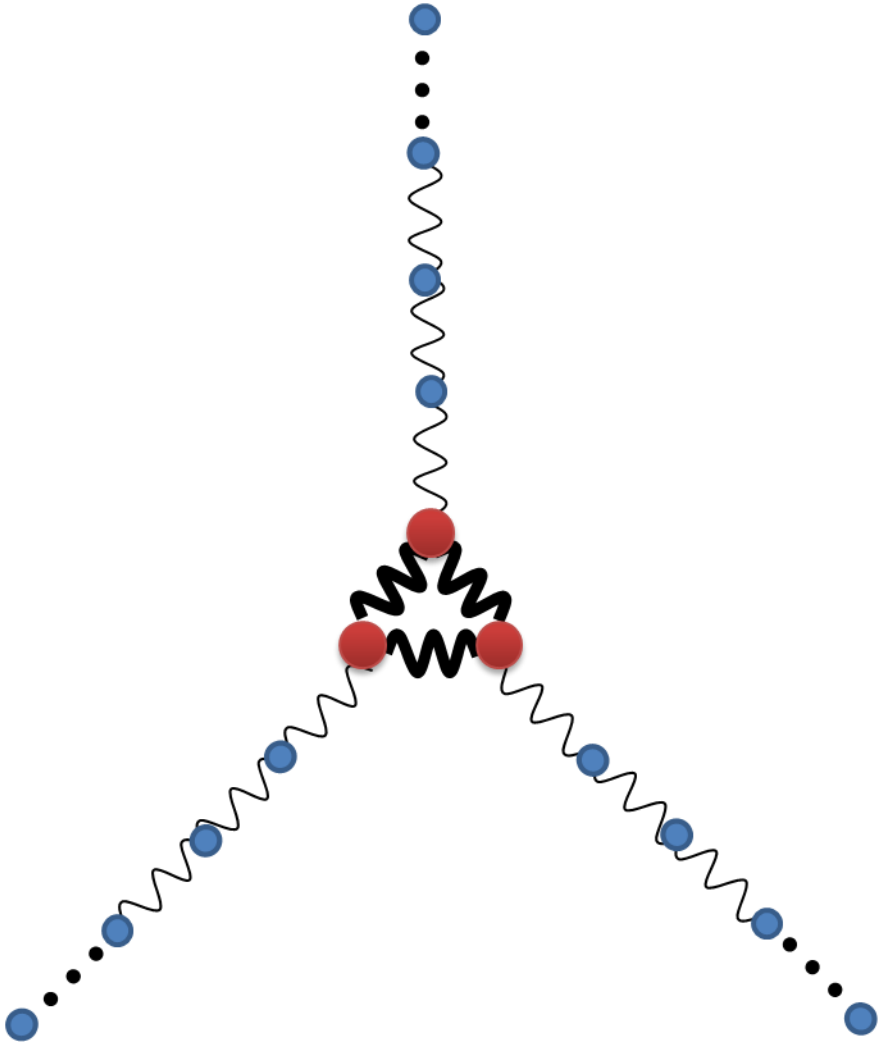

Modeling system-environment interaction in the non- perturbative regime

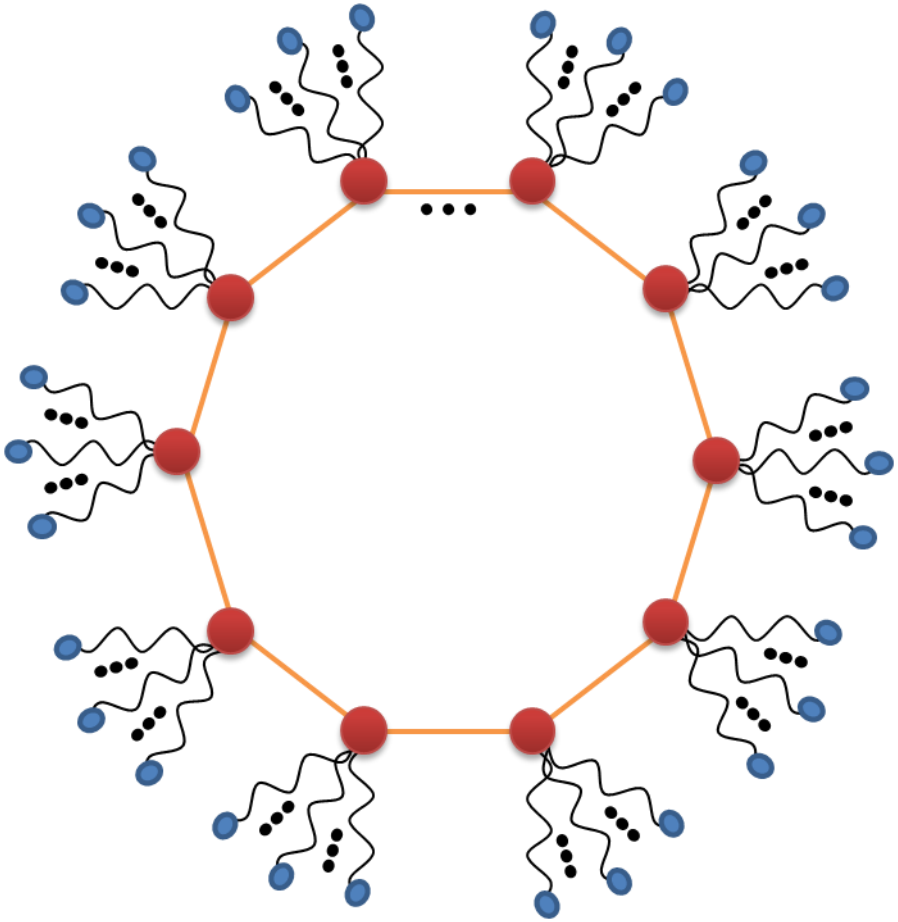

Modeling system-environment interaction in the non- perturbative regime

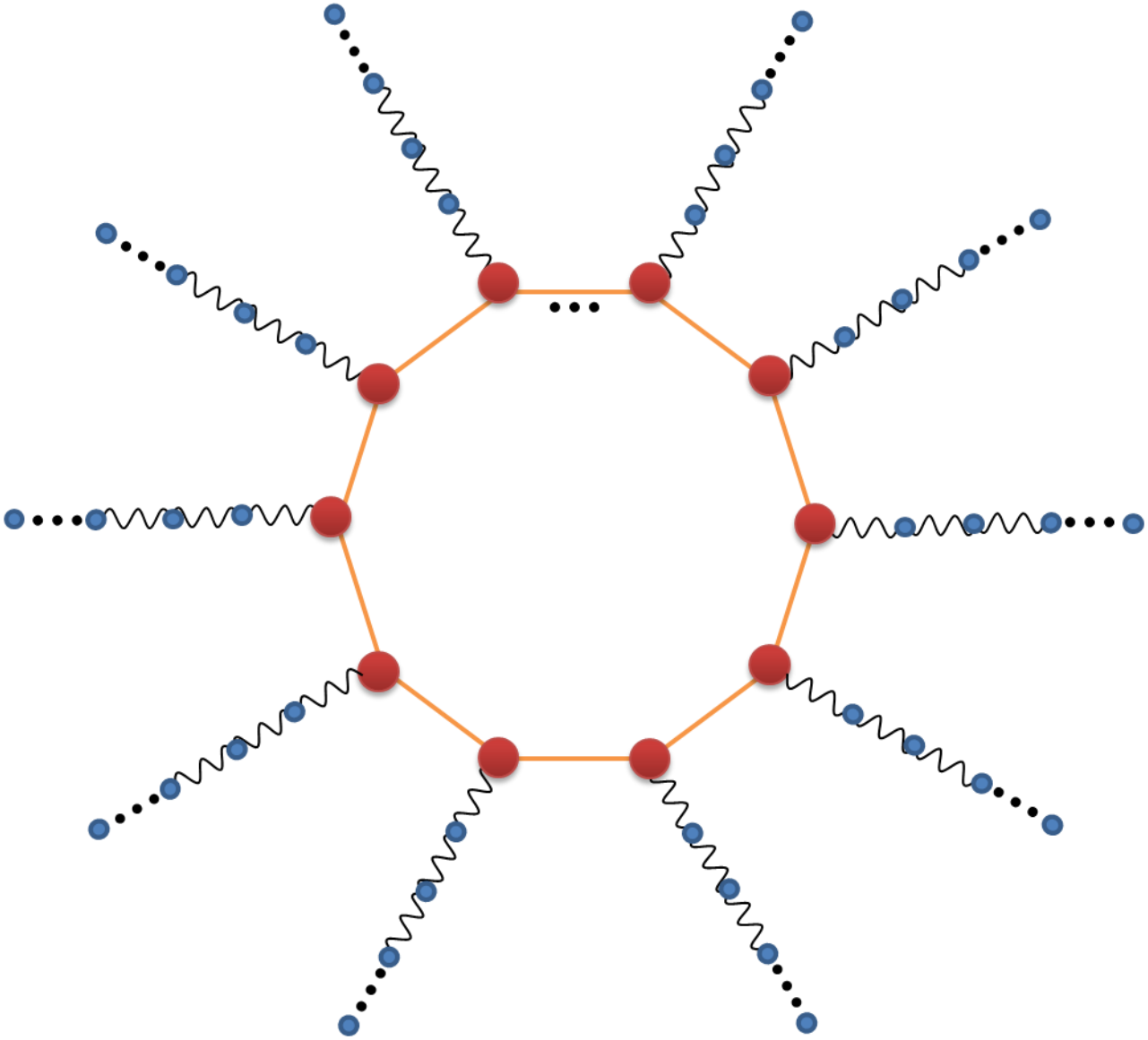

Exciton transport enhancement across quantum Su-Schrieer-Heeger lattices with quartic non linearity

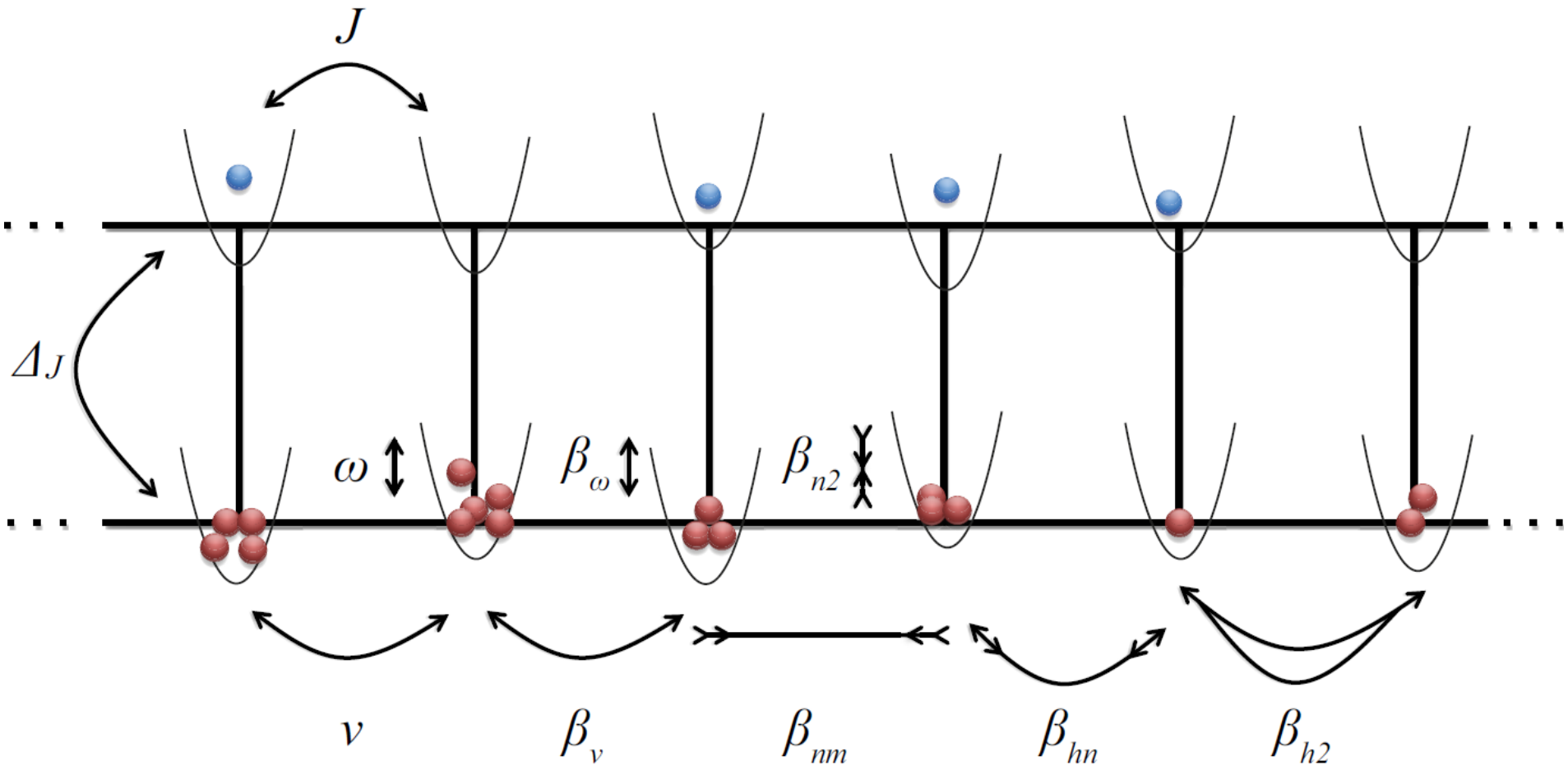

Exciton transport enhancement across quantum Su-Schrieer-Heeger lattices with quartic non linearity

Exciton transport enhancement across non-linear oscillating lattices

J. J. Mendoza-Arenas[1], D. F. Rojas-Gamboa[1], M. B. Plenio[2] and J. Prior[3,4]
[1] *Departamento de Física, Universidad de los Andes, A.A. 4976, Bogotá D. C., Colombia*
[2] *Institut für Theoretische Physik & IQST, Albert-Einstein Allee 11, Universität Ulm, D-89081 Ulm, Germany*
[3] *Departamento de Física Aplicada, Universidad Politécnica de Cartagena, Cartagena E-30202, Spain and*
[4] *Departamento de Física Aplicada, Universidad de Granada, Granada E-30202, Spain*
(Dated: January 9, 2019)

In the present work we discuss the propagation of excitons across a one-dimensional mobile underlying lattice, which possesses both harmonic and weak anharmonic oscillations. When quantizing these vibrational degrees of freedom we identify several types of phonon non-linearities, each one with a different impact on the excitonic dynamics. Our analysis of the dynamics identifies a dominant non-linear correction to the phonon hopping which leads to a strong enhancement of exciton transport compared to a purely linear vibrational dynamics. Thus lattice non-linearities can be exploited to induce transitions from localized to delocalized conduction, even for very weak amplitudes.

PACS numbers: 05.60.Gg, 05.10.-a, 63.20.Ry, 68.65.-k

Exciton transport enhancement across quantum Su-Schrieer-Heeger lattices with quartic non linearity

$$H = H_{ex} + H_{lat} + H_{in}$$

$$H_{ex} = J \sum_{j=1}^{N-1} \left(C_j^{\dagger} C_{j+1} + hc \right)$$

Exciton transport enhancement across quantum Su-Schrieer-Heeger lattices with quartic non linearity

$$H = H_{ex} + H_{lat} + H_{in}$$

$$H_{lat} = \sum_{j=0}^{N+1} \frac{p_j^2}{2m} + \frac{\alpha}{2} \sum_{j=0}^{N} \left(u_{j+1} - u_j\right)^2 + \frac{\lambda}{4} \sum_{j=0}^{N} \left(u_{j+1} - u_j\right)^4$$

$$u_j = \sqrt{\frac{1}{2m\omega}} \left(a_j^\dagger + a_j\right) \qquad p_j = \sqrt{\frac{m\omega}{2}} \left(a_j^\dagger - a_j\right)$$

Exciton transport enhancement across quantum Su-Schrieer-Heeger lattices with quartic non linearity

$$H_{lat-lin} = \omega \sum_{j=1}^{N} n_j - \nu \sum_{j=1}^{N-1} \left(a_j^{\dagger} a_{j+1} + hc\right)$$

$$H_{lat-nl} = \beta \left[9 \sum_{j=1}^{N} n_j - 3 \sum_{j=1}^{N-1} \left(a_j^{\dagger} a_{j+1} + hc\right) - 3 \sum_{j=1}^{N} n_j^2 + 6 \sum_{j=1}^{N-1} n_j n_{j+1} + \frac{3}{2} \sum_{j=1}^{N-1} \left(\left(\left(a_j^{\dagger}\right) \right)^2 a_{j+1}^2 + hc \right) + 3 \sum_{j=1}^{N-1} \left(a_j^{\dagger} a_{j+1} + hc\right)\left(n_j + n_{j+1}\right) \right]$$

Exciton transport enhancement across quantum Su-Schrieer-Heeger lattices with quartic non linearity

$$H = H_{ex} + H_{lat} + H_{in}$$

$$H_{in} = \Delta_J \sum_{j=1}^{N-1} \left(C_j^\dagger C_{j+1} + hc\right)\left(a_{j+1} + a_{j+1}^\dagger - a_j - a_j^\dagger\right)$$

Exciton transport enhancement across quantum Su-Schrieer-Heeger lattices with quartic non linearity

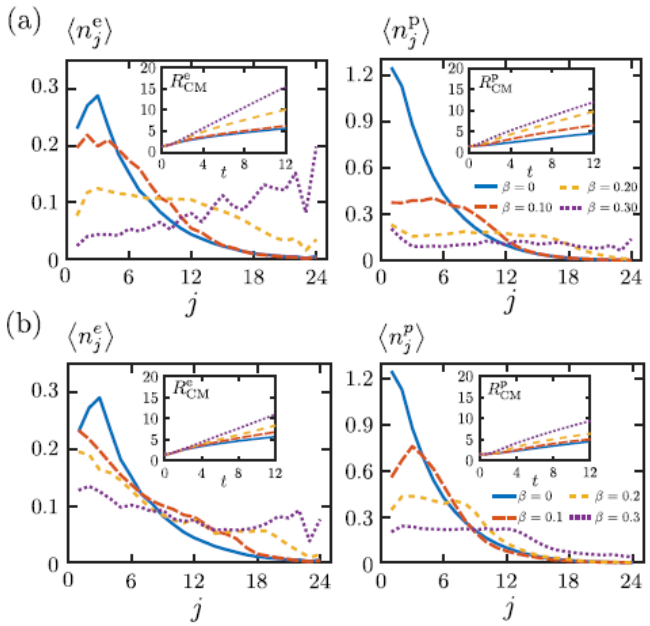

FIG. 6: Final exciton (left) and phonon (right) profiles for higher-order non-linear phonon hopping processes, Eqs. (8c) and (8d). The results are for $\nu = 6.25 \times 10^{-2}$, $\Delta_J = 0.25$ and several values of β. (a) Double phonon hopping. (b) Density-modulated phonon hopping. Insets: Corresponding CM position as a function of time.

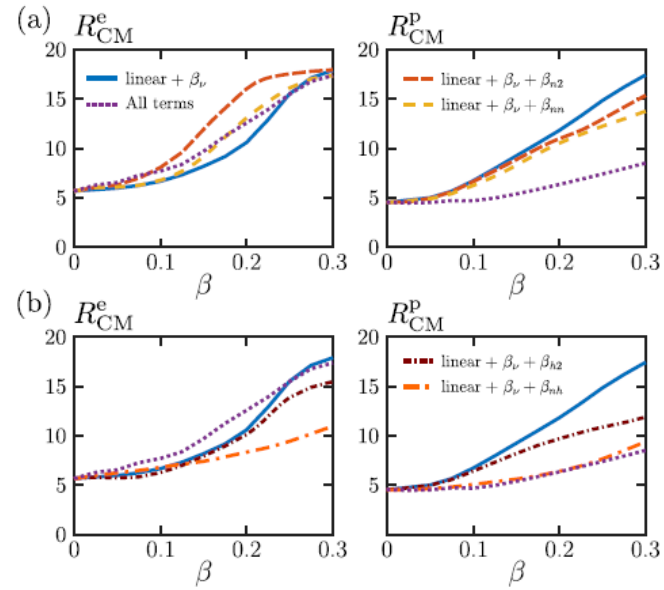

FIG. 7: Final position of the CM for excitons (left) and phonons (right) as a function of β, for the different non-linearities. All panels include the results for the linear plus the non-linear hopping correction of Eq. (8a), and the total non-linearity. The upper panels correspond to density-density non-linearities of Eq. (8b), and the lower panels to the high-order hopping terms of Eqs. (8c) and (8d).

Conclusions

- ***An efficient method for simulating archetypal models of open quantum system is implemented combining an analytical chain transformation with t-DMRG methods.***

- ***Orthogonal polynomials theory shows the baths only differ in the first 10 -20 sites of chain representation. Universal truncation schemes are possible***

- ***Chain mapping works for bosons and fermions. Wide range of applications***

- ***Extension to finite temperatures, multiple sites, and spatially-correlated baths – compared with existing techniques***

TEDOPA: Time Evolving Density with Orthogonal Polynomial Algorithm

THANKS

Funding:

GOBIERNO DE ESPAÑA
MINISTERIO DE CIENCIA, INNOVACIÓN Y UNIVERSIDADES

f SéNeCa(+)
Agencia de Ciencia y Tecnología
Región de Murcia

Tensor Network States, an Introduction and Applications to Quantum Coherent Processes:II

Javier Prior

Universidad Politécnica de Cartagena

iCI Instituto Carlos I
Física teórica y computacional

Long-lasting coherence in biological complexes: from microscopic models to actual experiments

Javier Prior

Universidad Politécnica de Cartagena

iCI Instituto Carlos I
Física teórica y computacional

From the classical to the quantum world

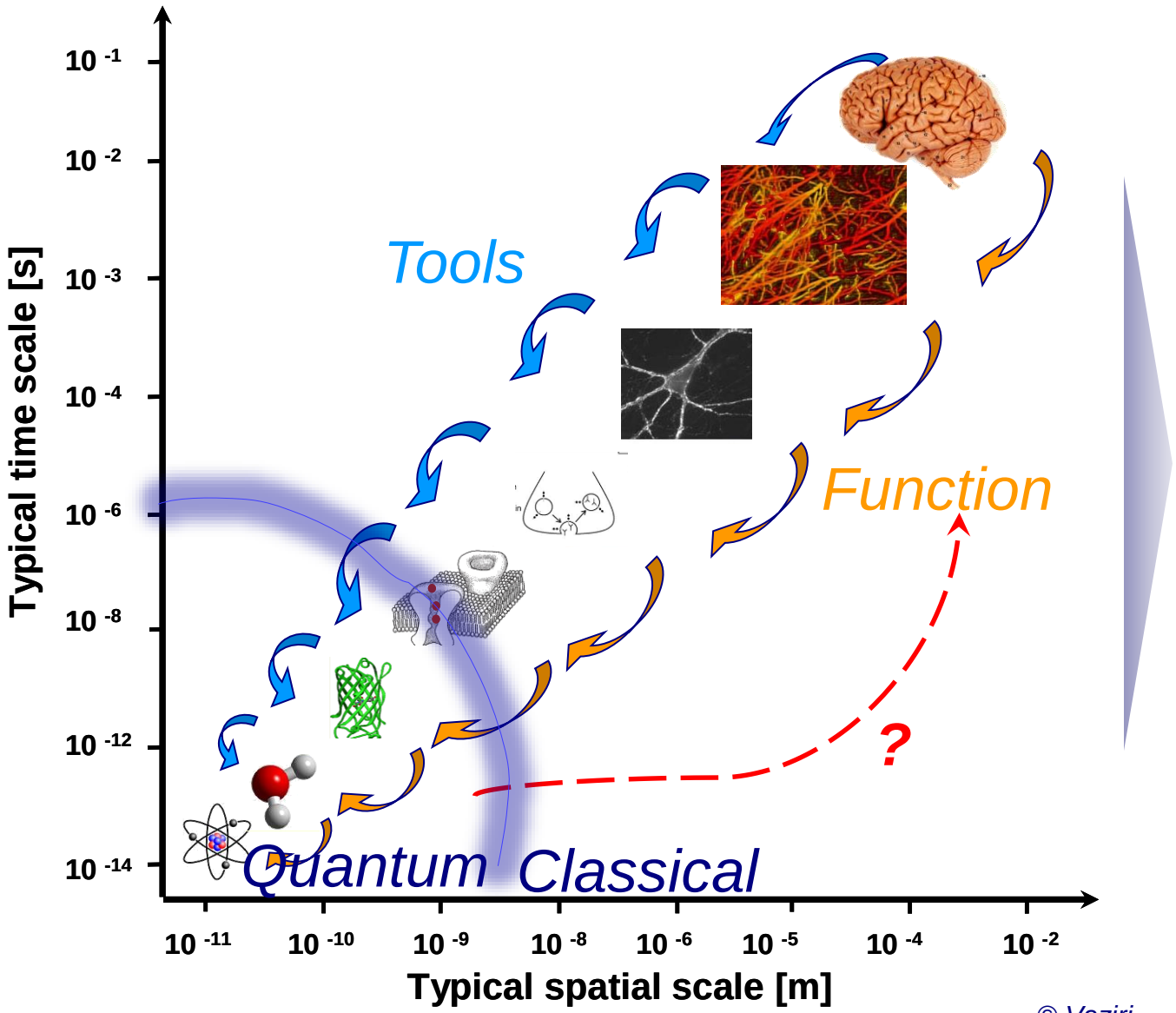

Can quantum coherence be relevant for biological function?

Requires tools for studying biological structure and function at unprecedented spatial and temporal resolution

From the classical to the quantum world

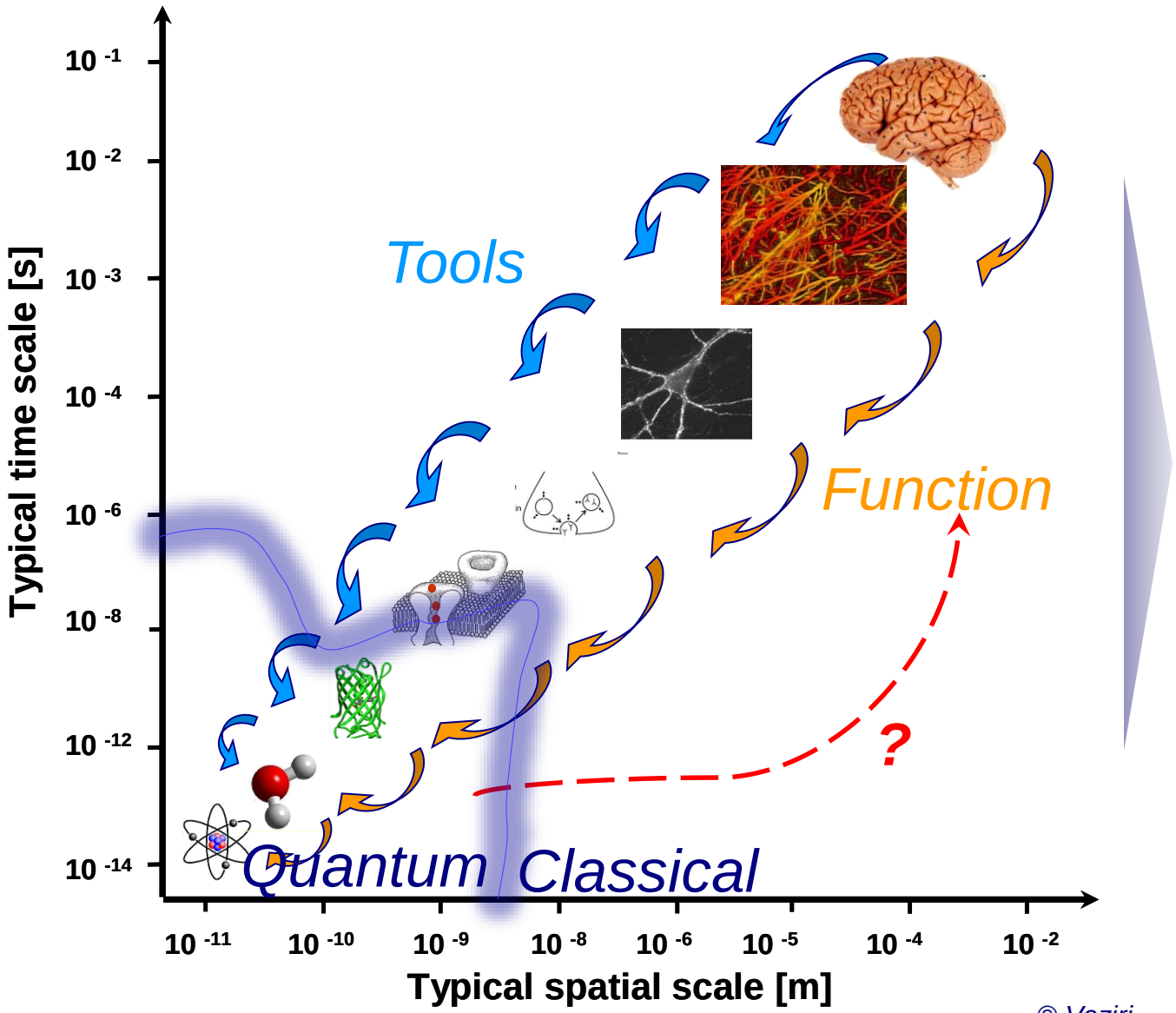

Can quantum coherence be relevant for biological function?

Requires tools for studying biological structure and function at unprecedented spatial and temporal resolution

From the classical to the quantum world

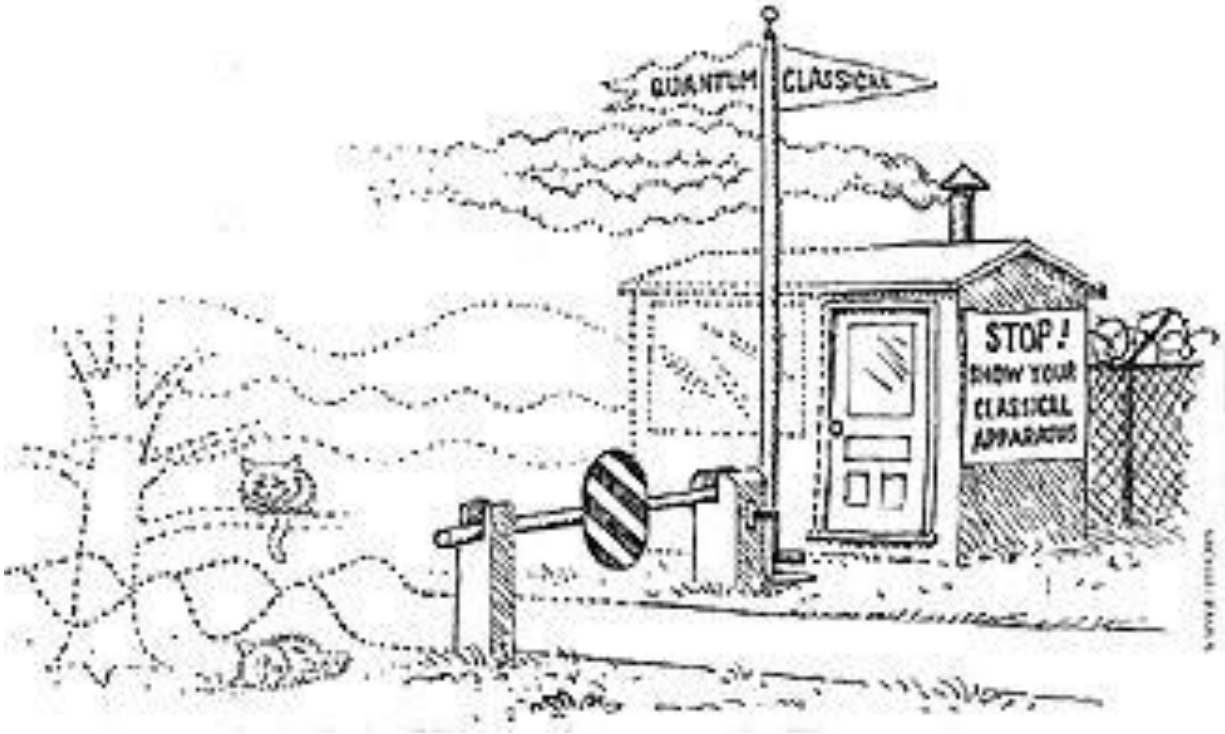

Quantum biology

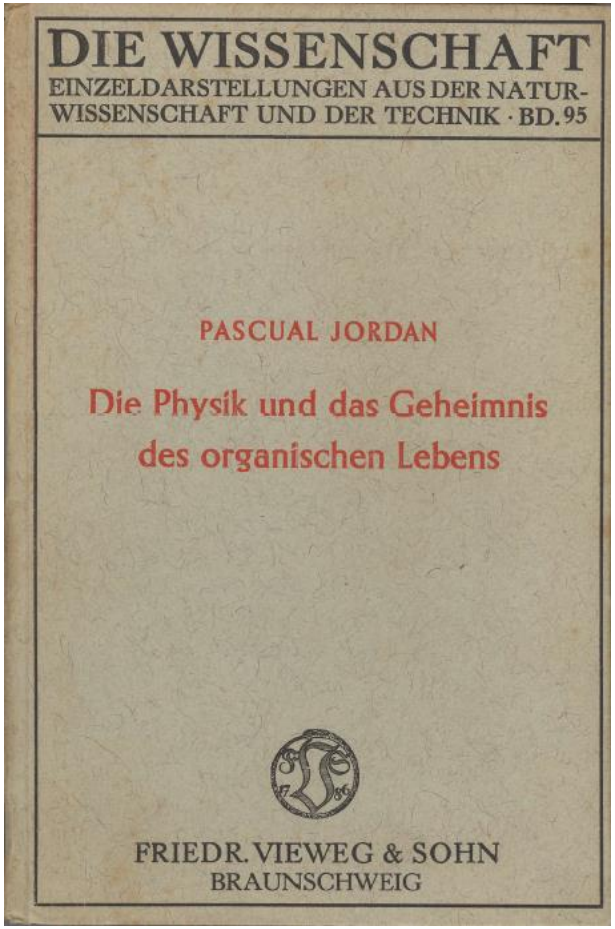

1943

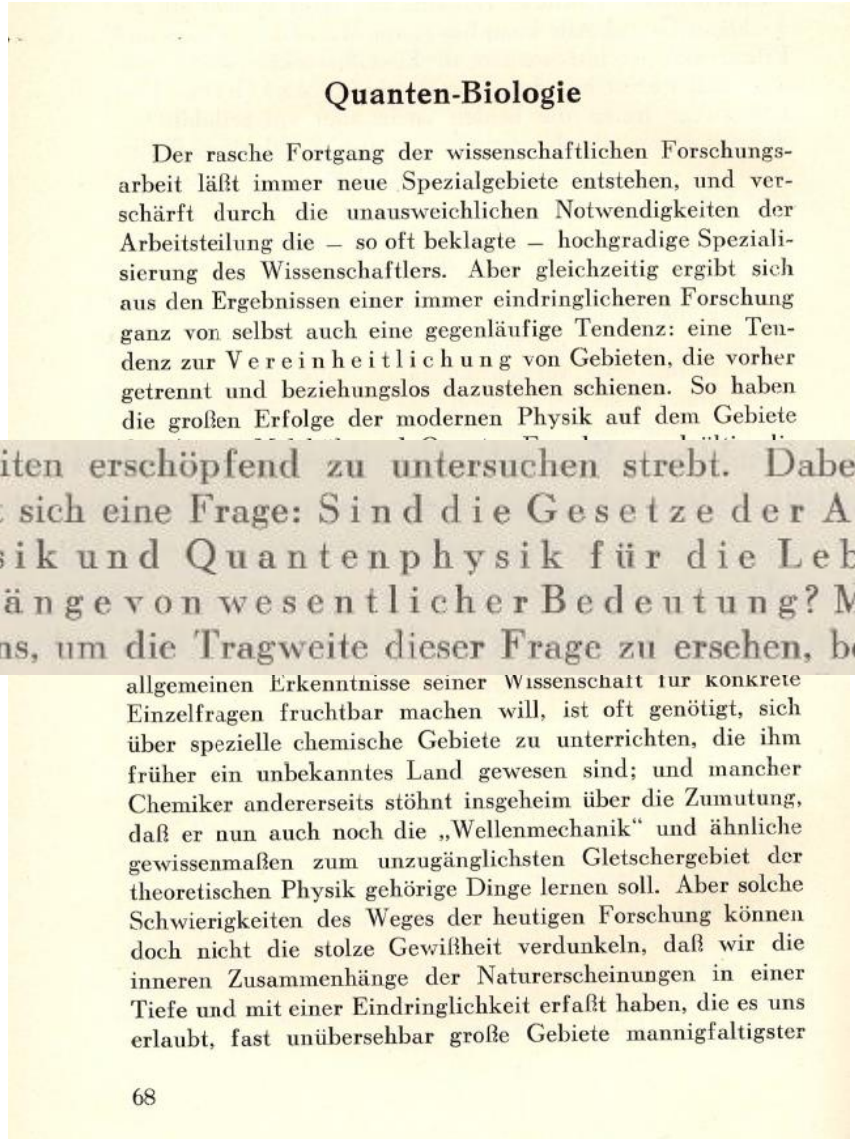

Quanten-Biologie

Der rasche Fortgang der wissenschaftlichen Forschungsarbeit läßt immer neue Spezialgebiete entstehen, und verschärft durch die unausweichlichen Notwendigkeiten der Arbeitsteilung die – so oft beklagte – hochgradige Spezialisierung des Wissenschaftlers. Aber gleichzeitig ergibt sich aus den Ergebnissen einer immer eindringlicheren Forschung ganz von selbst auch eine gegenläufige Tendenz: eine Tendenz zur Vereinheitlichung von Gebieten, die vorher getrennt und beziehungslos dazustehen schienen. So haben die großen Erfolge der modernen Physik auf dem Gebiete

lichkeiten erschöpfend zu untersuchen strebt. Dabei aber erhebt sich eine Frage: Sind die Gesetze der Atomphysik und Quantenphysik für die Lebensvorgänge von wesentlicher Bedeutung? Machen wir uns, um die Tragweite dieser Frage zu ersehen, bewußt,

allgemeinen Erkenntnisse seiner Wissenschaft für konkrete Einzelfragen fruchtbar machen will, ist oft genötigt, sich über spezielle chemische Gebiete zu unterrichten, die ihm früher ein unbekanntes Land gewesen sind; und mancher Chemiker andererseits stöhnt insgeheim über die Zumutung, daß er nun auch noch die „Wellenmechanik" und ähnliche gewissenmaßen zum unzugänglichsten Gletschergebiet der theoretischen Physik gehörige Dinge lernen soll. Aber solche Schwierigkeiten des Weges der heutigen Forschung können doch nicht die stolze Gewißheit verdunkeln, daß wir die inneren Zusammenhänge der Naturerscheinungen in einer Tiefe und mit einer Eindringlichkeit erfaßt haben, die es uns erlaubt, fast unübersehbar große Gebiete mannigfaltigster

68

Quantum biology

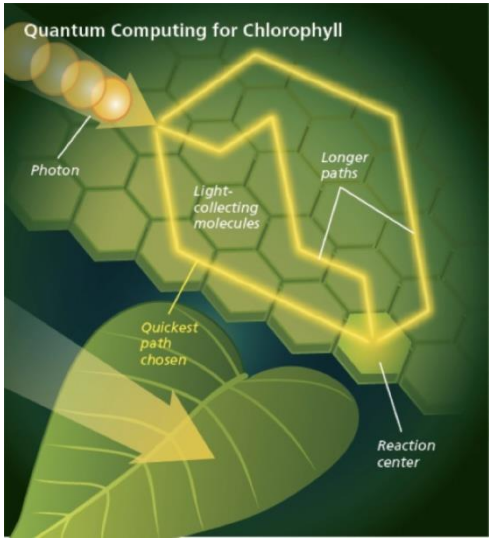

1. Quantum transport in photosynthesis

2. Photon-assisted tunnelling in olfaction

3. Magnetic sensing in birds

4. Others, General anaesthesia, etc

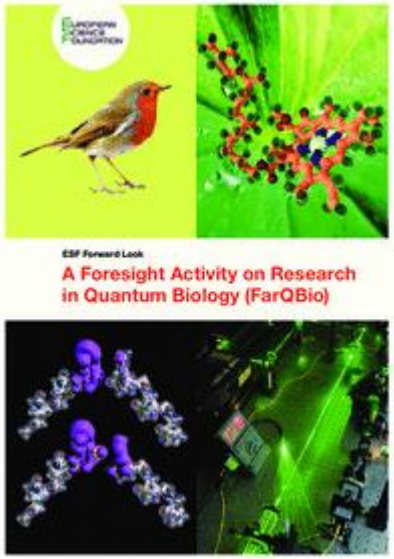

2D spectroscopy

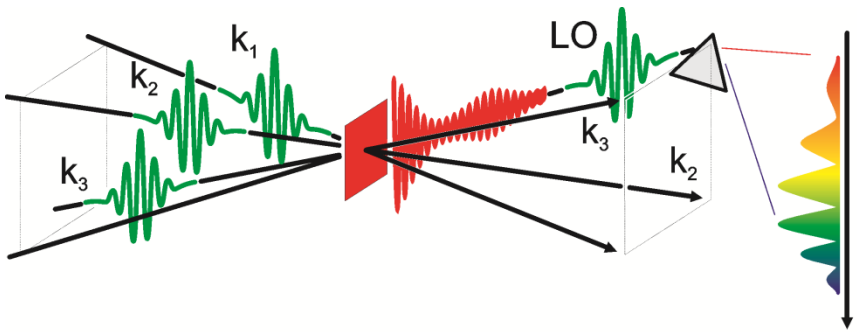

$k_S = -k_1 + k_2 + k_3$

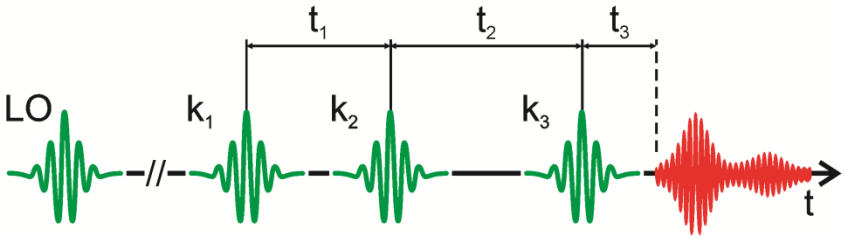

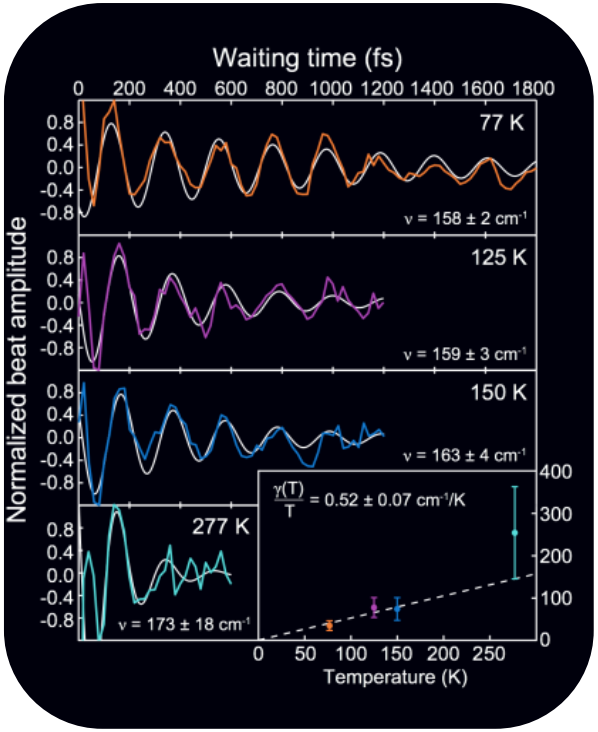

• **Evidence for wavelike energy transfer through quantum coherence in photosynthetic systems**
GS Engel, TR Calhoun, EL Read, TK Ahn, T Mančal, YC Cheng, Robert E Blankenship, Graham R Fleming
Nature 446 (7137), 782-786.

Long lived *coherence*

How can quantum coherence persist during relevant time scales and at room temperature?

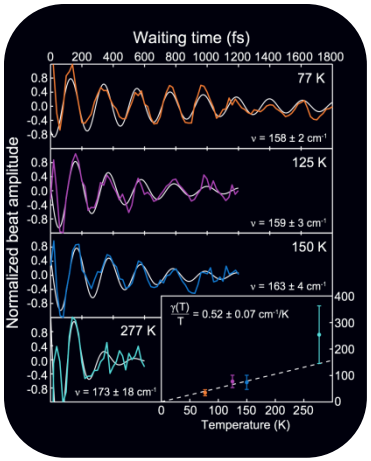

From theory to actual experiments

Spectral properties of the proposed model

Illustration: 2D ES in J-aggregates and PSII RC

Environment assisted quantum dynamics

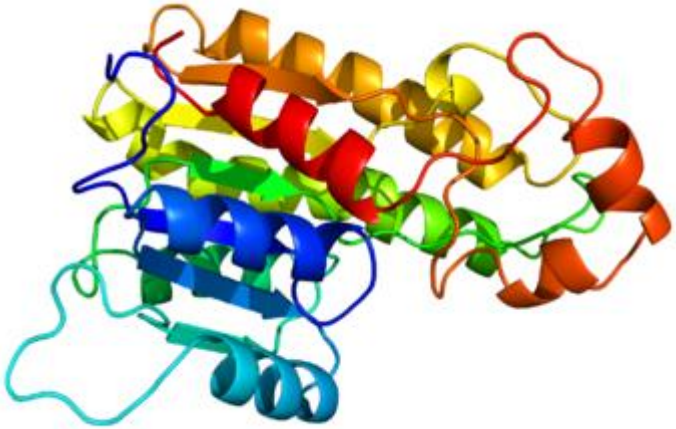

Controlled Arrangements

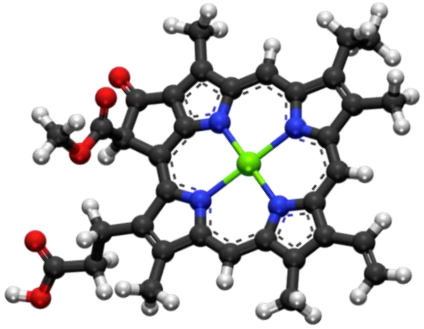

Molecules

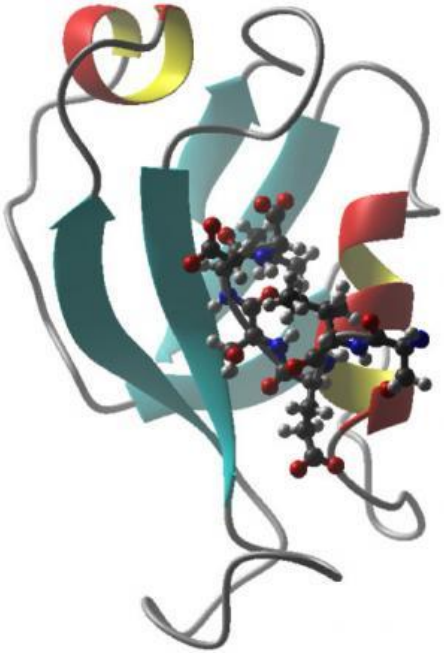

Optimized Function

Light harvesting systems

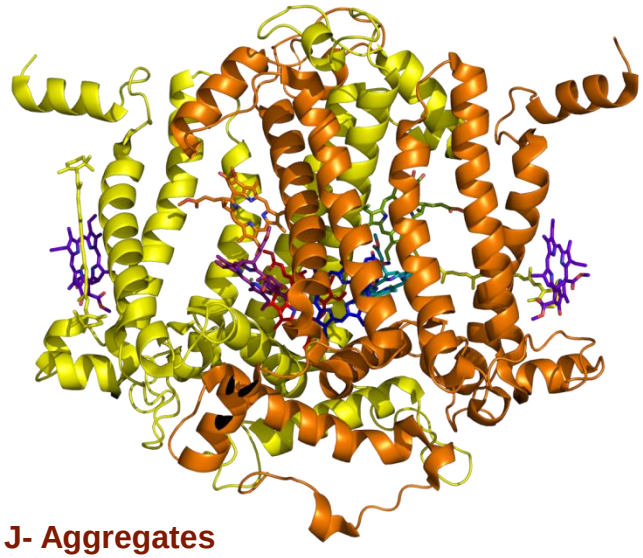

Photosynthesis II Reaction Center PSIIRC

- VI. Novoderezhkin, E. Romero, JP, R van Grondelle
Physical Chemistry Chemical Physics 19 (7), 5195-5208. (2017).
- E. Romero, JP, et al., Rienk van Grondelle,
Scientific reports (2017).
- Elisabet Romero, et. al, Rienk Van Grondelle,
Nature physics 10 (9), 676-682.(2014).

J- Aggregates

- Lim, Palecek, Caycedo-Soler, Lincoln, JP, Berlepsch,
Huelga, Plenio, Zigmantas, Hauer, Nat. Comm. 6, 7755 (2015).

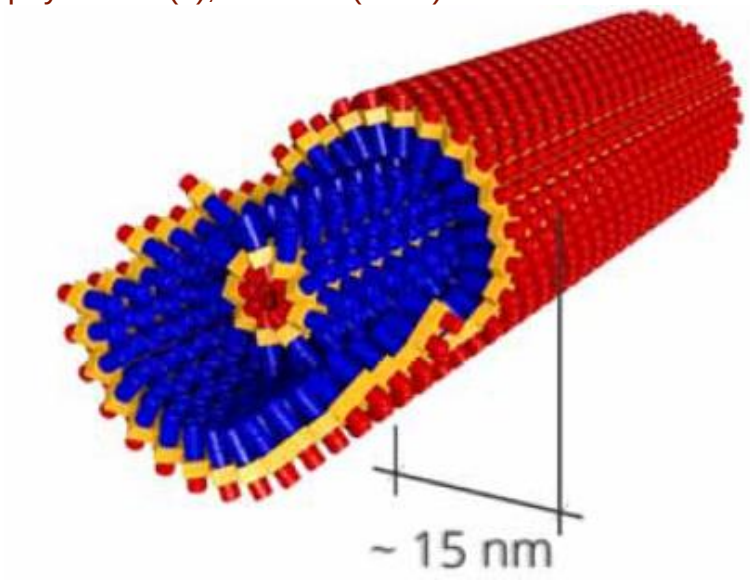

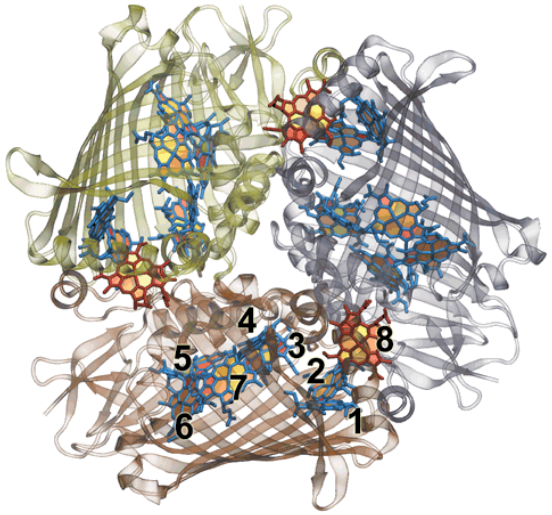

Fenna-Matthews-Olson complex

- A. Chin, JP, R. Rosenbach, F. Caycedo-Soler, S. Huelga and M.Plenio,
Nature Phys. 9, 113 (2013).

Photovoltaic solar cells

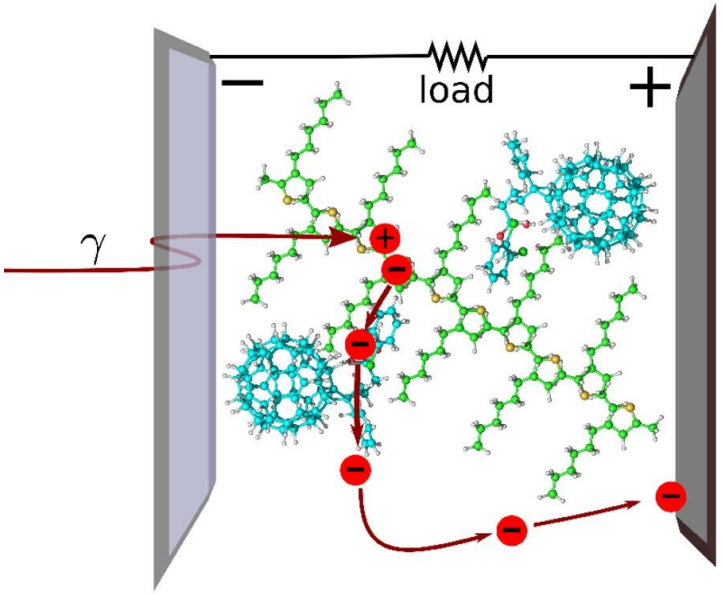

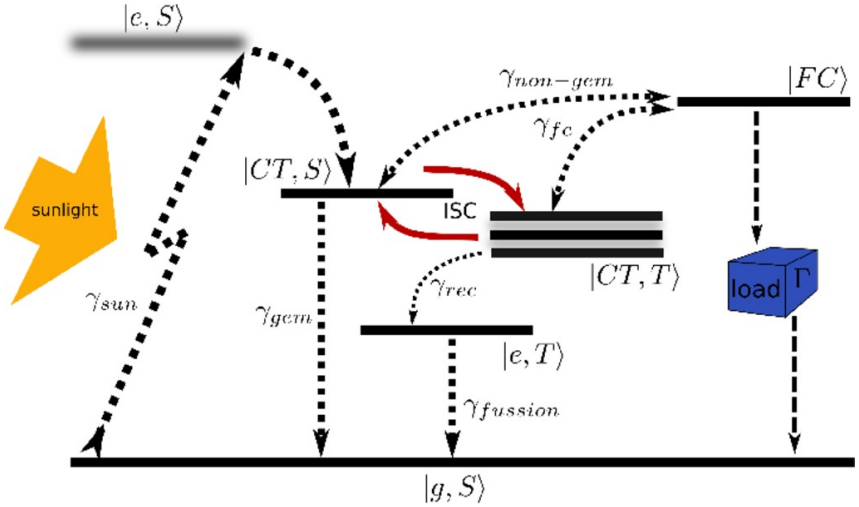

P3HT:PCBM solar cell

• S Oviedo-Casado, A Urbina, J P, Scientific reports (2017).

Green sulphur bacteria

Fenna-Matthews-Olsen complex (FMO)

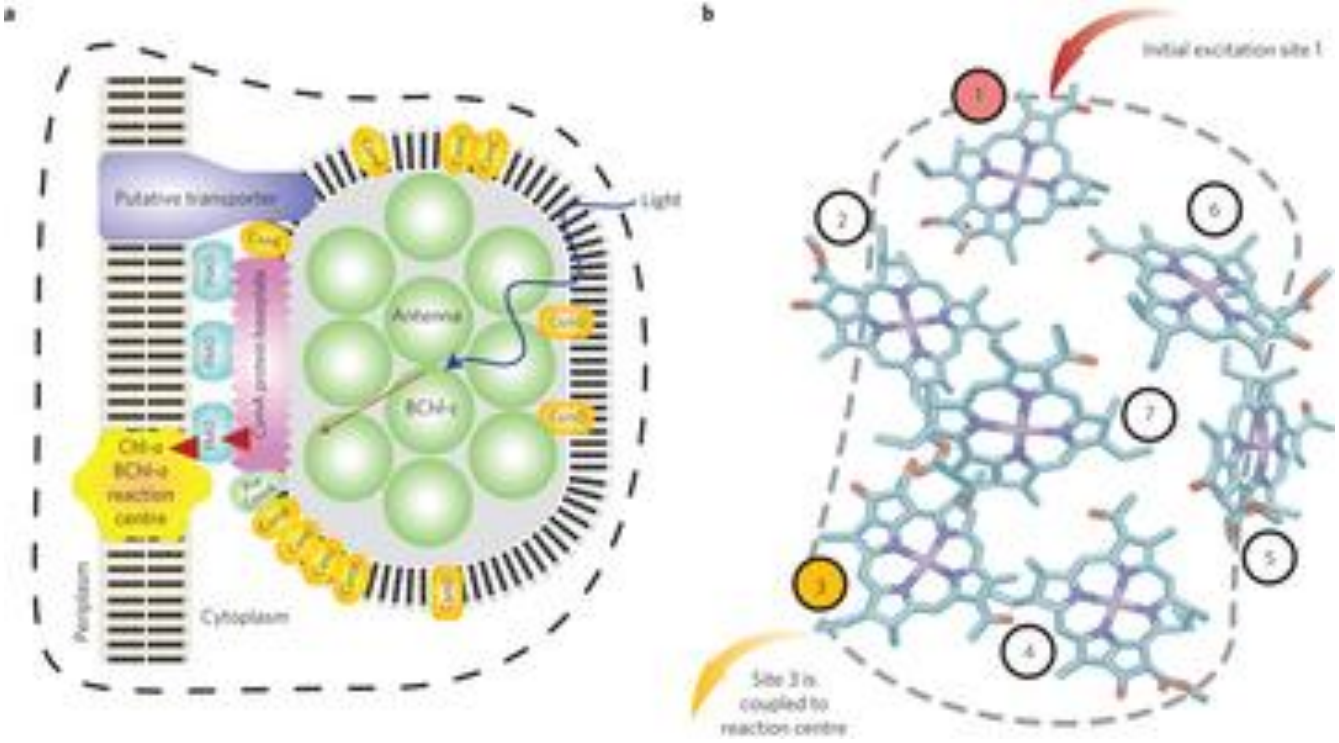

Exciton transport

Transport time ~ 5-6 ps

Long lived oscillatory features (*coherence)* in PPCs
A microscopic model and its associated spectral response

- A. Chin, JP, R. Rosenbach, F. Caycedo-Soler, S. Huelga and M.Plenio,
Nature Phys. 9, 113 (2013).

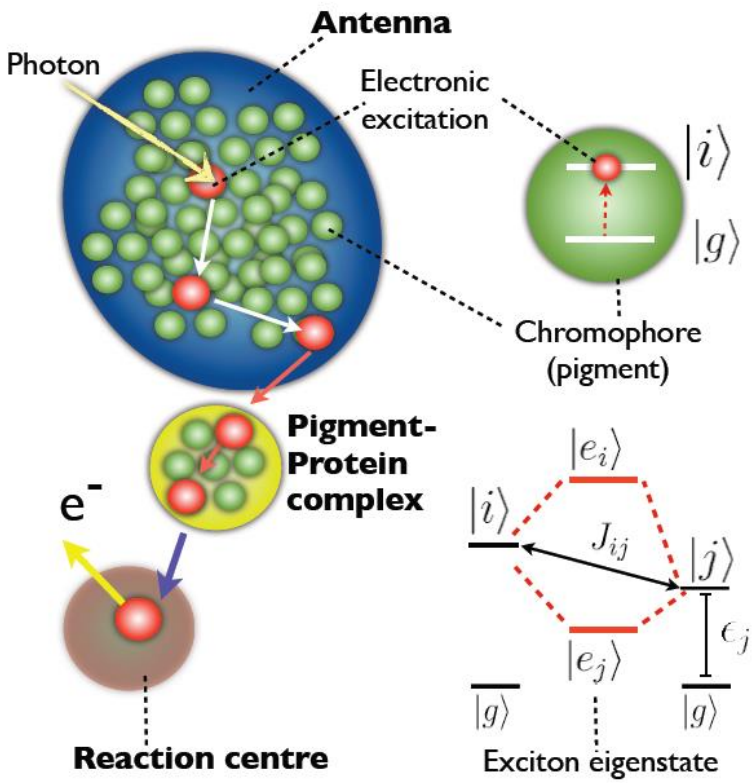

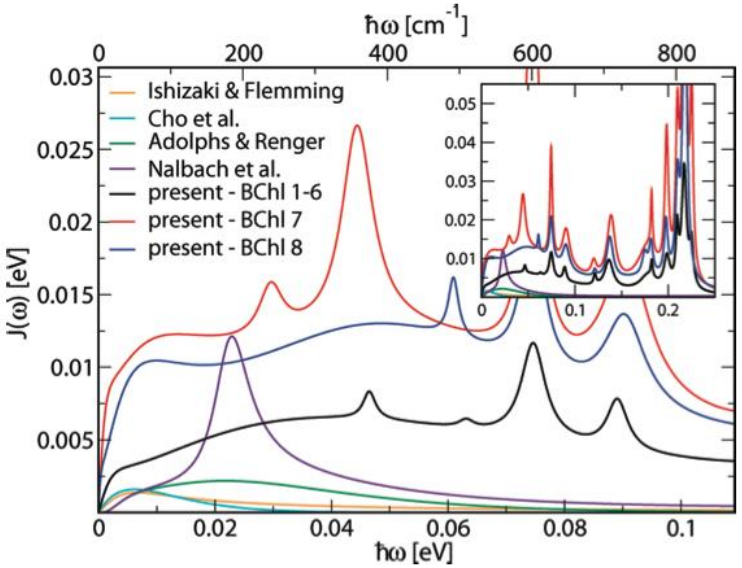

- Olbrich et al. J. Phys. Chem Lett. 2. 2011
Aspuru-Guzik et al J. Chem. Phys. 137, 224103 (2012)

SYSTEM **ENVIRONMENT**

Dealing with highly structured environments
Efficient exact simulation of many body systems (TEDOPA)

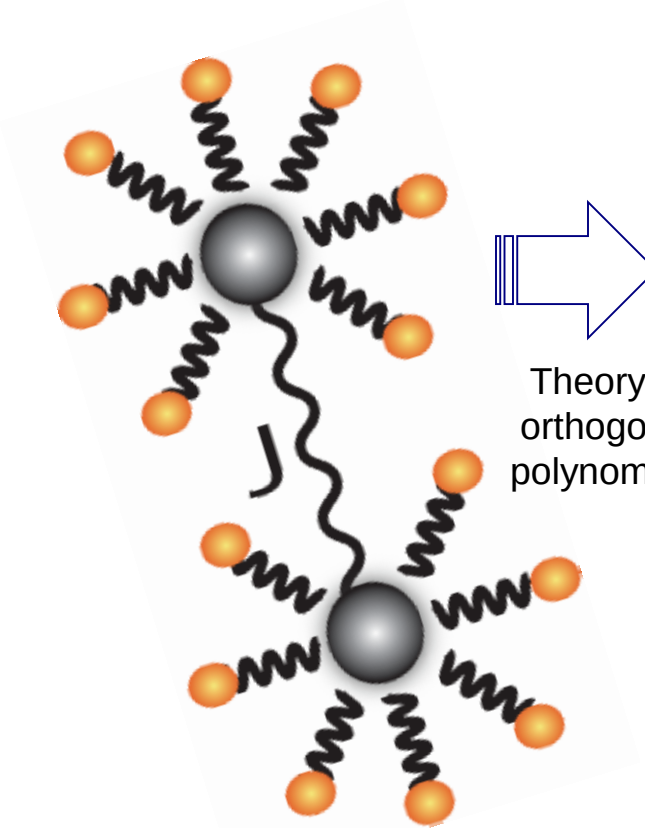

Theory of orthogonal polynomials

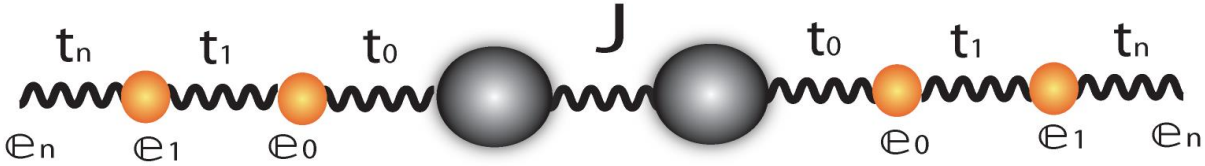

$$J(\omega) = \frac{2\pi\lambda[1000\omega^5 e^{-(\omega/\omega_1)(1/2)} + 4.3\omega^5 e^{-(\omega/\omega_2)(1/2)}]}{9!(1000\omega_1^5 + 4.3\omega_2^5)} + 4\pi S_H \omega_H^2 \delta(\omega - \omega_H),$$

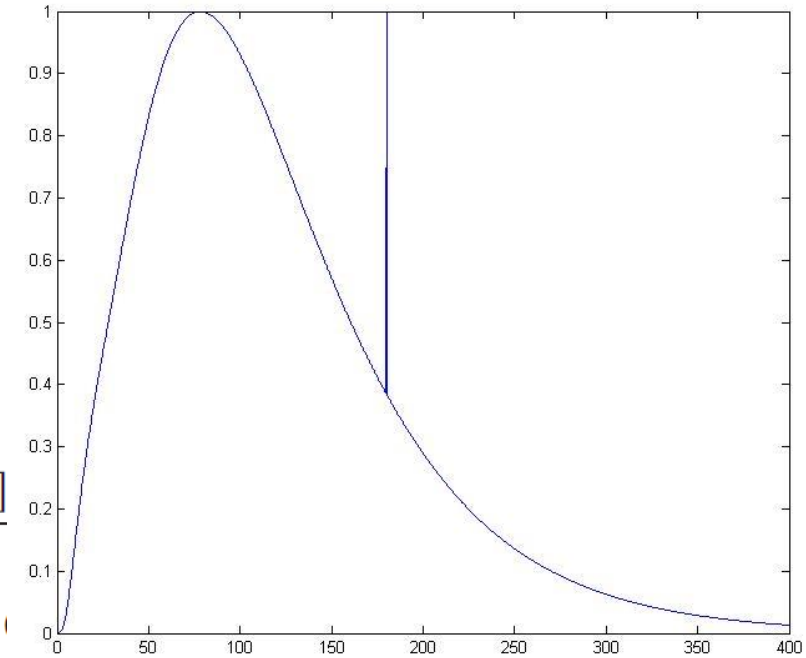

- J. Adolphs and T. Renger, Biophysical Journal 91, 2778 (2006)

- Prior, Chin, Huelga, Plenio, PRL 2010
- Rosenbach, Prior, Chin, Huelga, Plenio, 2011

TEDOPA in action. Exact simulation at T=77k

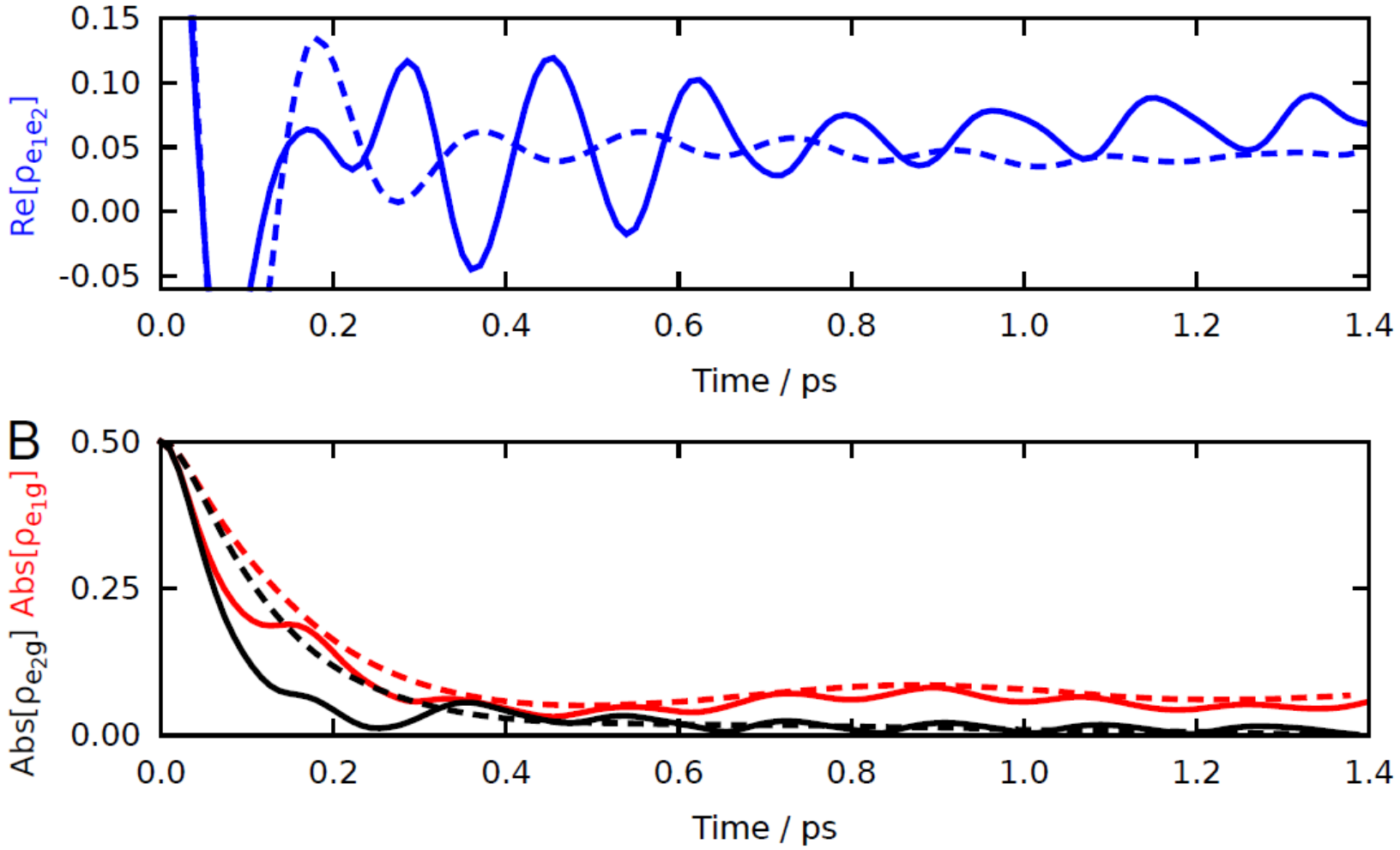

TEDOPA – Long lived coherence at 277k

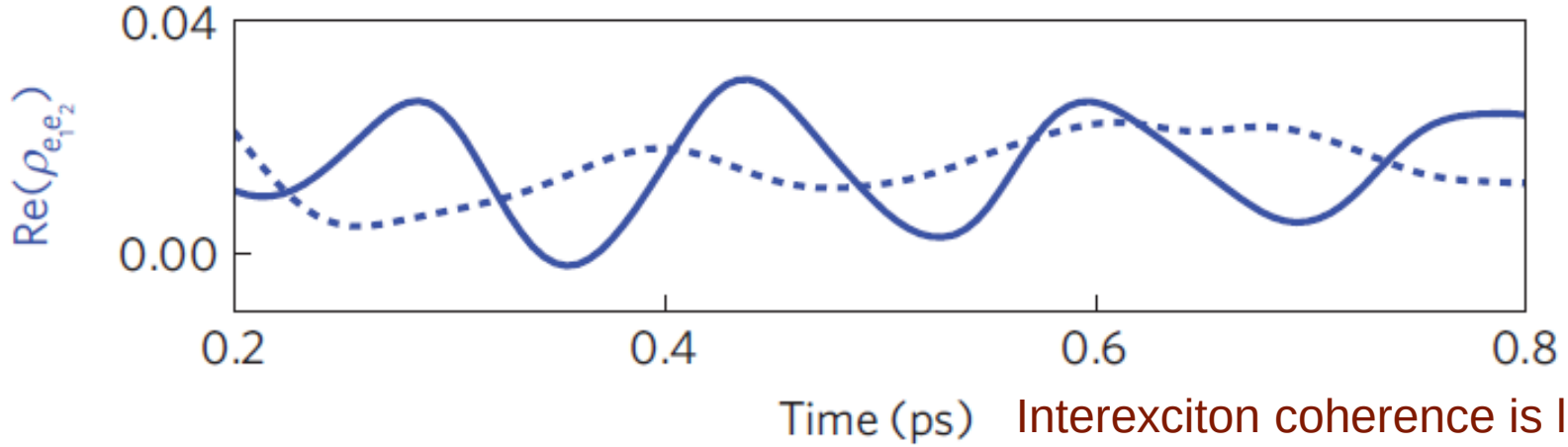

Interexciton coherence is long lived

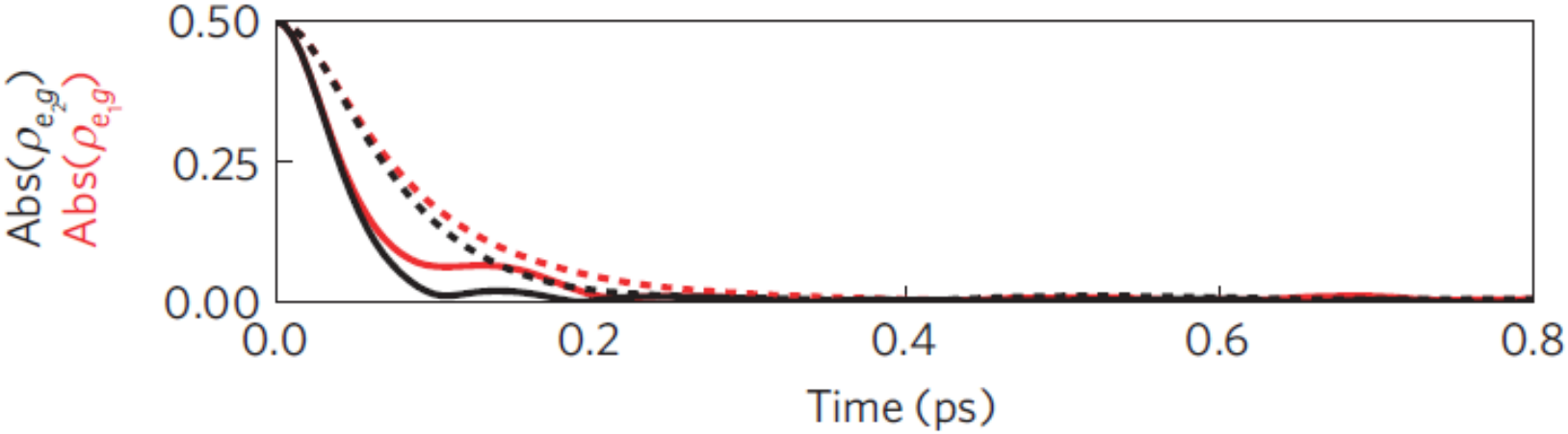

- - - - Without 180^{-1}cm mode
------ Without 180^{-1}cm mode

Ground-excited state coherence vanishes rapidly

• A. Chin, JP, R. Rosenbach, F. Caycedo-Soler, S. Huelga and M. Plenio, Nature Phys. 9, 113 (2013).

2D spectroscopy

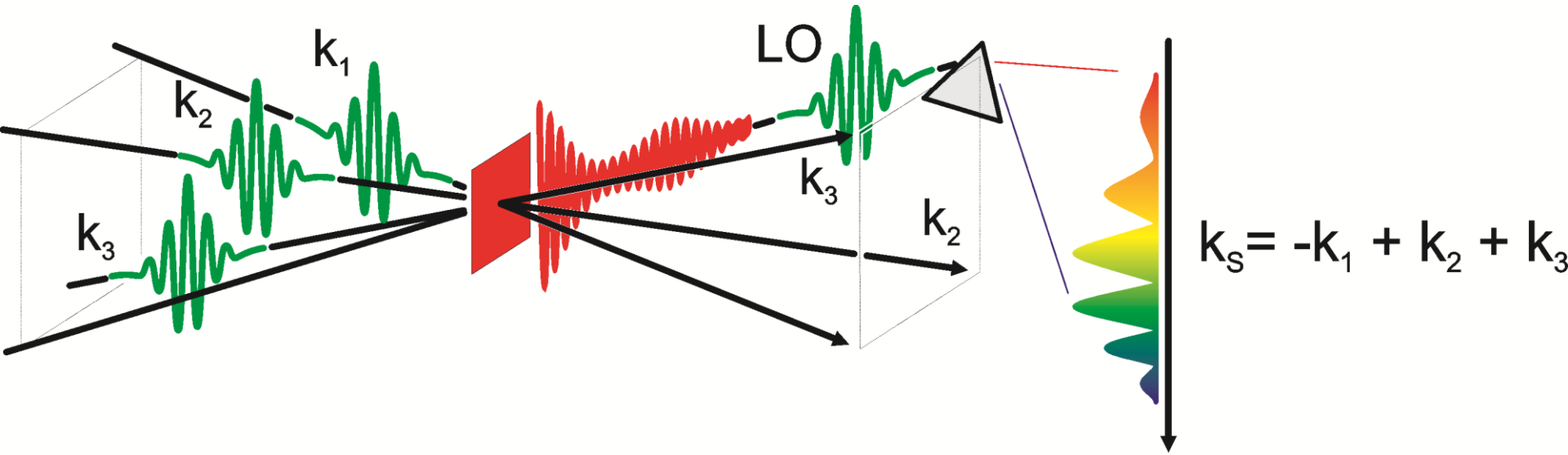

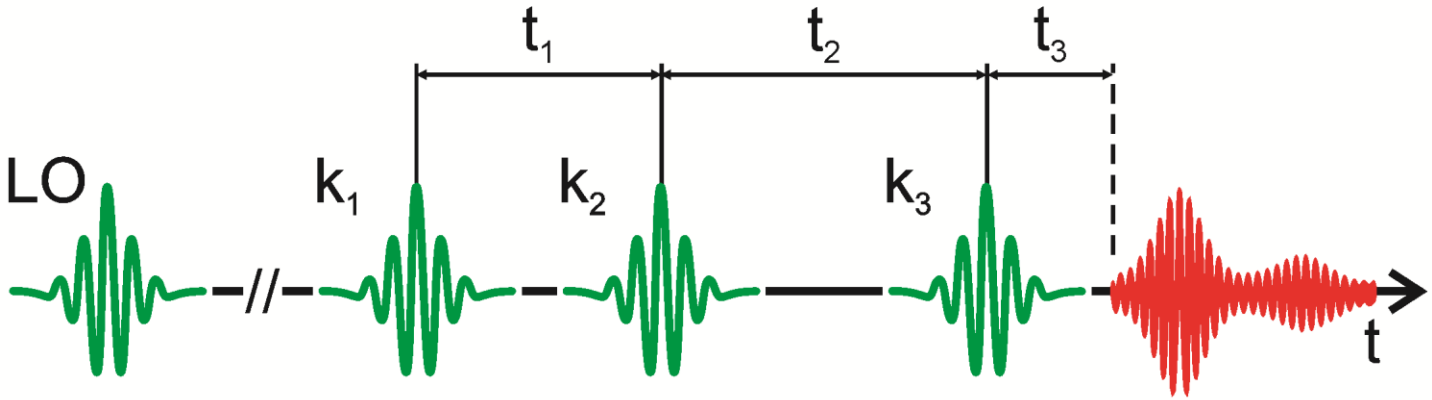

Schematic 2D signals

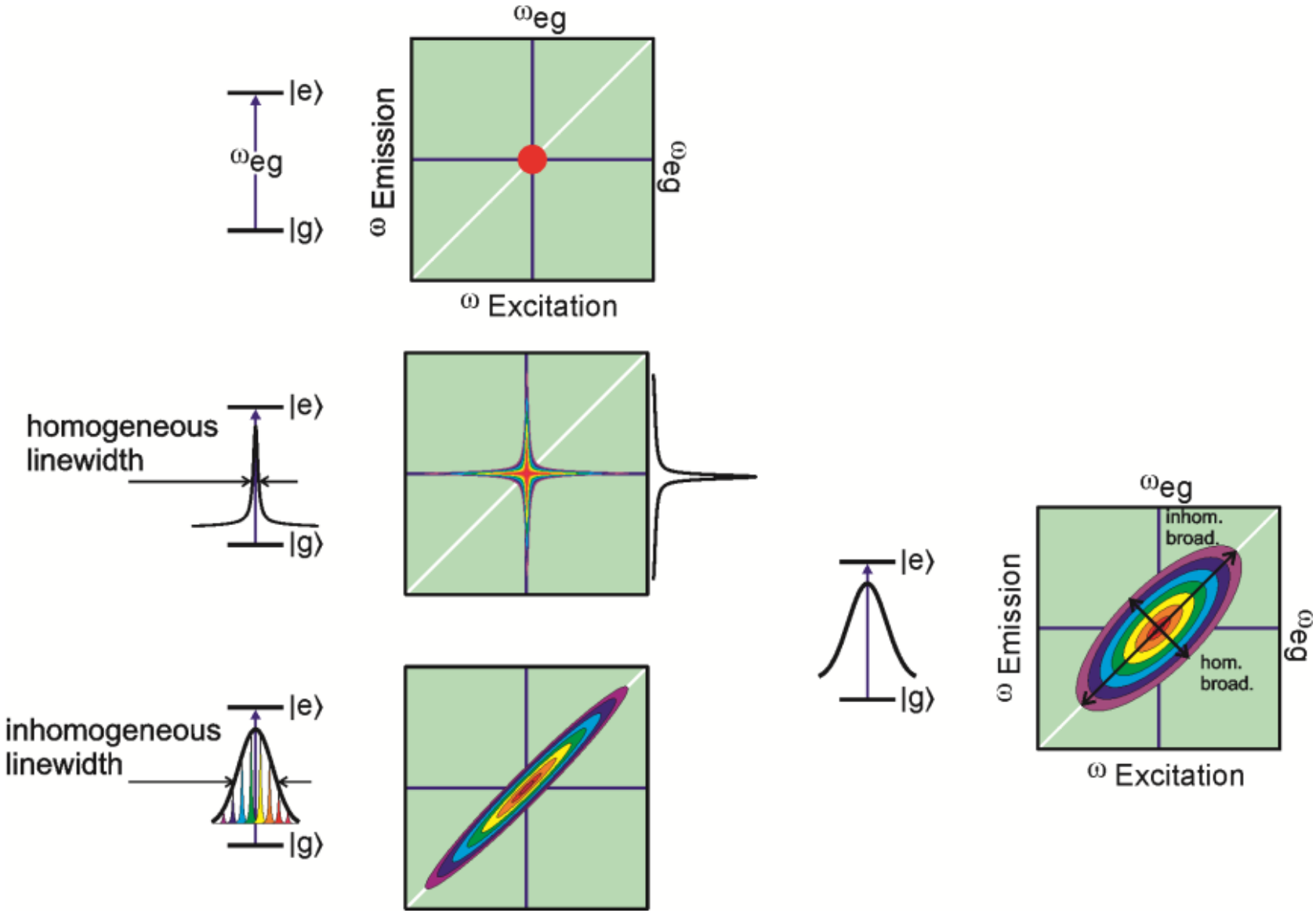

Schematic 2D signals

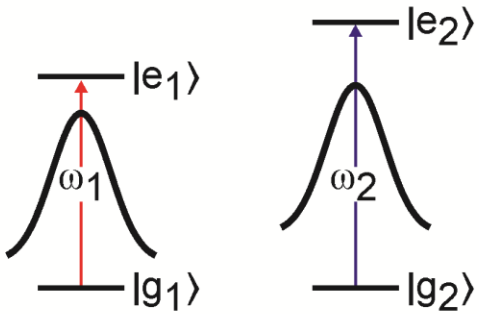

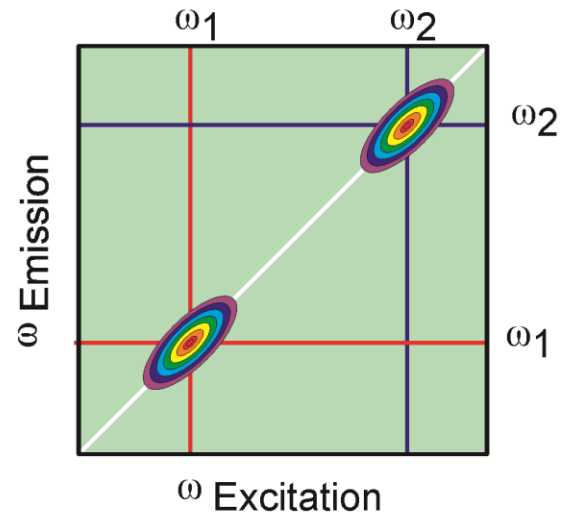

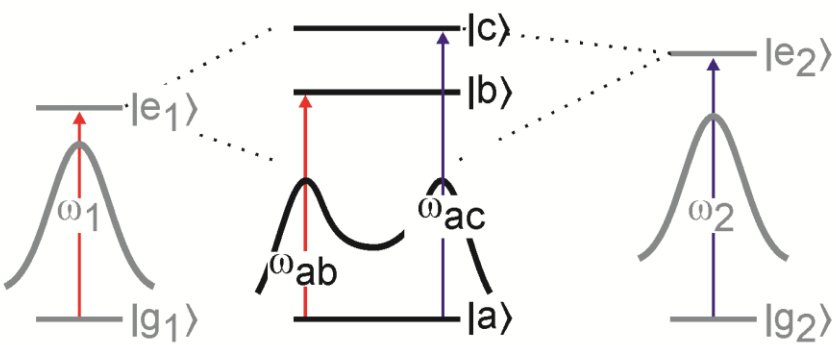

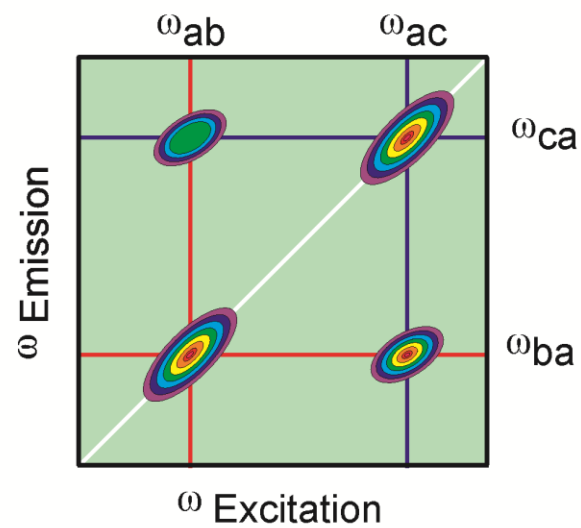

Electronic 2D-spectroscopy

Stimulated Emission

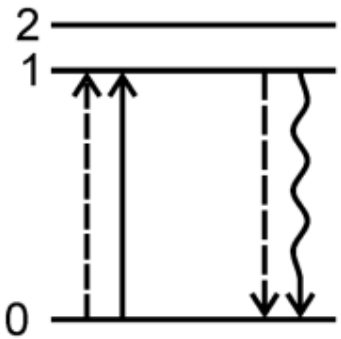

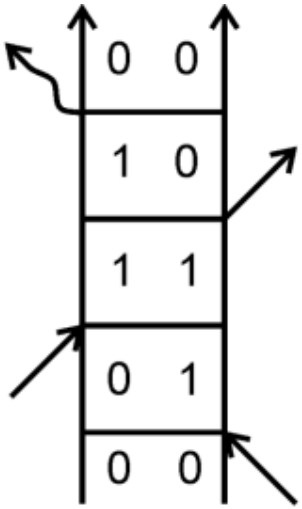

Excitonic Coherence

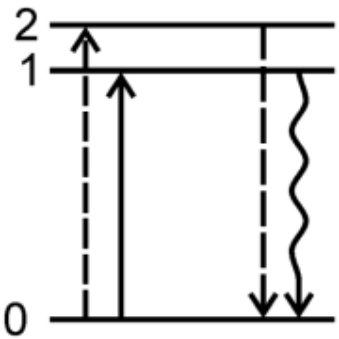

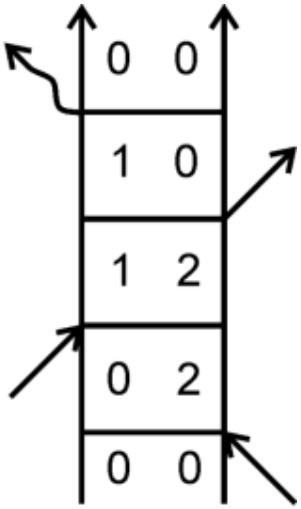

Ground State Bleach

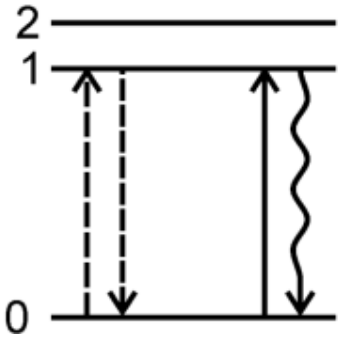

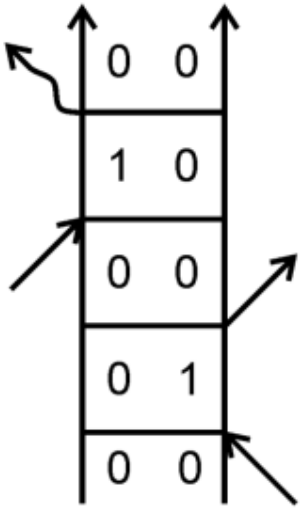

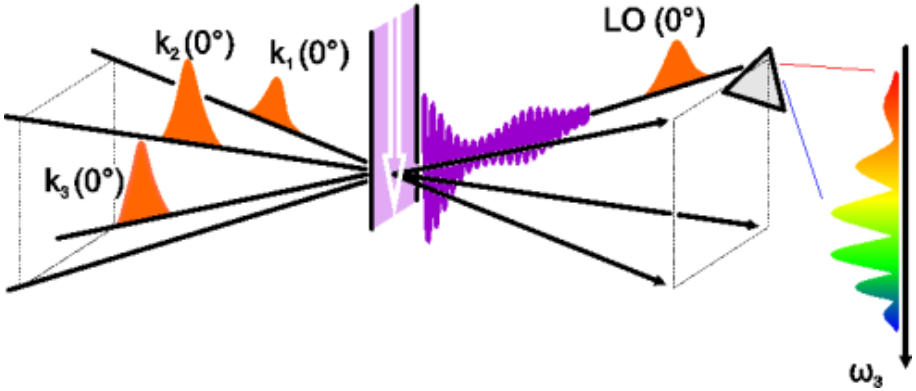

Types of coherences

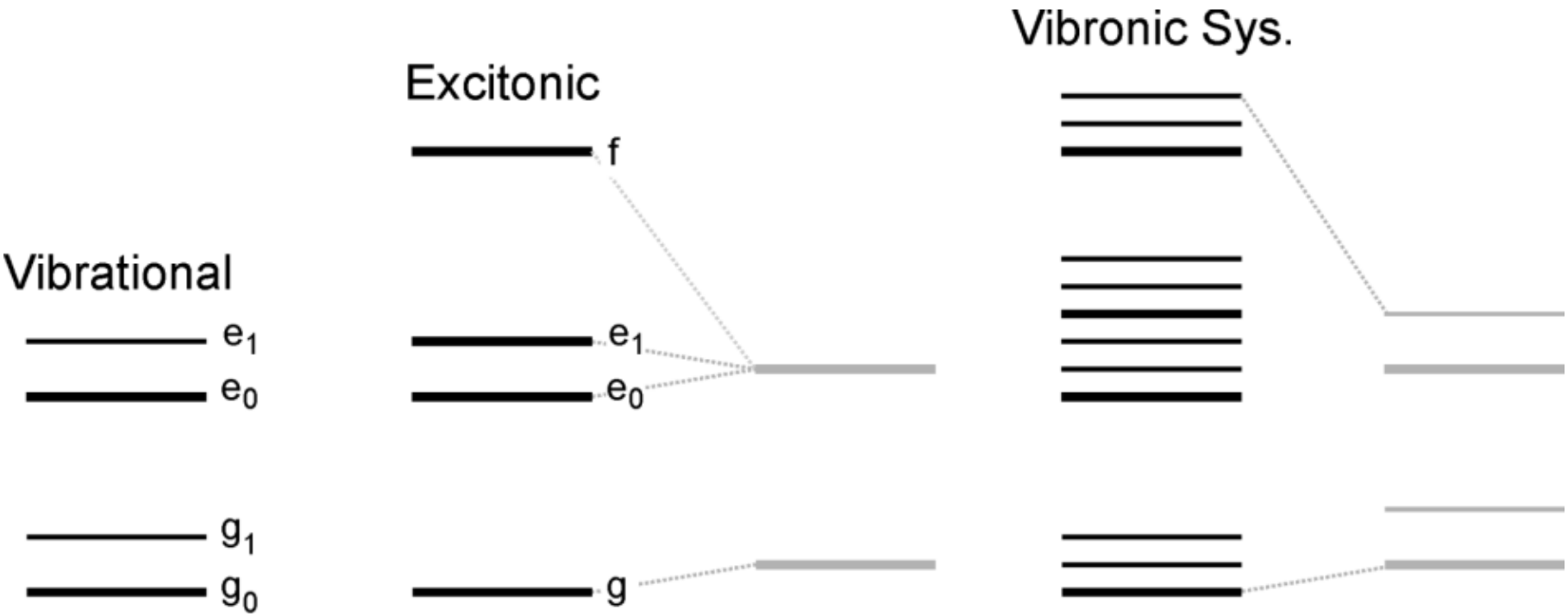

- An excitonic system and an electronic two-level-system with vibrational levels share many excitation pathways.
- It is a challenging problem to distinguish them

Fourier transform: From population time to frequency

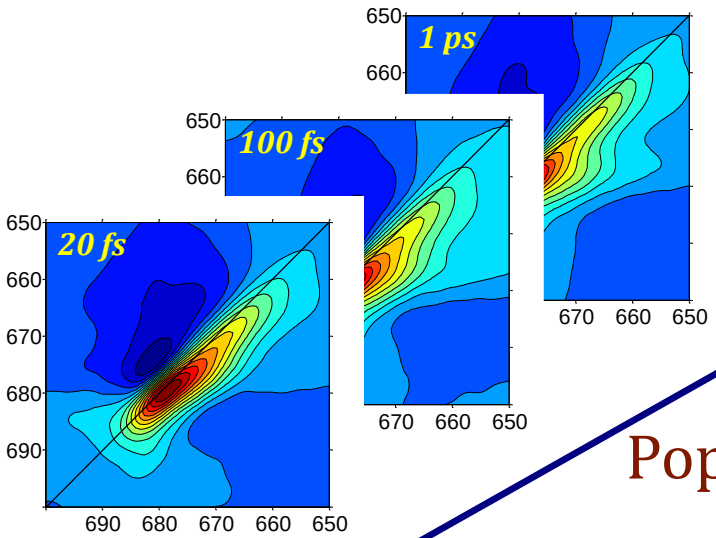

2D spectra
All absorbing and emitting states

Population Time, **T**

2D frequency maps
Only the states oscillating at certain frequency

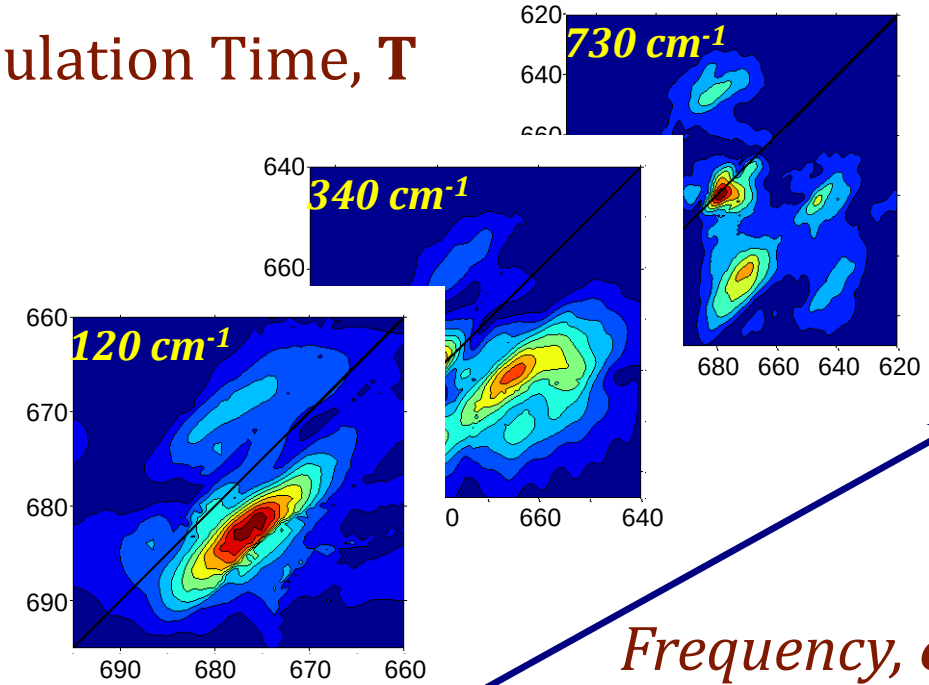

Fourier Transform

Frequency, $\boldsymbol{\omega_T}$

C803-a molecular J-aggregate

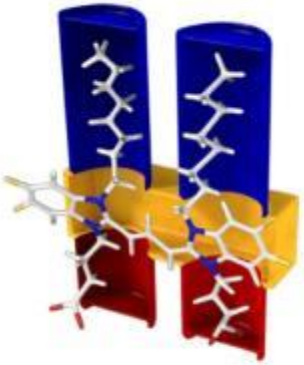

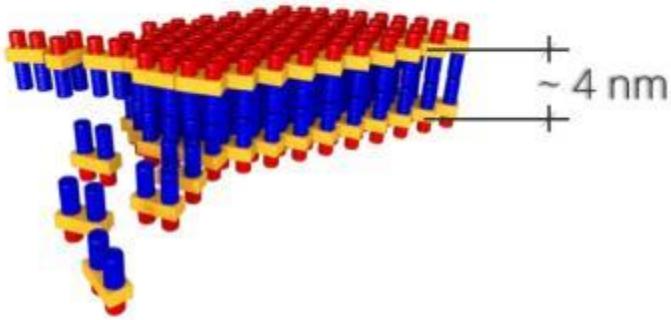

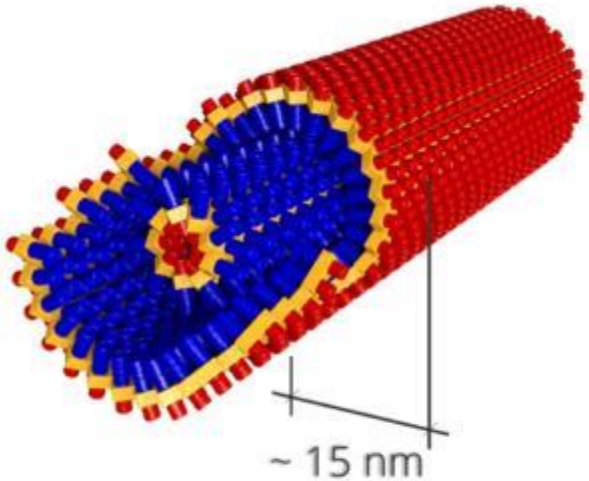

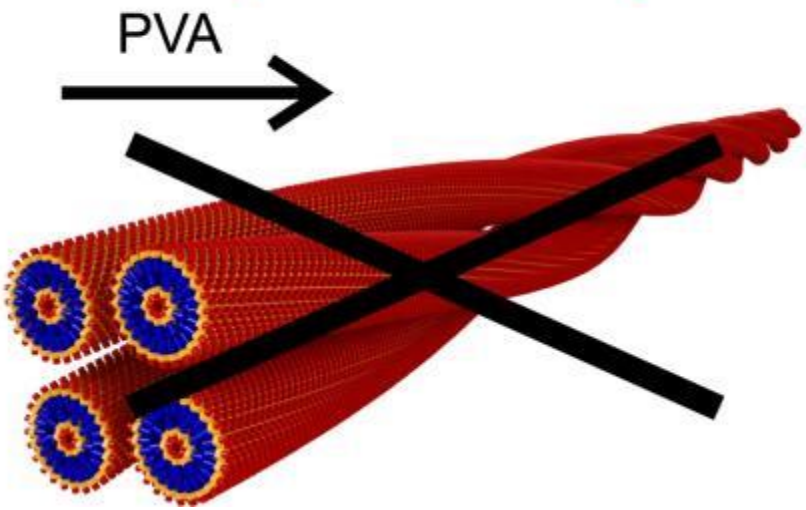

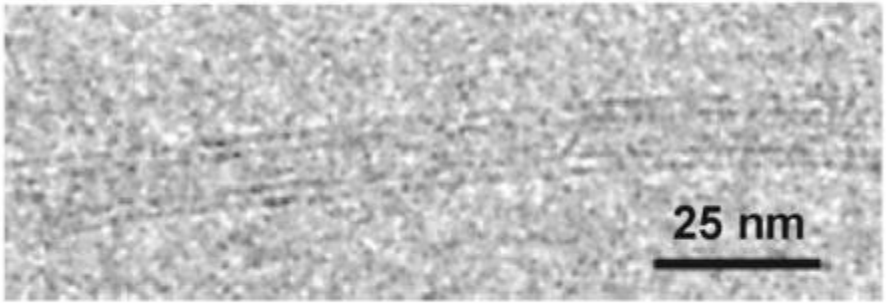

from von Berlepsch et al. J. Phys. Chem. B 2003, **107**, 14176

- Addition of Polyvinyl alcohol (PVA) prevents formation of super-helices
- In this aligned tubular system, polarization controlled 2D spectroscopy delivers an uncongested and specific optical response.

Aggregates show macroscopic orientation

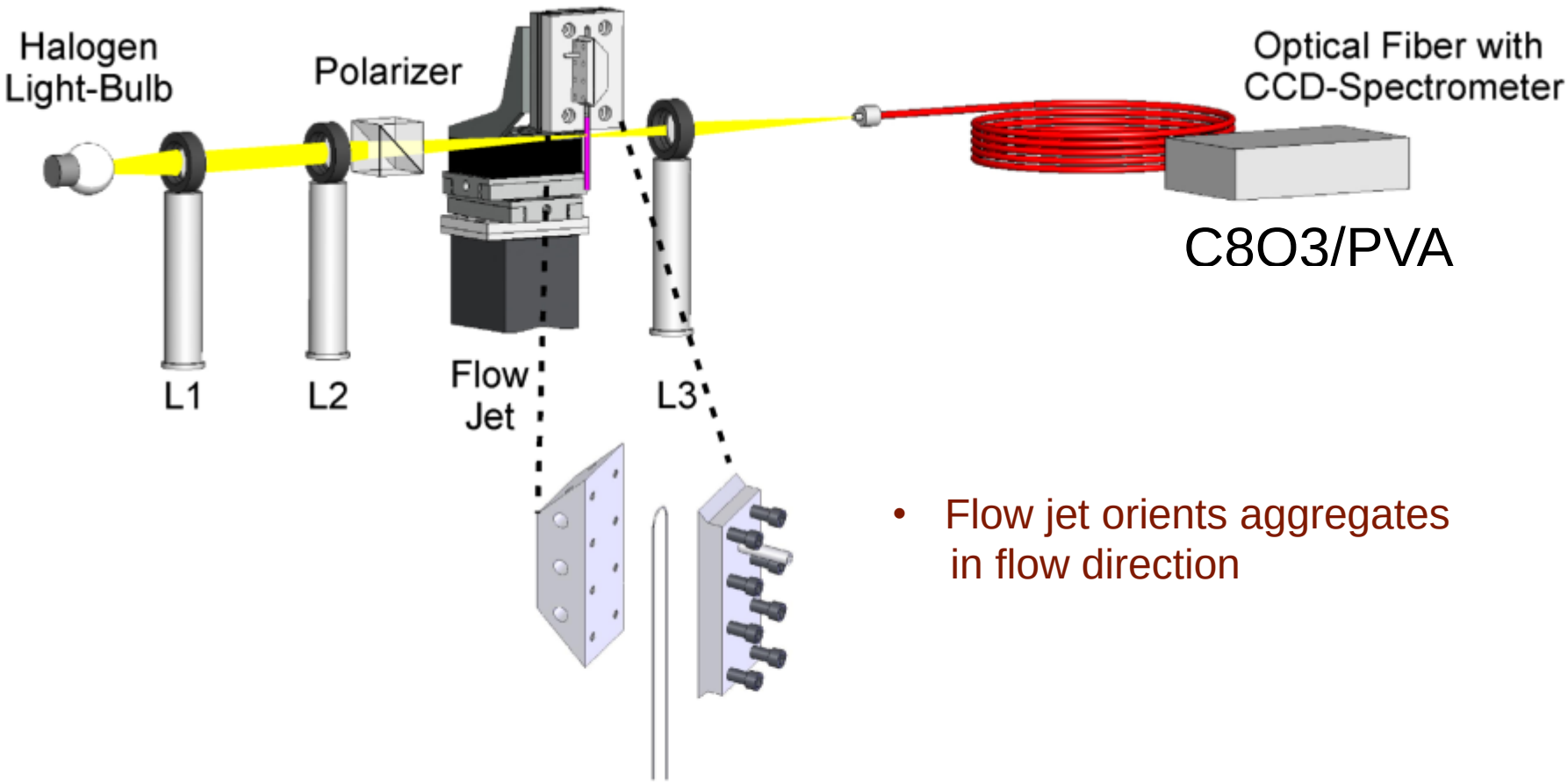

- Flow jet orients aggregates in flow direction

A transparent illustration of the proposed mechanism: J-aggregates

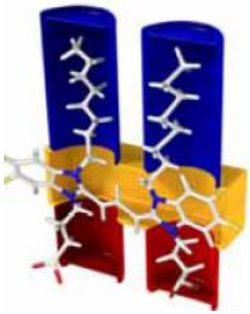

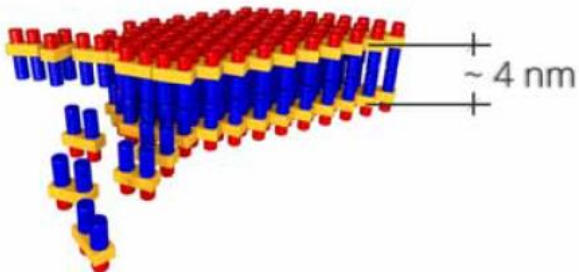

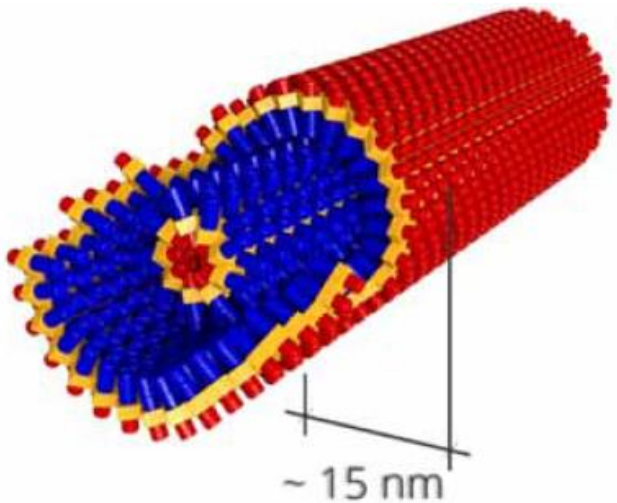

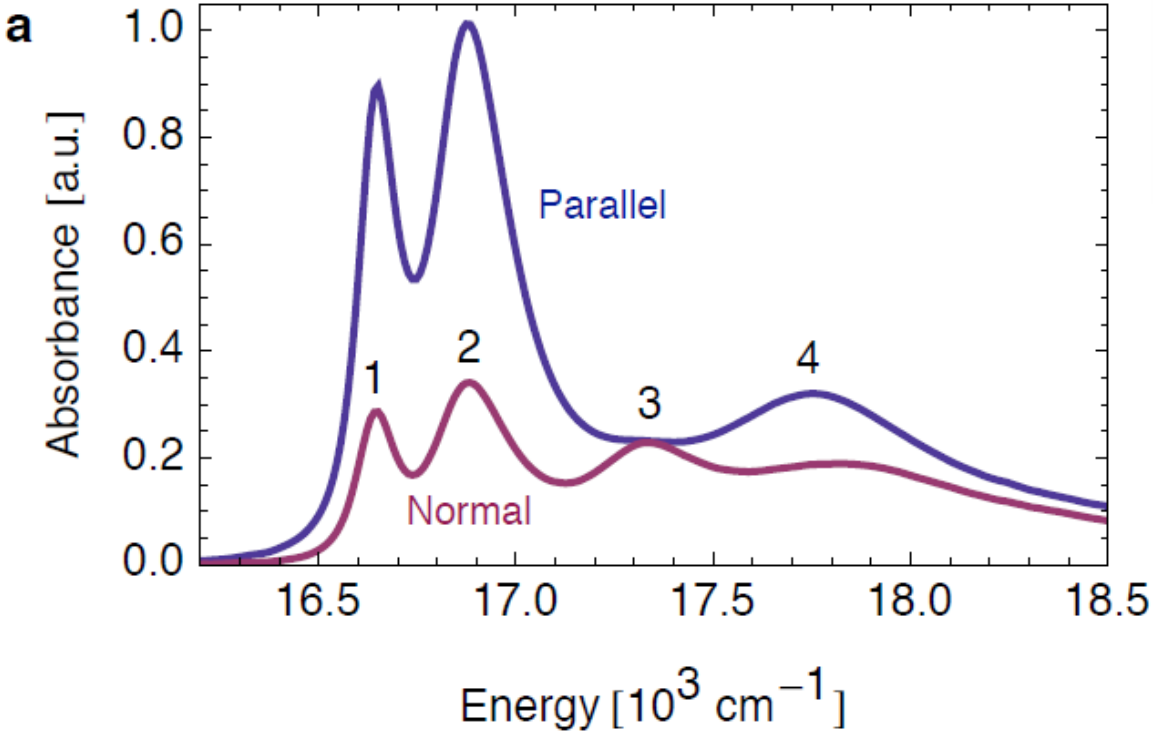

A transparent illustration of the proposed mechanism: J-aggregates

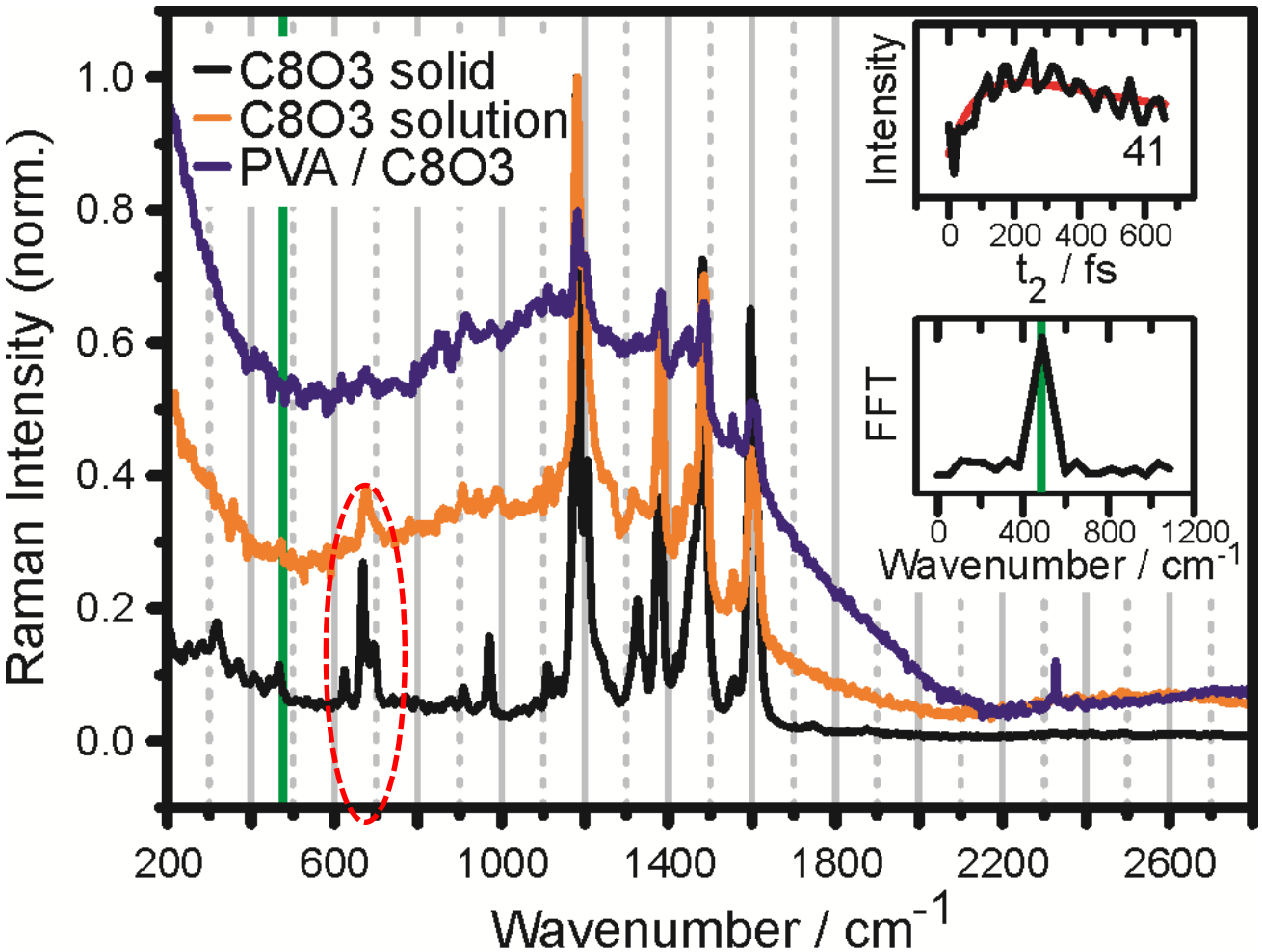

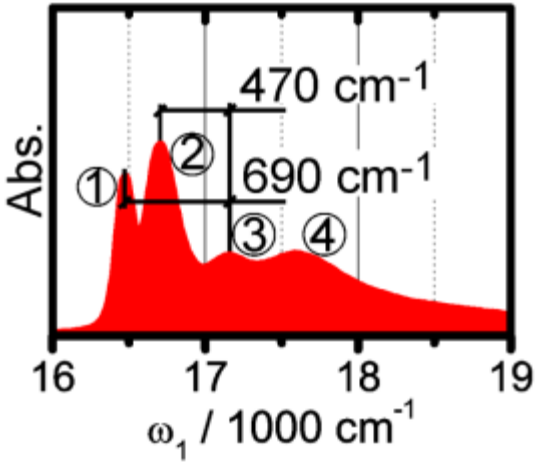

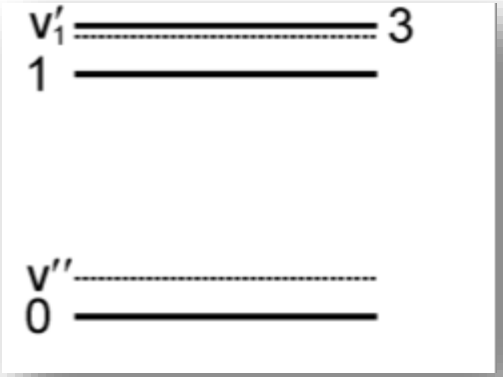

From F, Milota, V. I. Prokhorenko, T. Mancal, H. von Berlepsch, O. Bixner, H. F. Kauffmann, J. Hauer, “Vibronic and Vibrational Coherences in Two-Dimensional Electronic Spectra of Supramolecular J-Aggregates”. *JPCA* **2013**, *117*, 6007.

Electronic 2D-spectroscopy
All parallel pulses

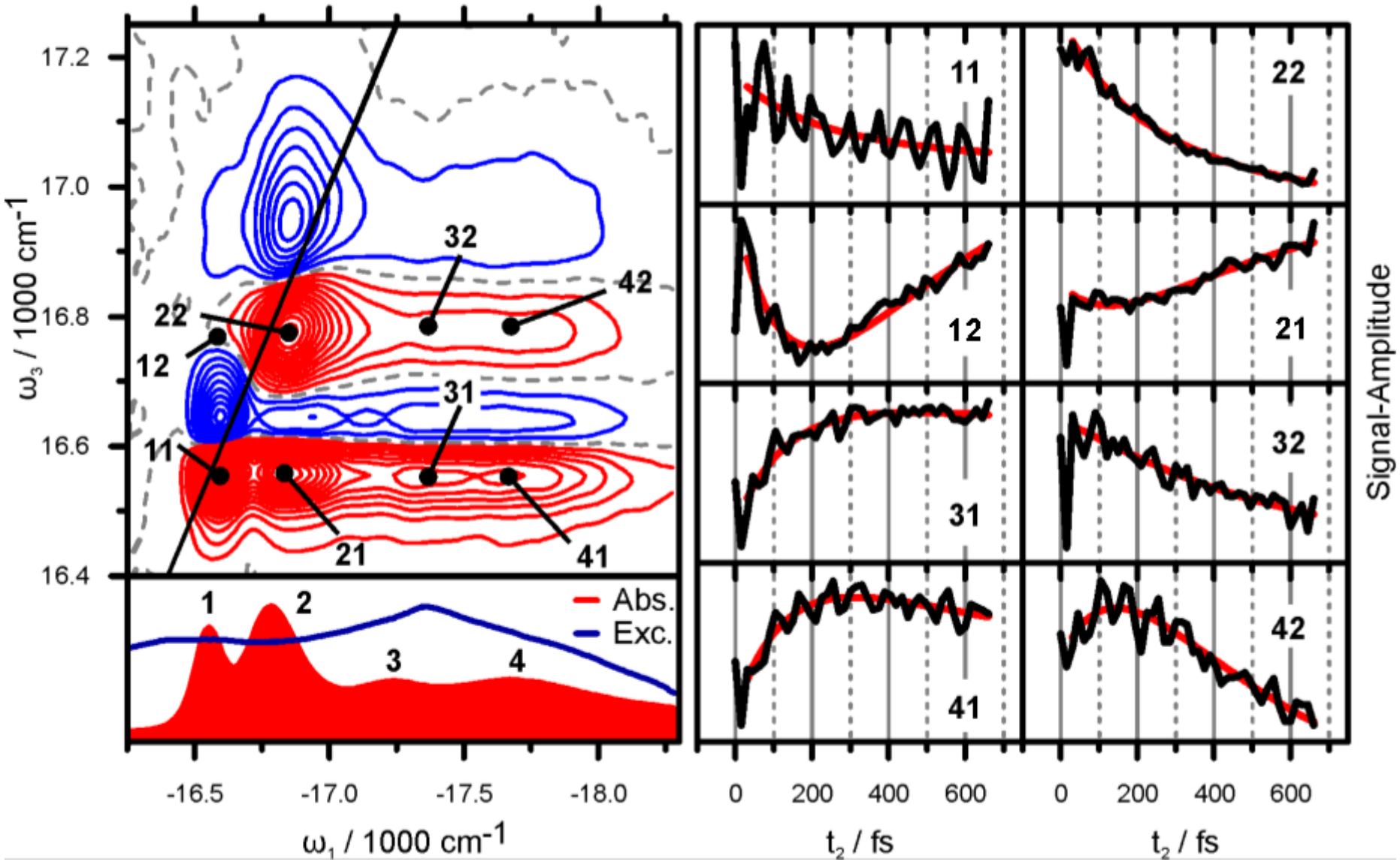

Electronic 2D-spectroscopy
All parallel pulses

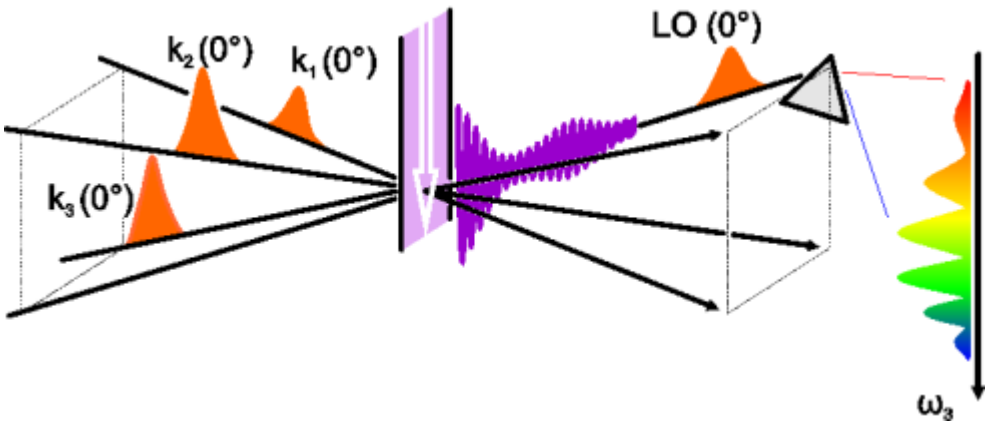

90-0-90-0 electronic 2D-spectroscopy excitation

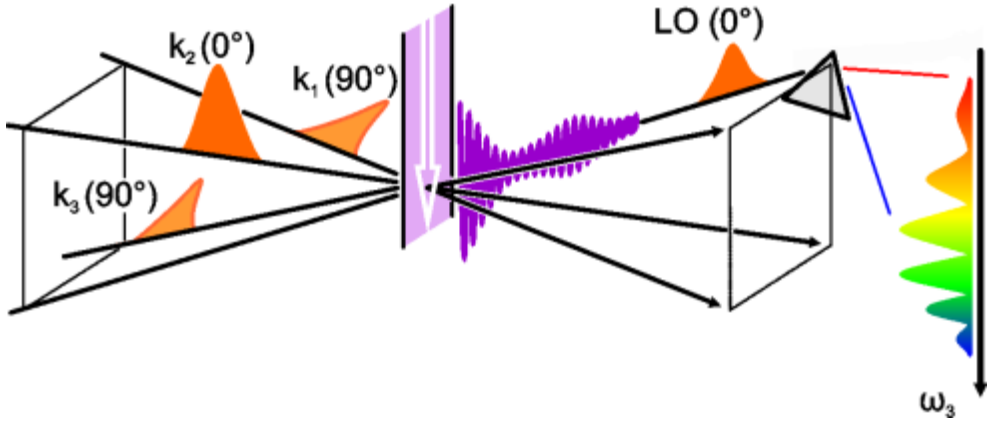

Electronic 2D-spectroscopy

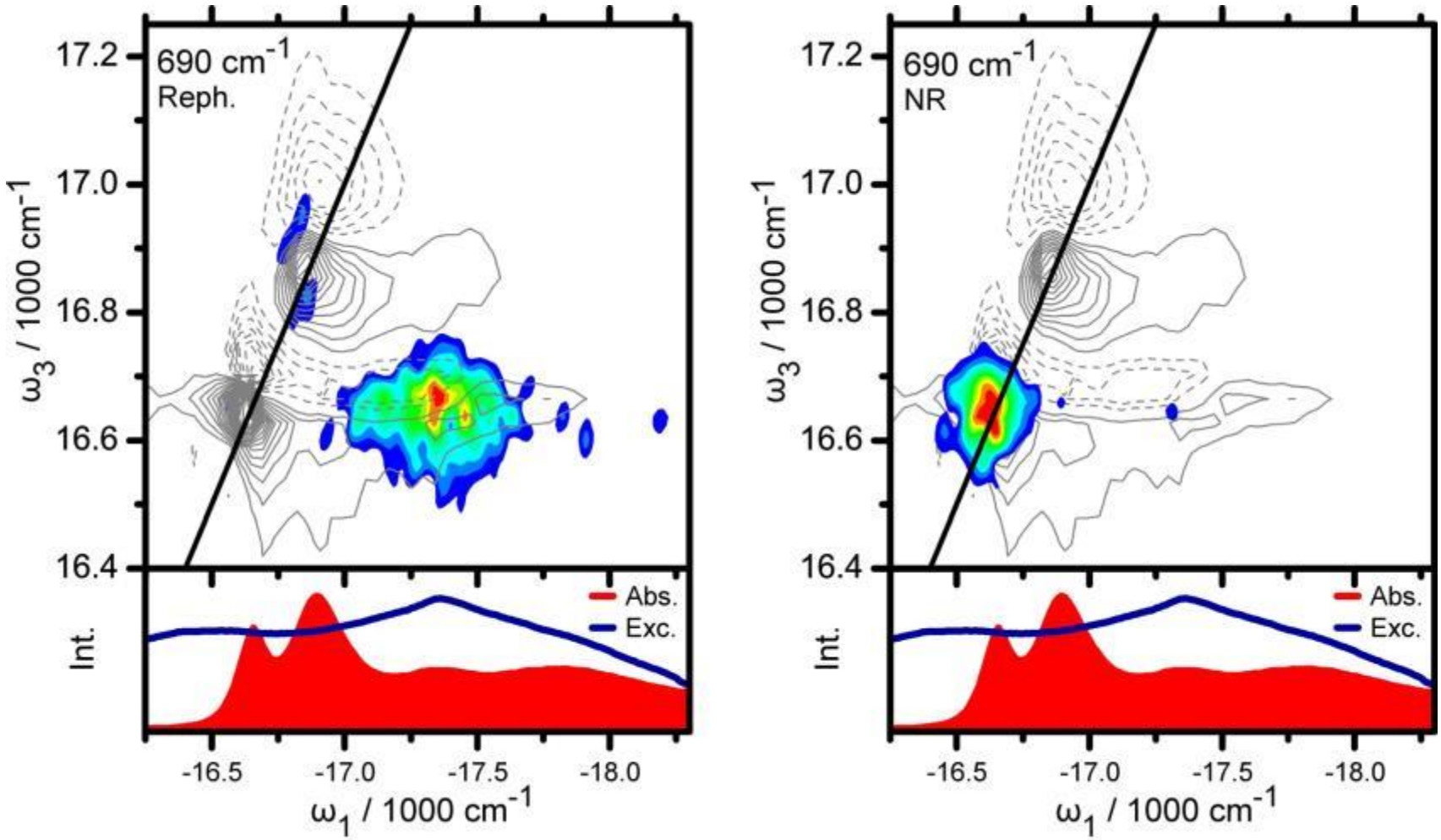

- Polarization-rotated 2D spectroscopy supresses population transfer pathways
- The FFT-amplitude pattern suggests **excitonic** (electronic) **coherence**

Electronic 2D-spectroscopy. 90-0-90-0 excitation

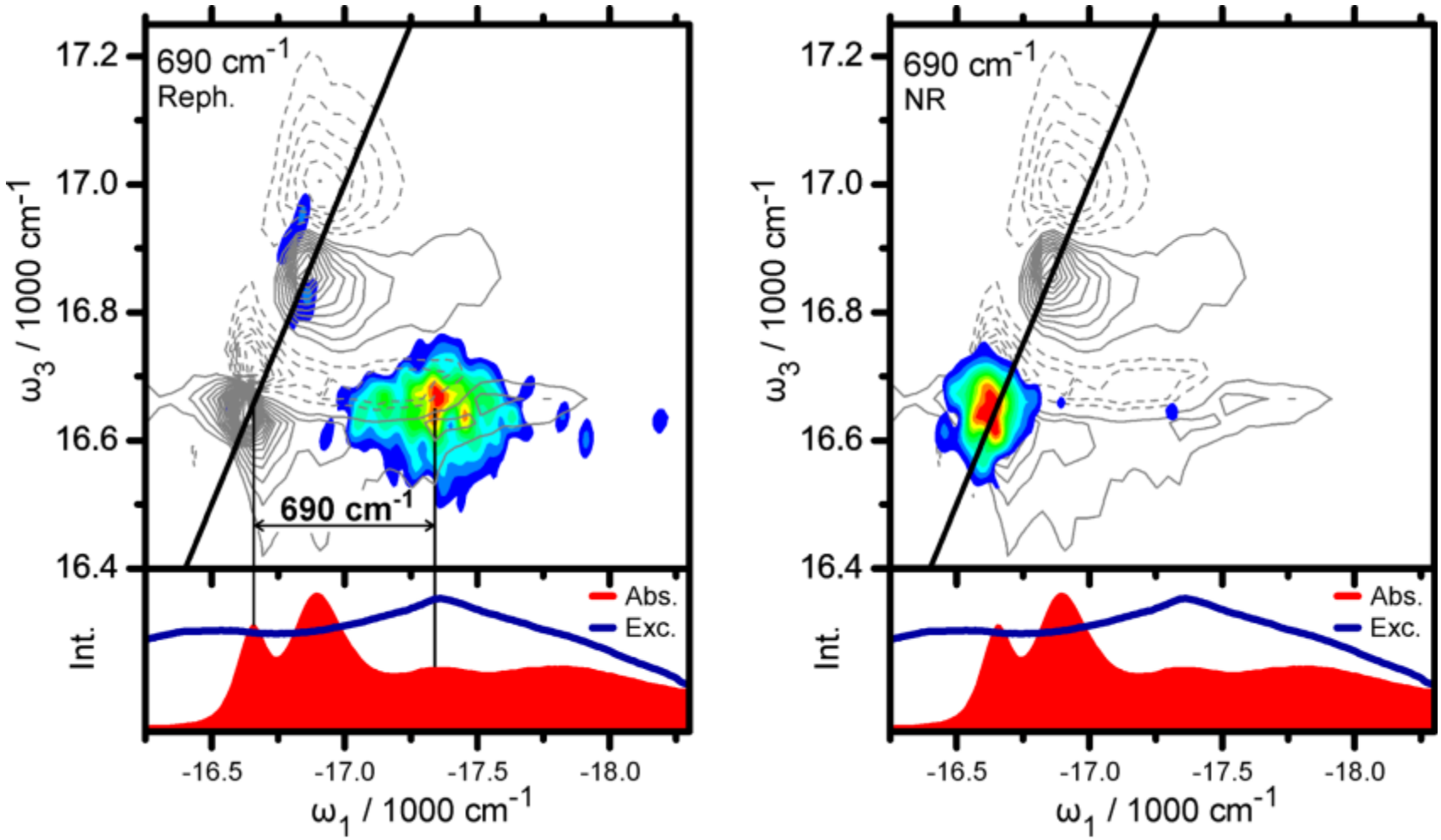

- Polarization-rotated 2D spectroscopy supresses population transfer pathways
- The oscillation frequency matches the energy spacing in the absorption spectrum!

2D signal from J-aggregates of cyanine dyes

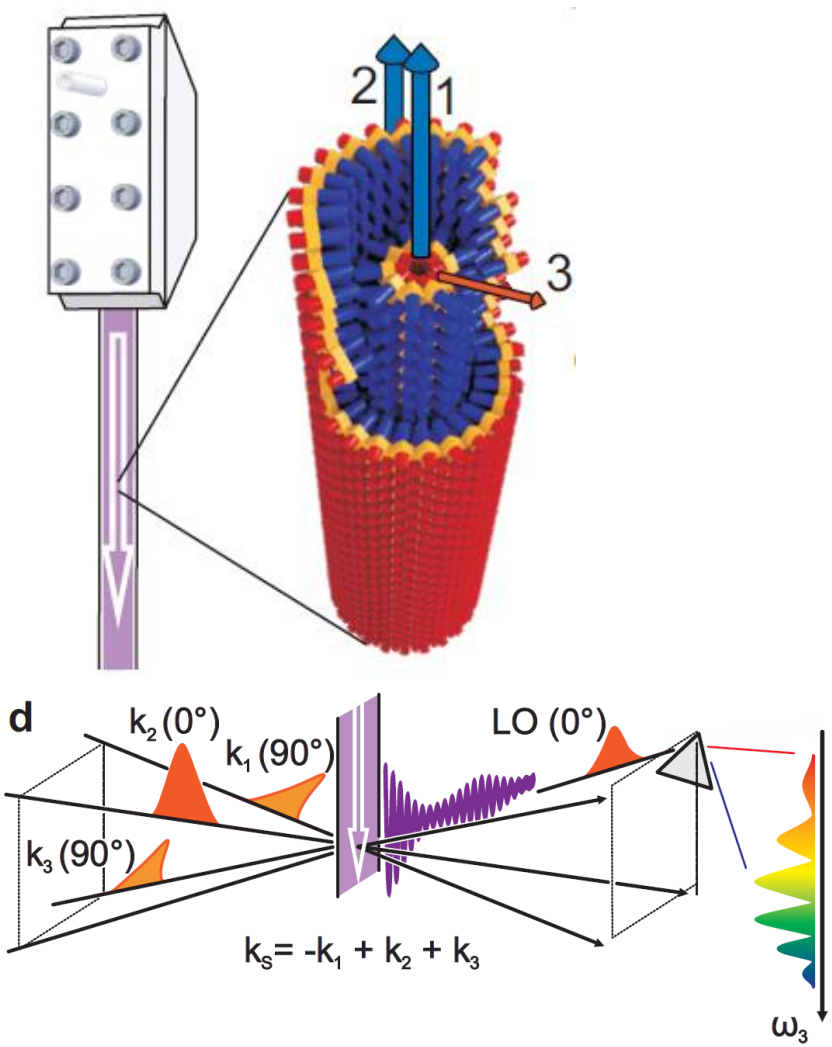

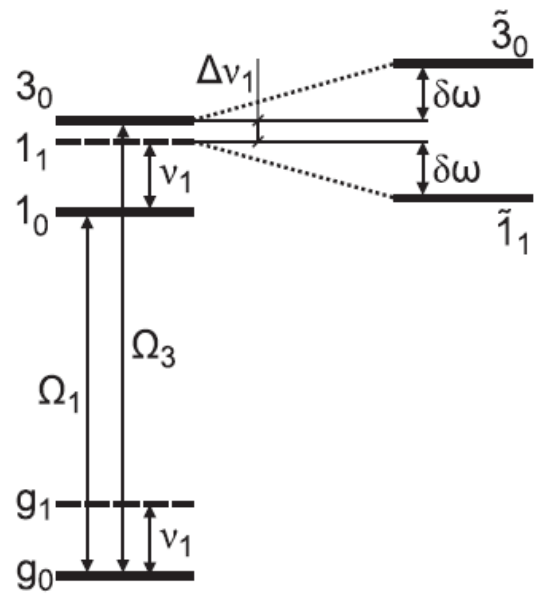

Experimental results

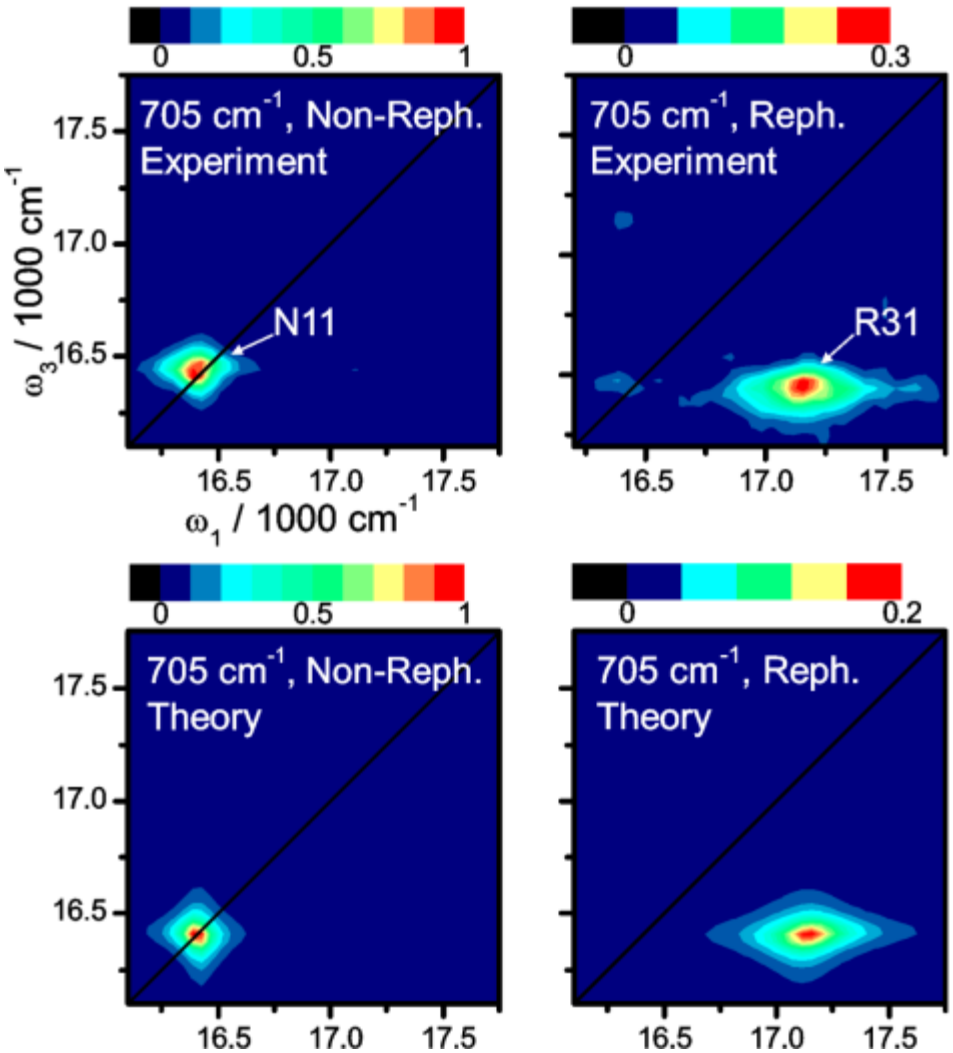

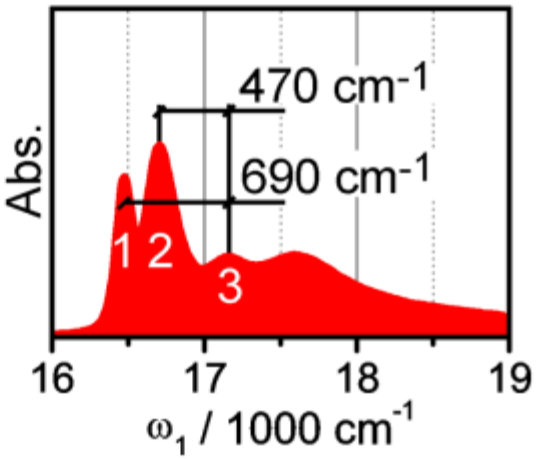

2D signal from J-aggregates of cyanine dyes

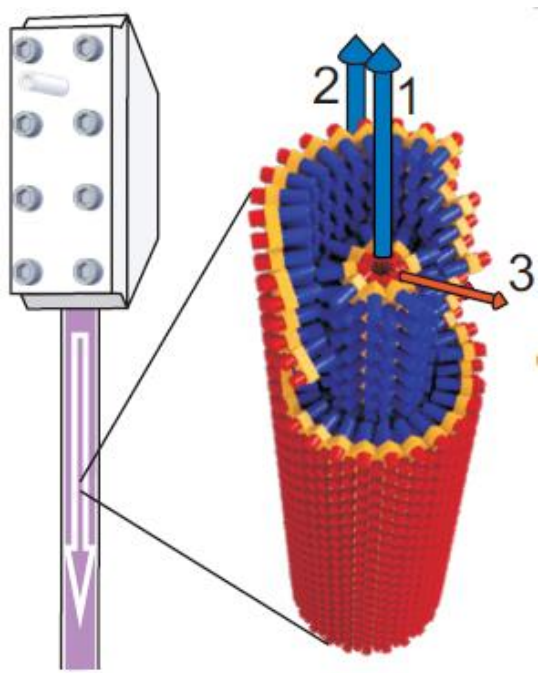

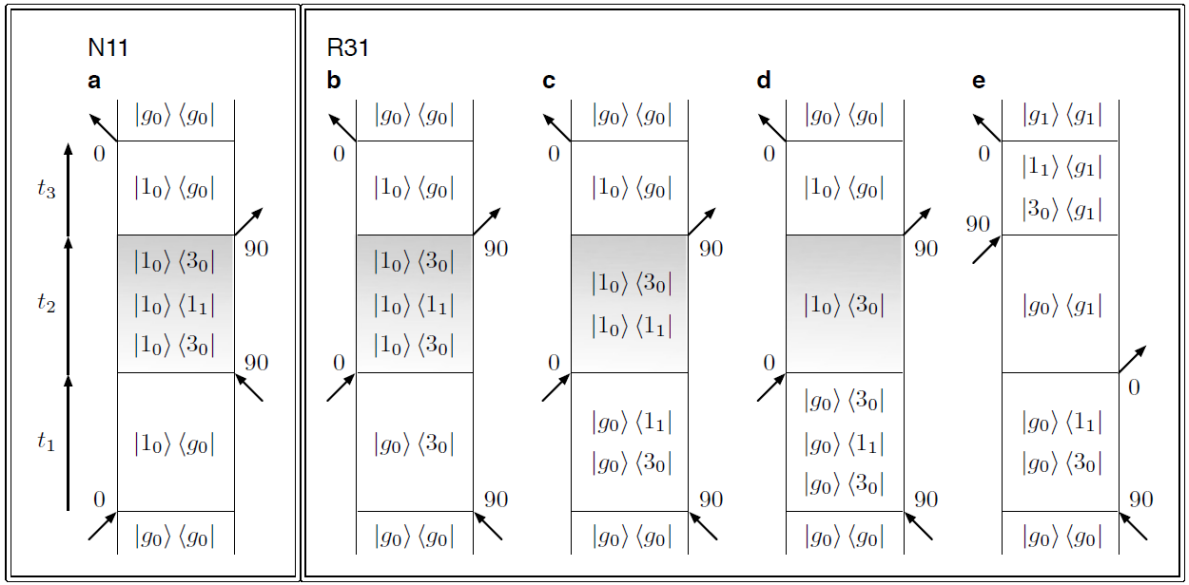

Non-rephasing:

vibronic

Rephasing:

vibronic and vibrational

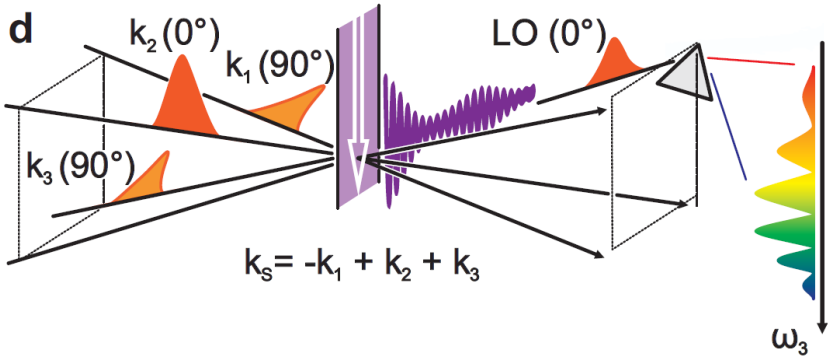

Comparison of non-rephasing and rephasing signals

Differentiate effects of ground state vibration and excited state vibronic coupling !

Feynman diagrams

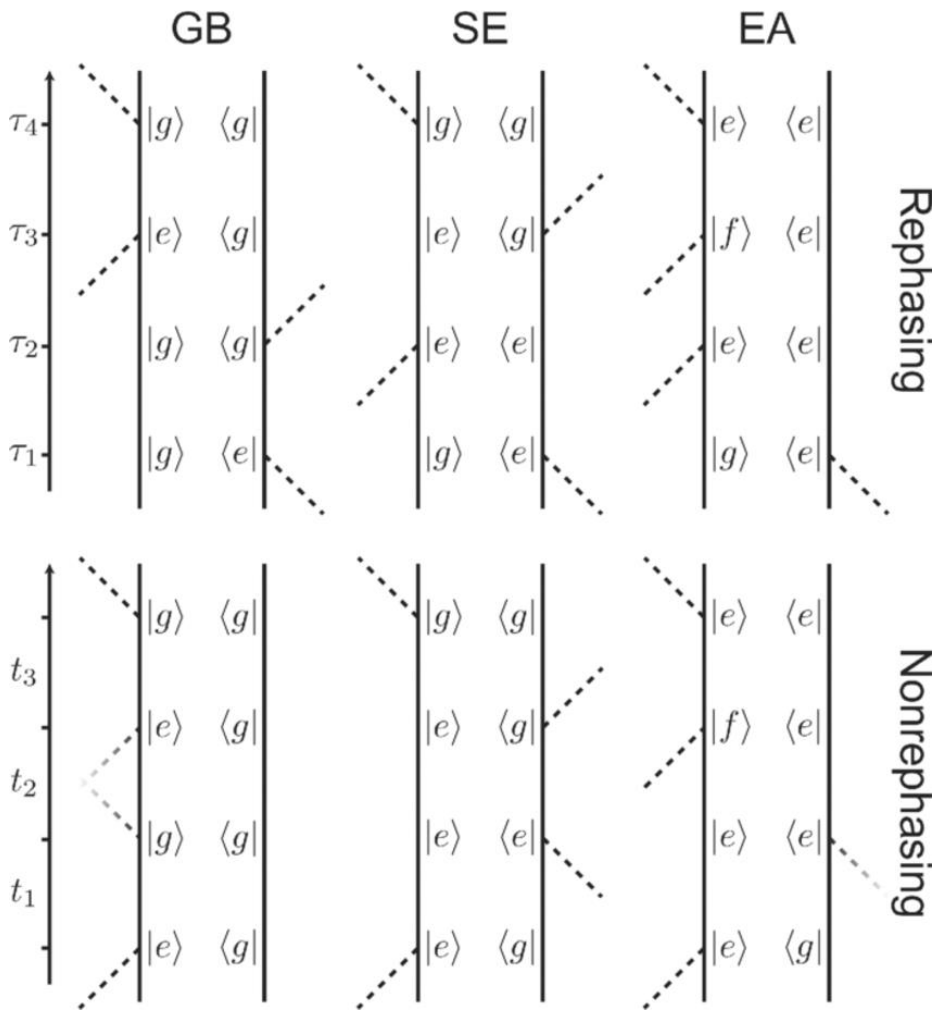

2D signal from J-aggregates of cyanine dyes

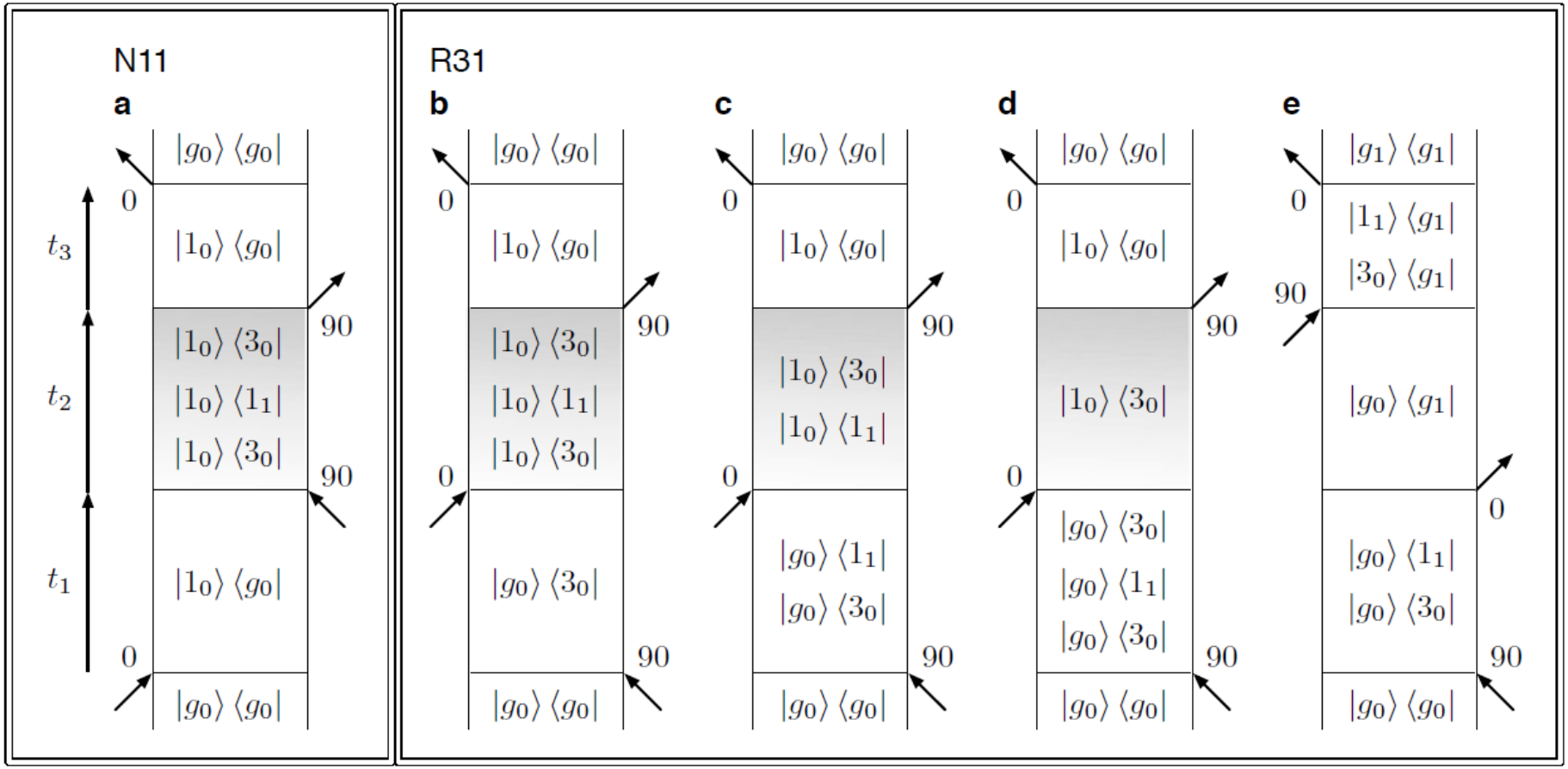

Non-rephasing:

vibronic

Rephasing:

vibronic and vibrational

Experimental results

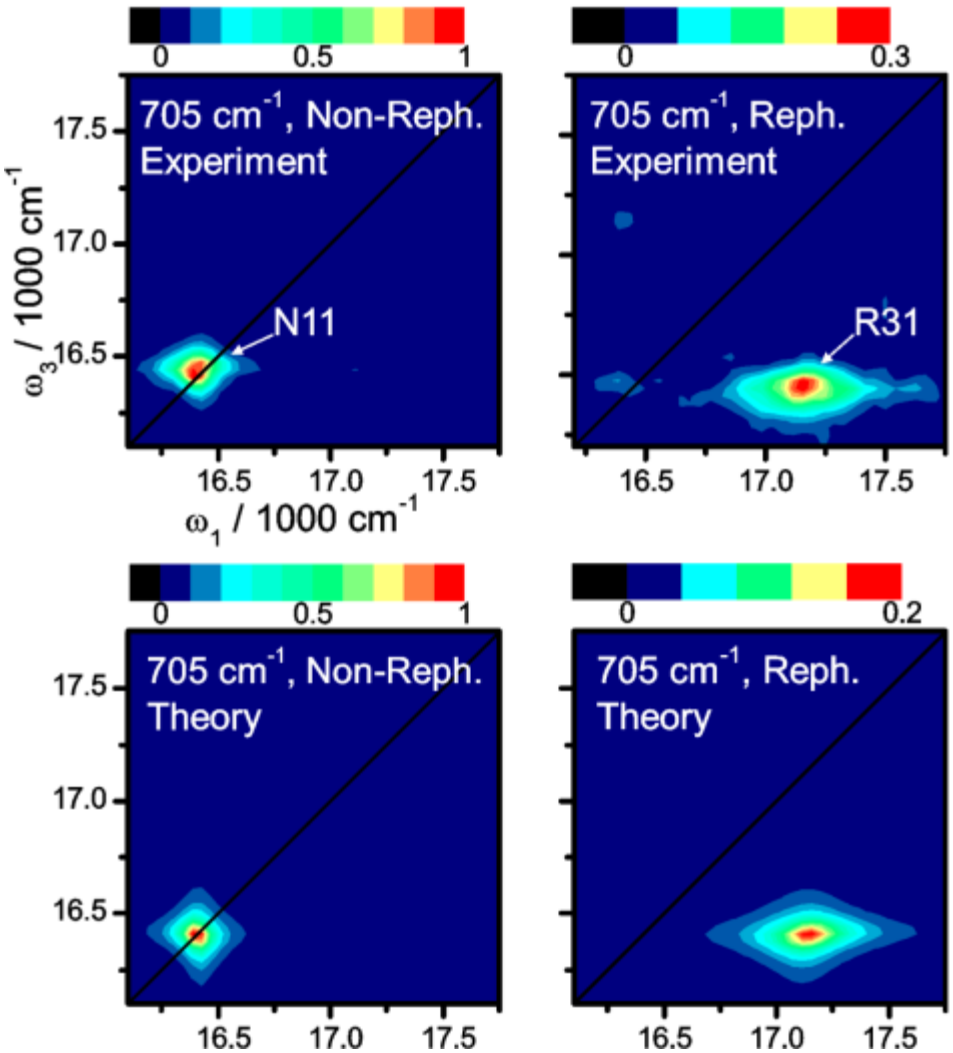

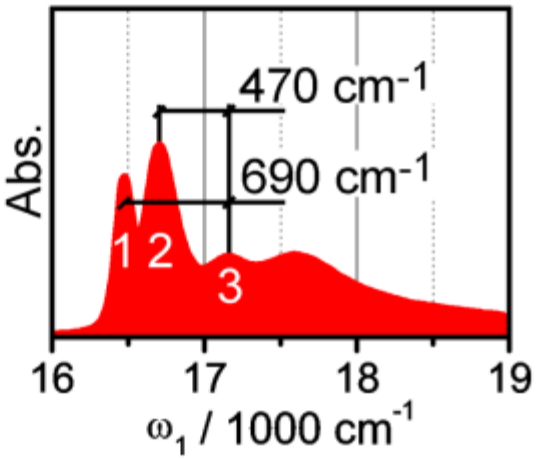

2D signal from J-aggregates of cyanine dyes

Analytics allow identification of short lived components

$$\frac{\left|R_{1g}^{N_{11}}(\omega_1 = \Omega_1, \omega_2 = \Delta\Omega_{31}, \omega_3 = \Omega_1)\right|}{\left|R_{2g}^{R_{31}}(\omega_1 = \Omega_3, \omega_2 = \Delta\Omega_{31}, \omega_3 = \Omega_1)\right|} \approx \frac{\Gamma_3}{\Gamma_1}$$

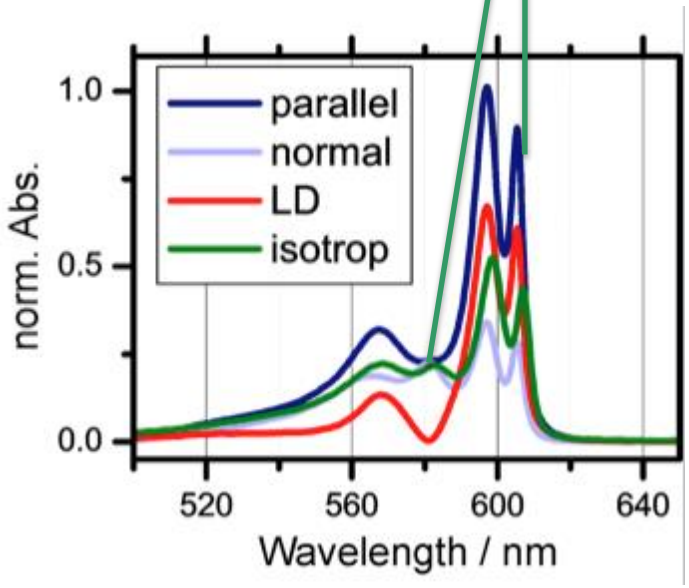

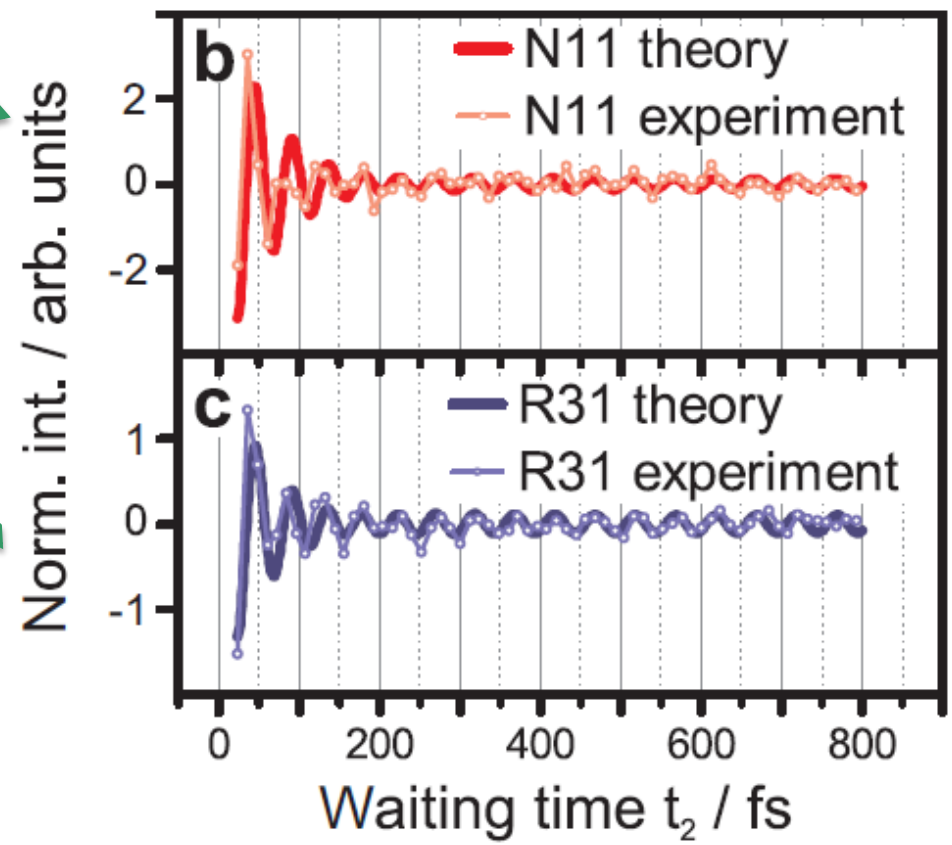

2D signal: Analytical model

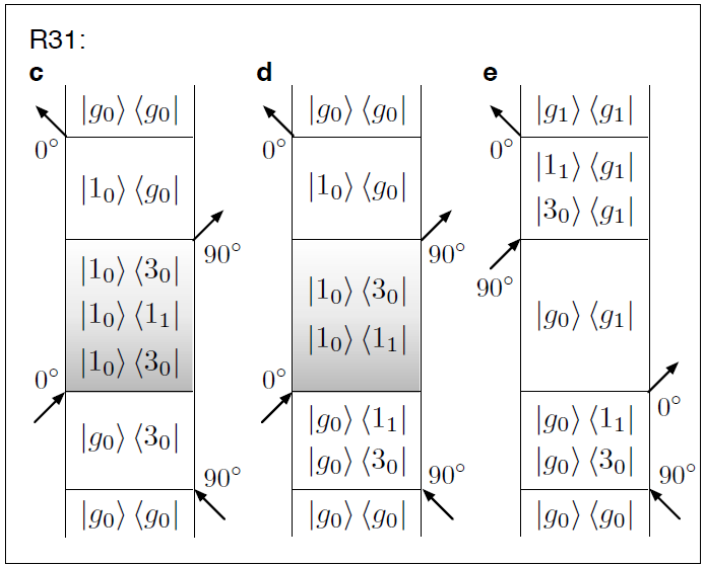

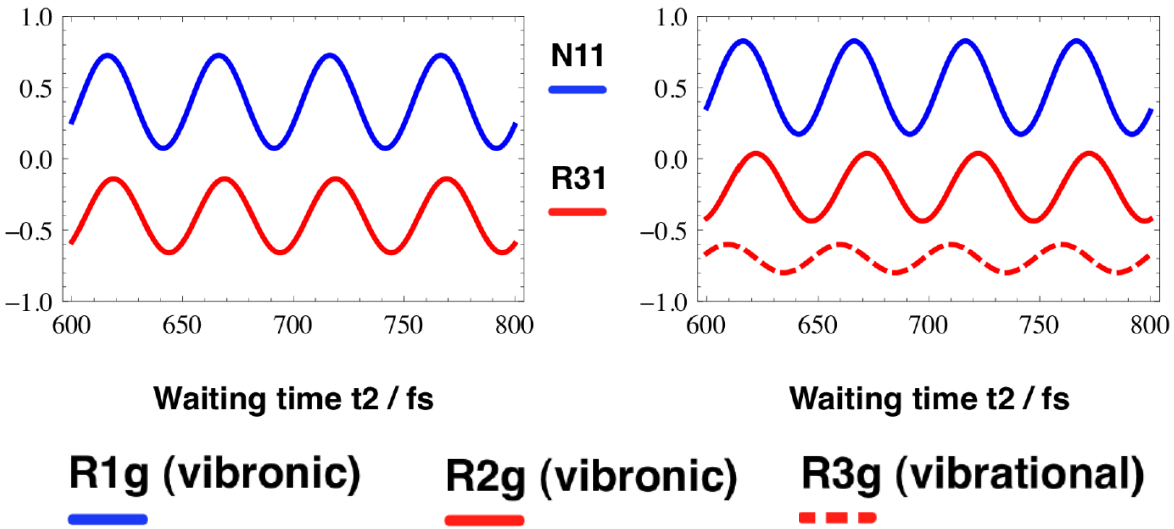

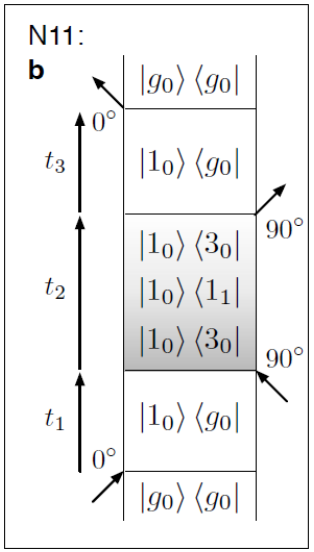

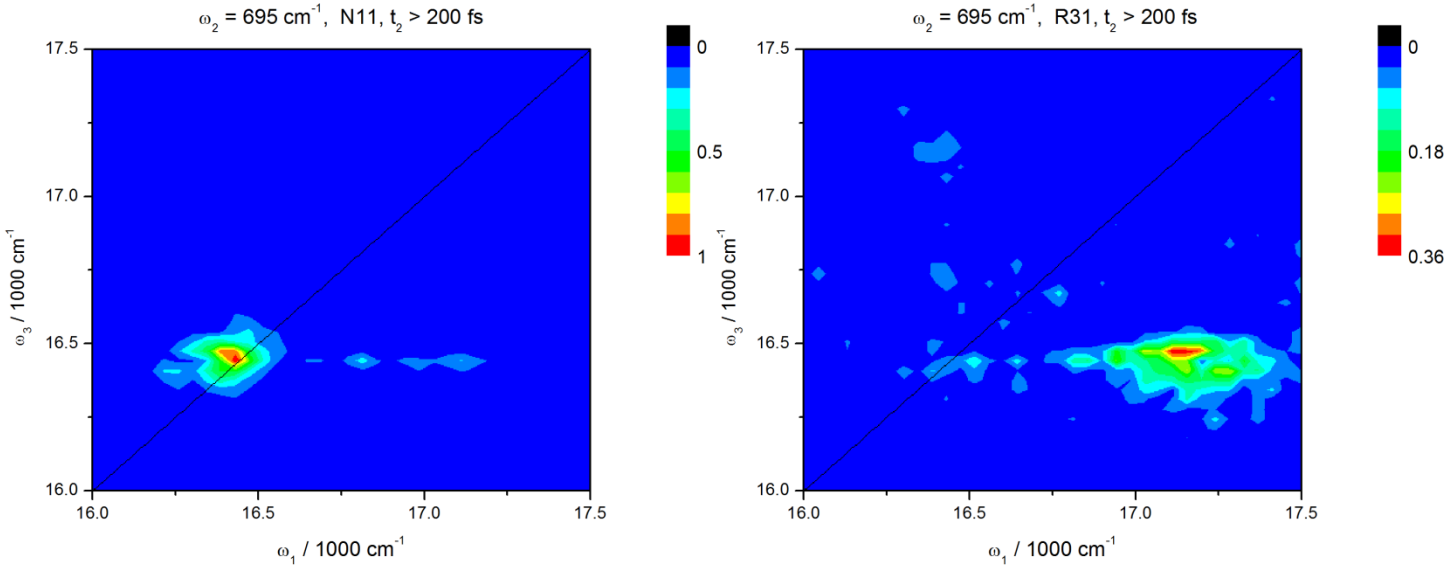

Correlated disorder in J-aggregates

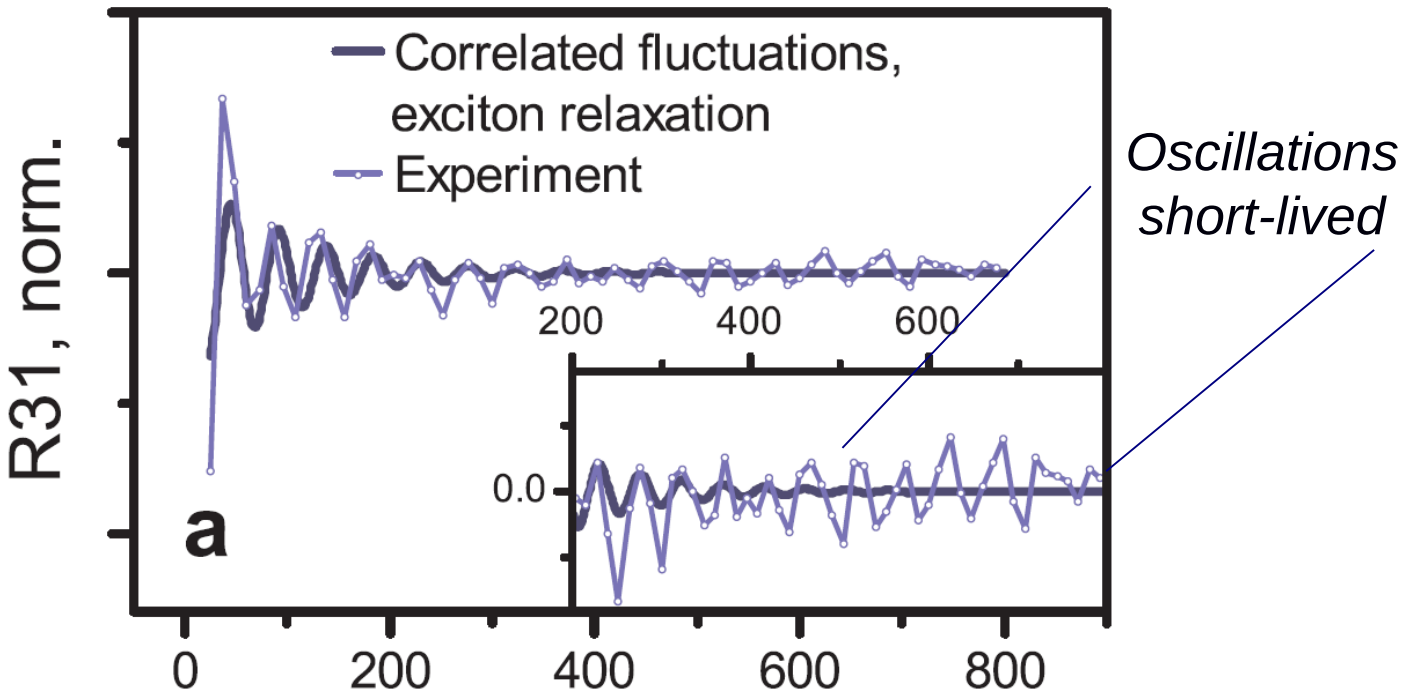

Correlated disorder: band 1 and 3 are coupled to a common environment.
The noise enables the inter-exciton coherence |1><3| to decohere very slowly compared to the coherence|g><1| and |g><3| between electronic ground state and excitons.

Correlated disorder in J-aggregates

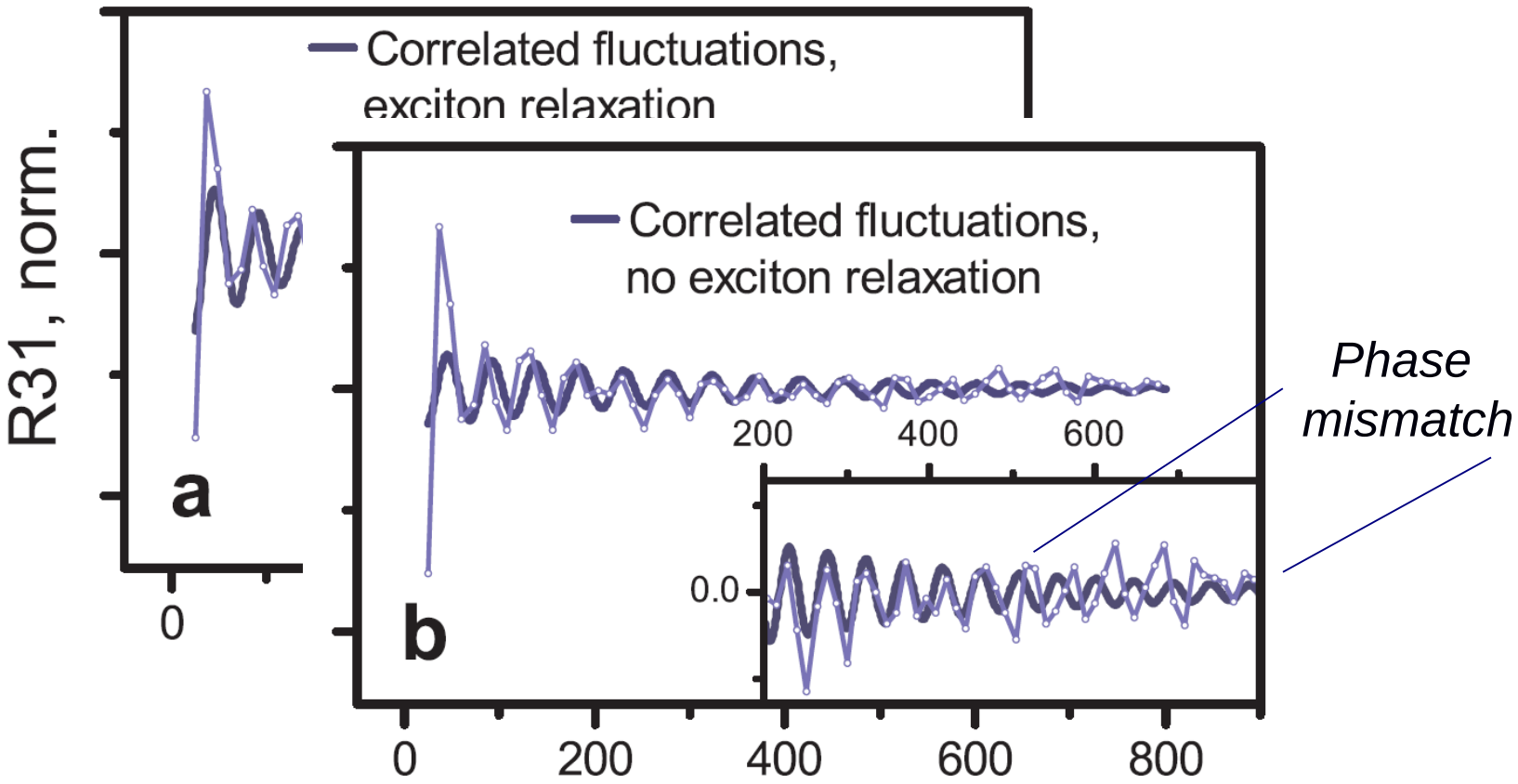

Correlated disorder in J-aggregates

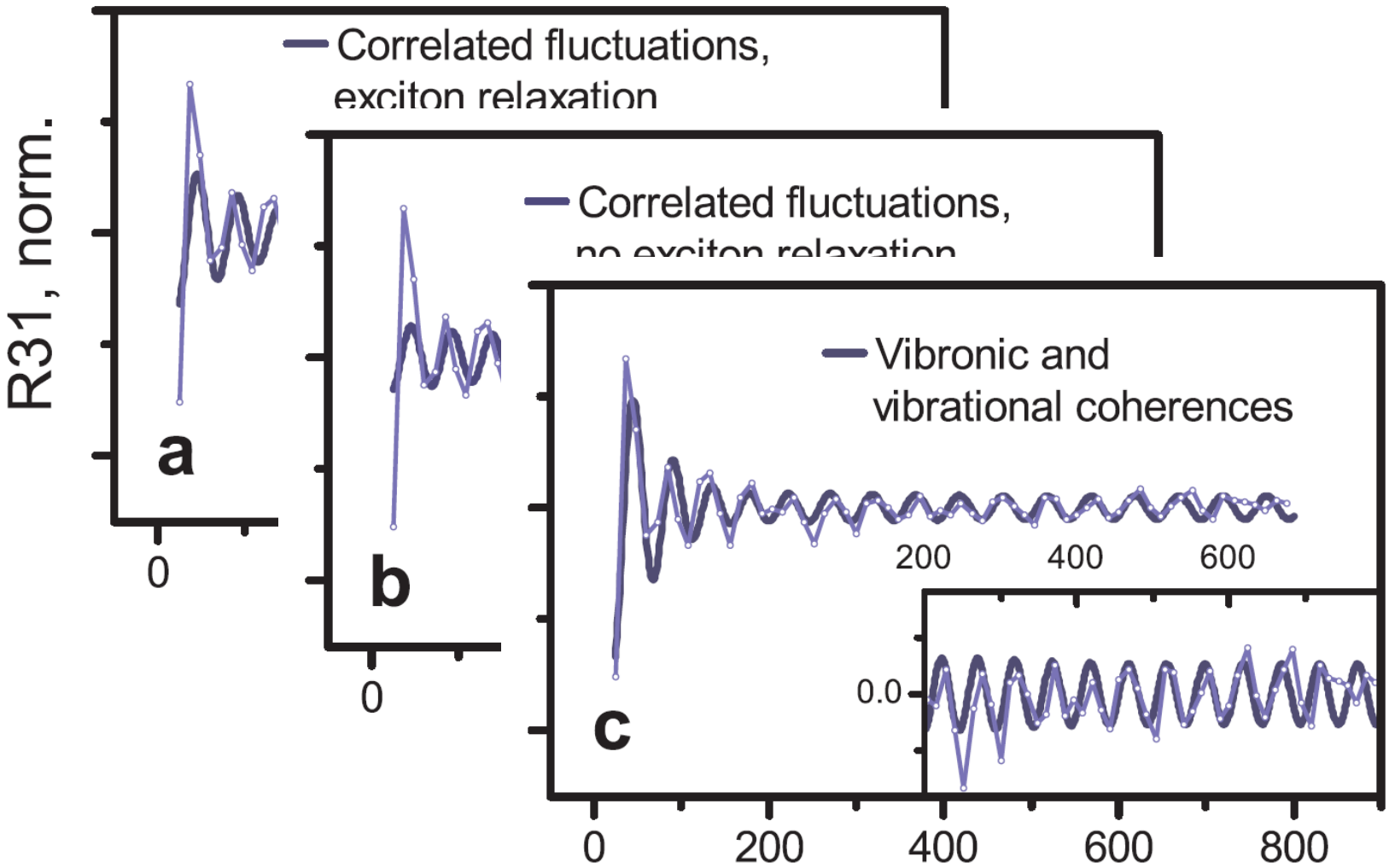

Correlated disorder in J-aggregates

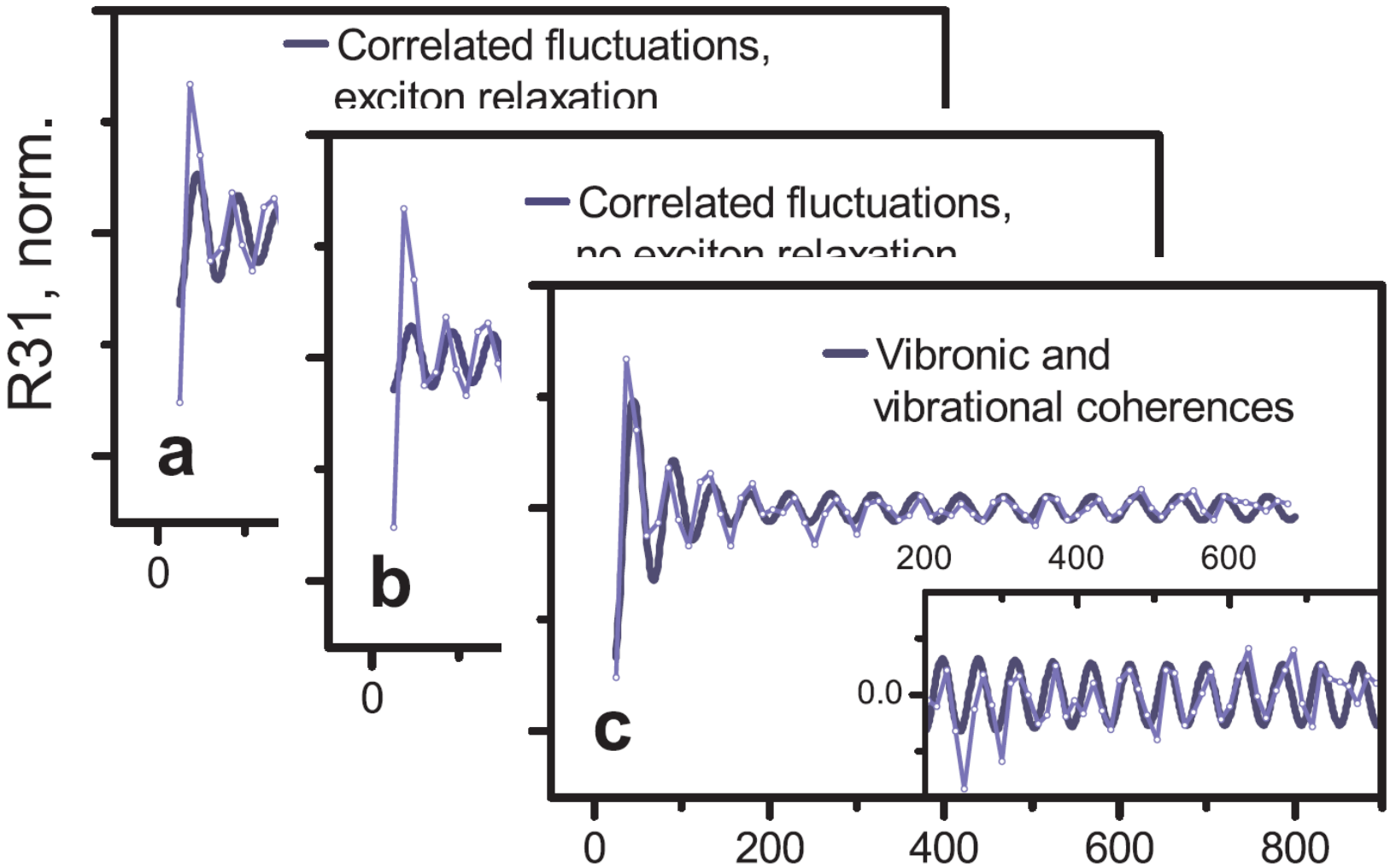

Only the vibronic model can reproduce the observations quantitatively on all timescales

Correlated disorder in J-aggregates

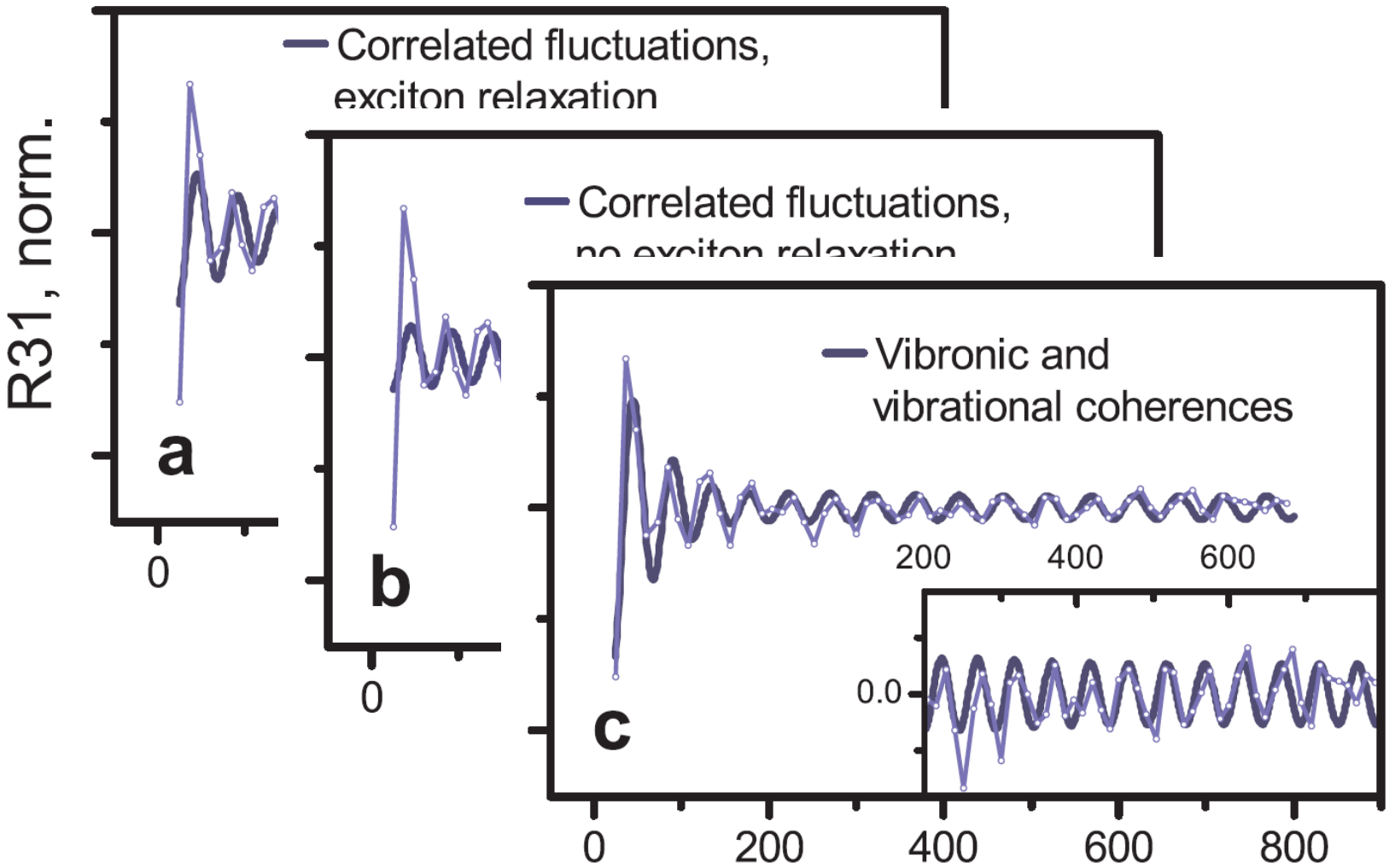

Only the vibronic model can reproduce the observations quantitatively on all timescales

Conclusions

- **Excited state exciton/vibrational coupling (vibronic) has functional relevance , (e.g. it can enhances transport).**

- **Vibronic model achieves quantitative agreement with experiment on J aggregates while correlated electronic dephasing does not.**

Long-lasting coherence in biological complexes: from microscopic models to actual experiments

THANKS

Javier Prior

Funding:

Universidad Politécnica de Cartagena

GOBIERNO DE ESPAÑA
MINISTERIO DE ECONOMÍA Y COMPETITIVIDAD

f SéNeCa (+)
Agencia de Ciencia y Tecnología
Región de Murcia

Photosystem II Reaction Center (PSII RC)

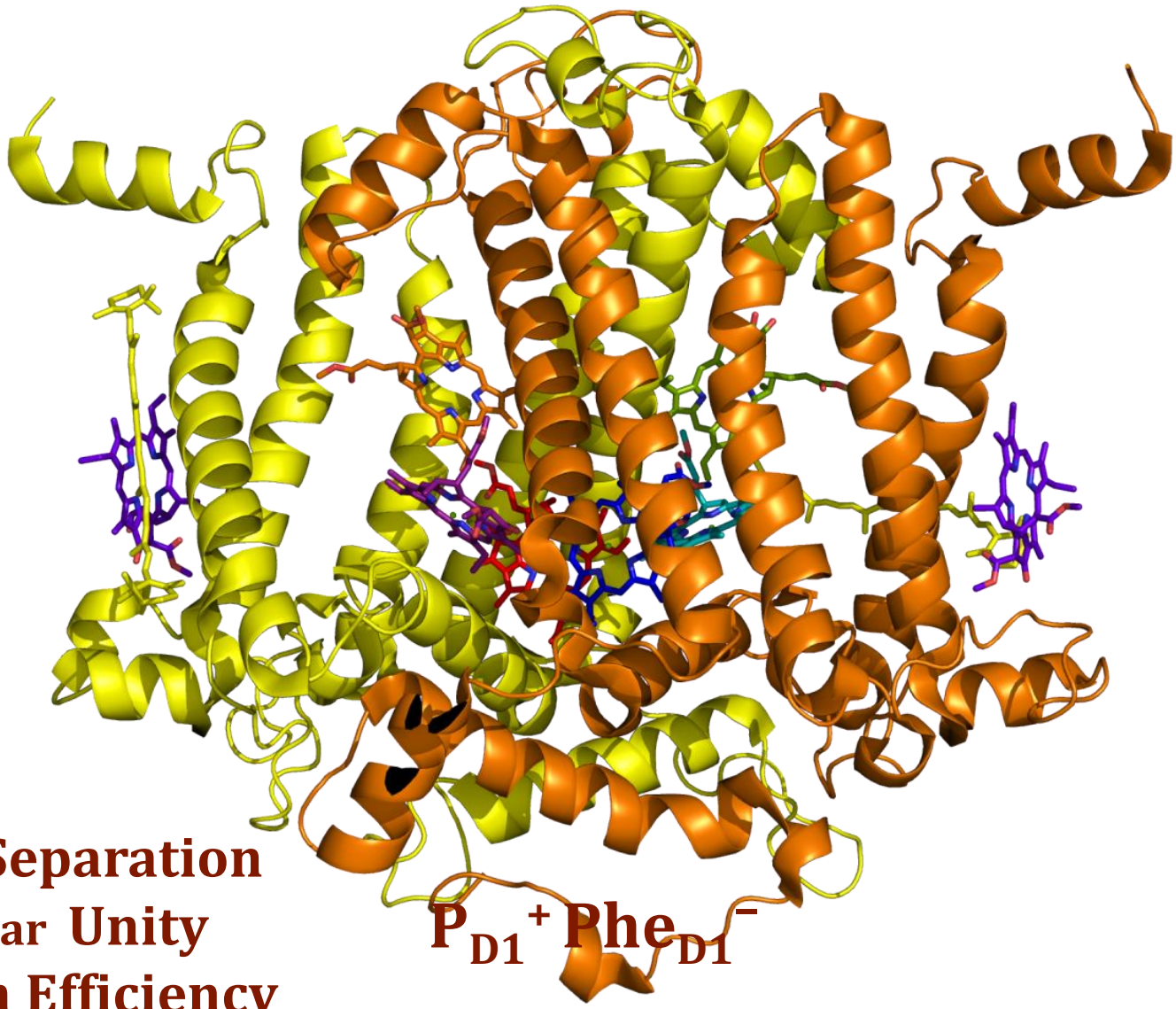

Charge Separation with near Unity Quantum Efficiency

$P_{D1}^{+} Phe_{D1}^{-}$

Photosystem II Reaction Center (PSII RC)

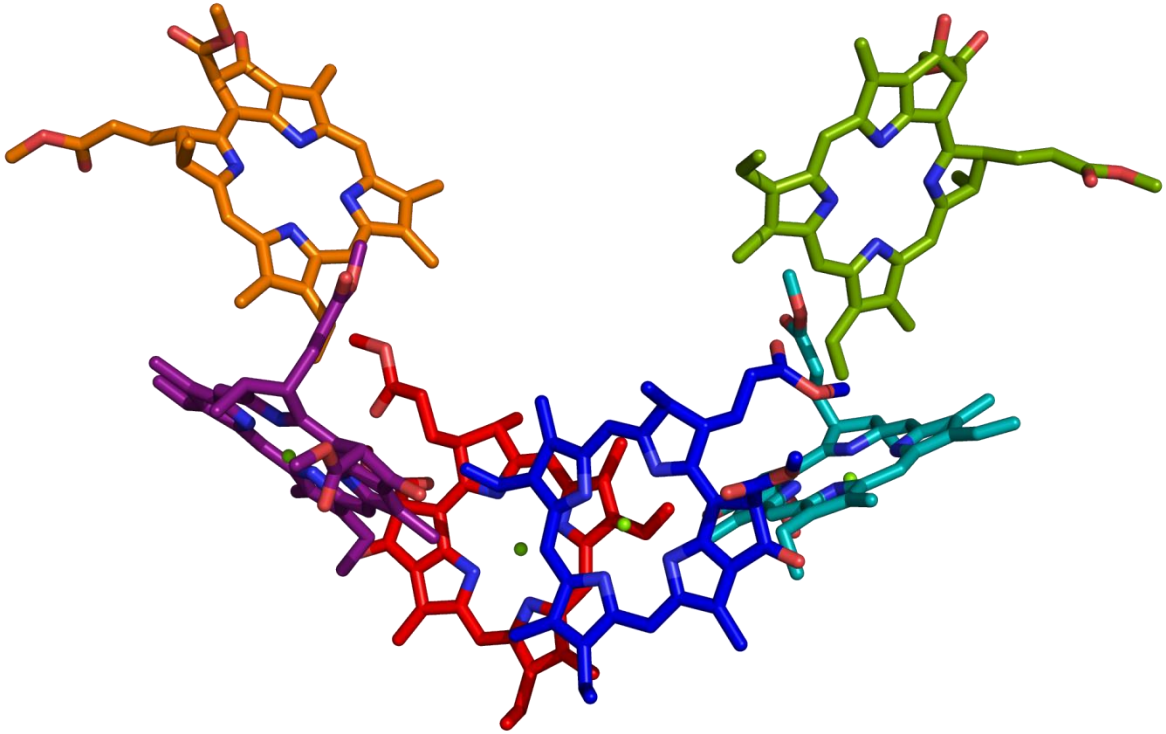

Excitons with charge transfer character

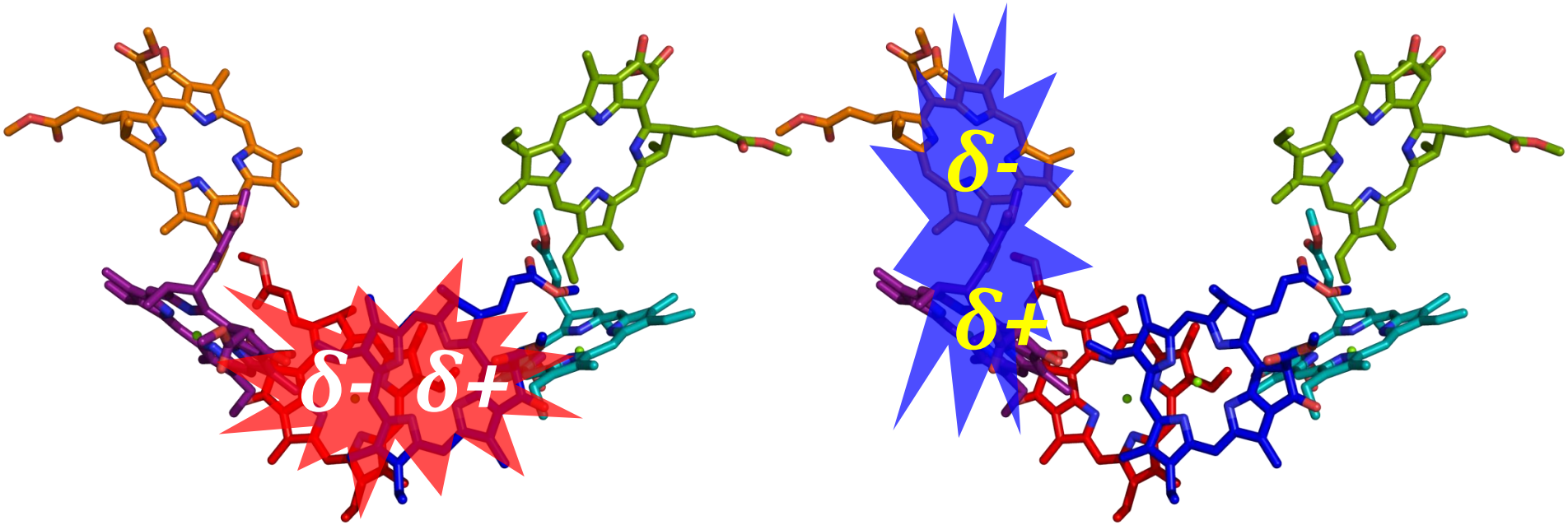

$P_{D2}^{\delta+} P_{D1}^{\delta-}$ $Chl_{D1}^{\delta+} Phe_{D1}^{\delta-}$

Novoderezhkin et al, Biophys. J., ***2007***
Romero et al,

Two different charge separation pathways

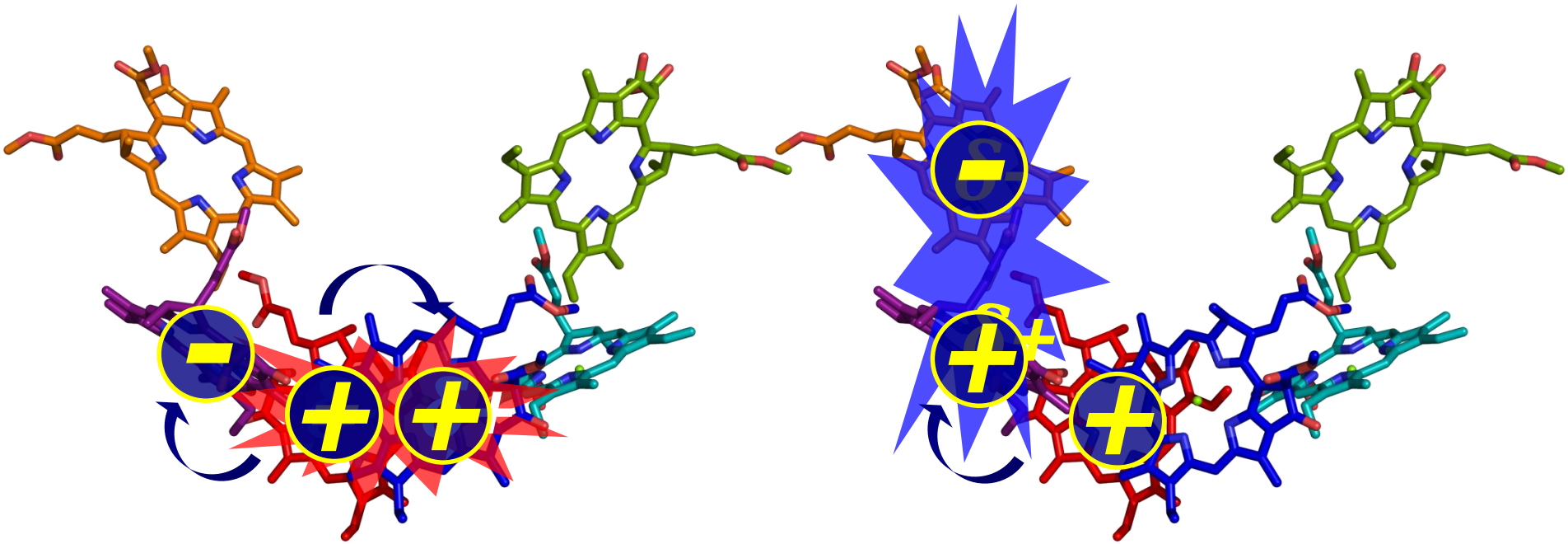

• VI Novoderezhkin, E Romero, J Prior, R van Grondelle
Physical Chemistry Chemical Physics 19 (7), 5195-5208

Electronic states in the PSII RC

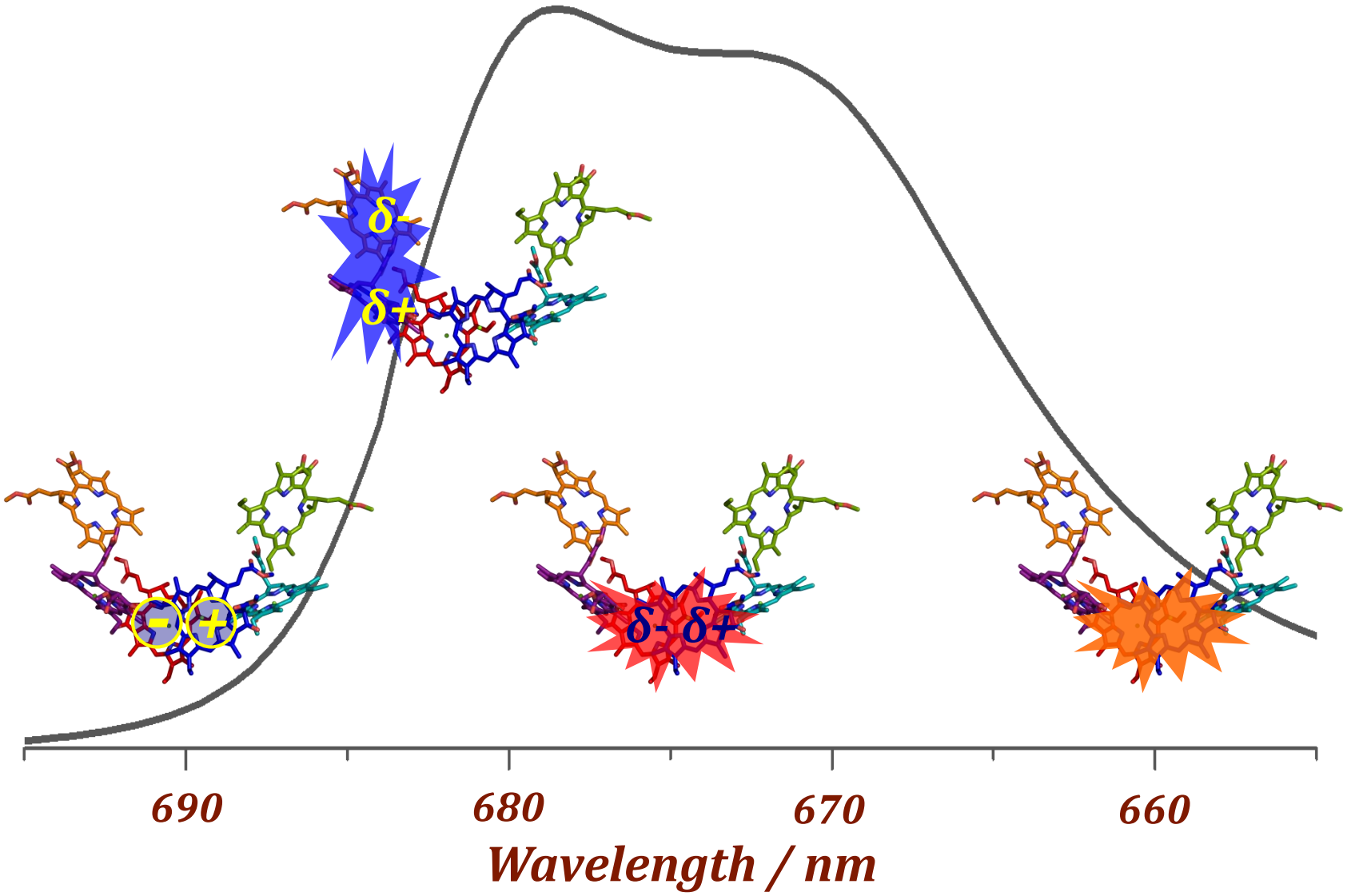

Quantum beats

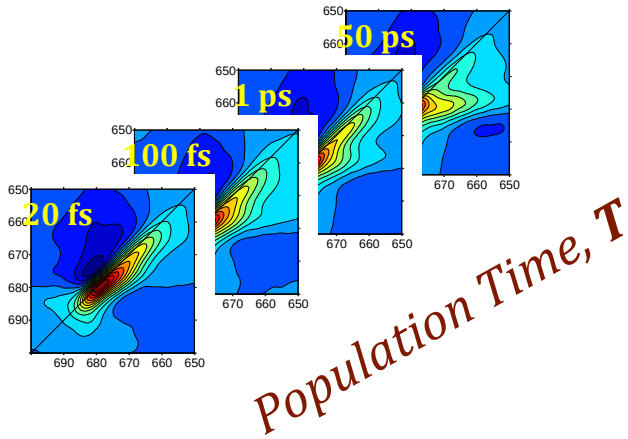

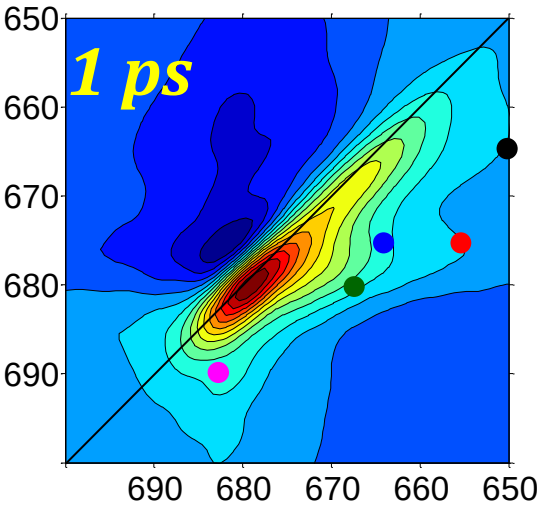

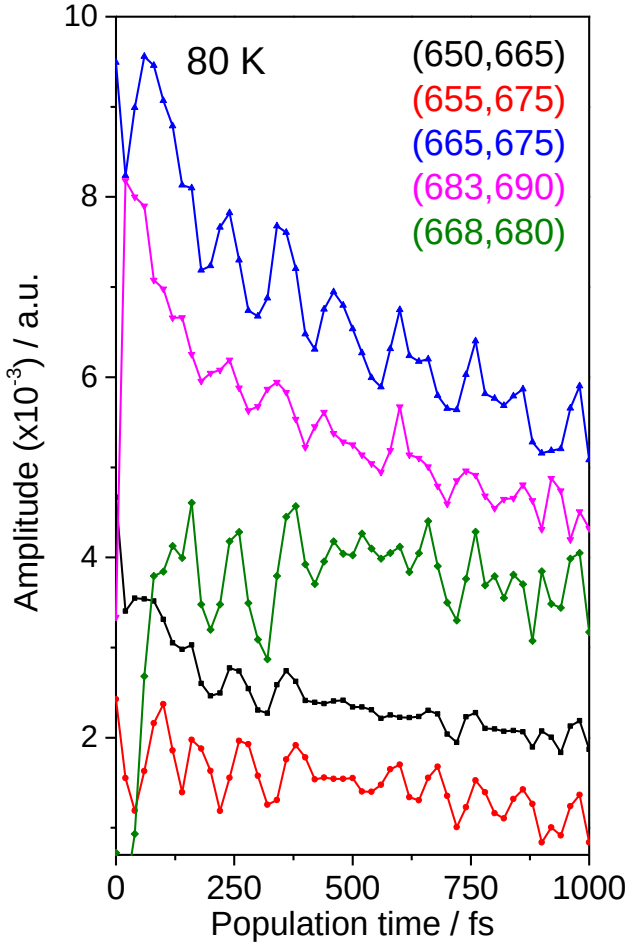

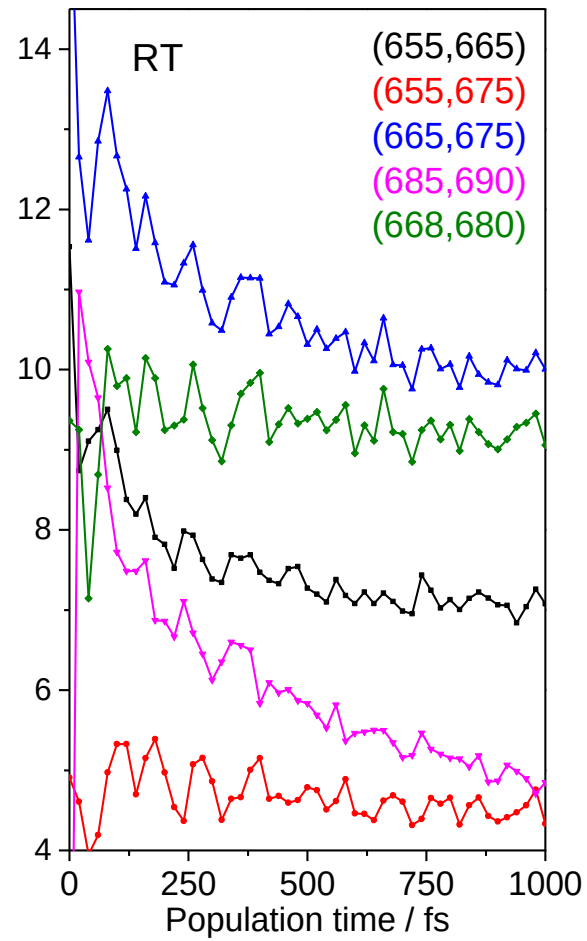

Fast Fourier transform: 2D frequencies

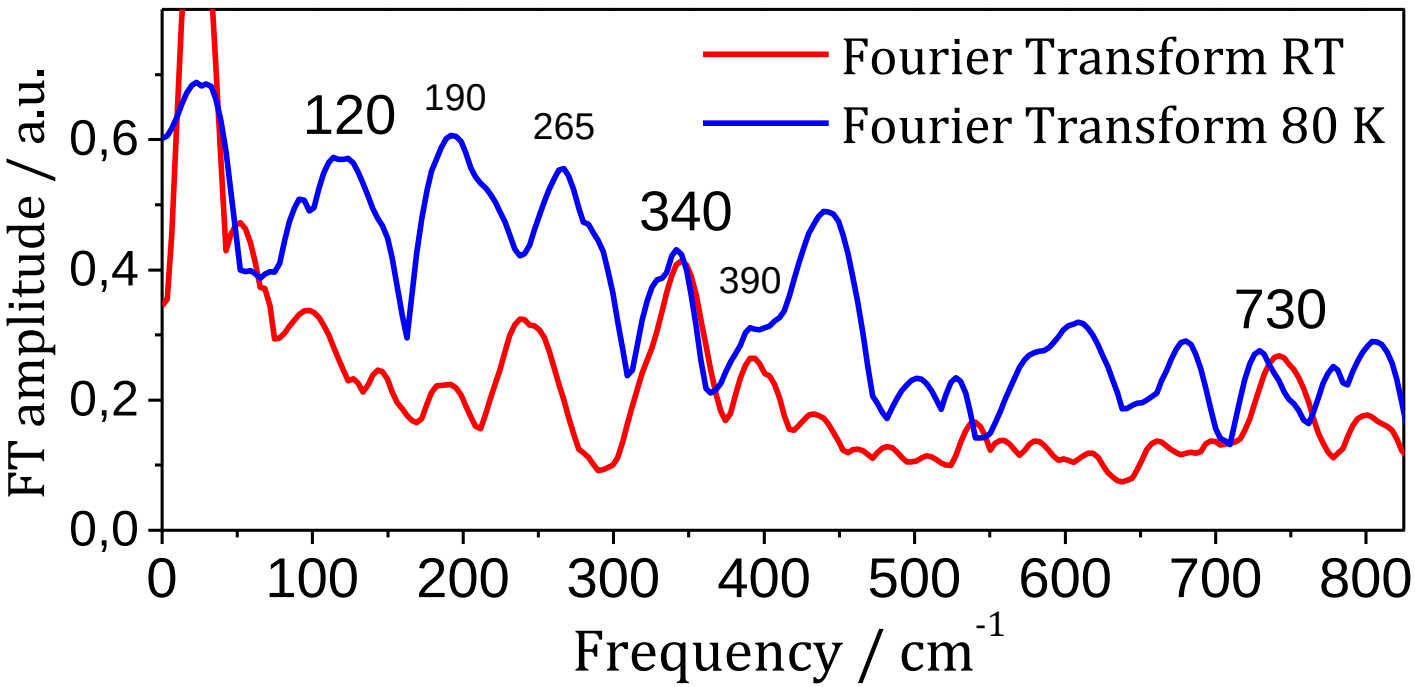

Optimal range to match energy differences between electronic states

Fourier transform: from population time to frequency

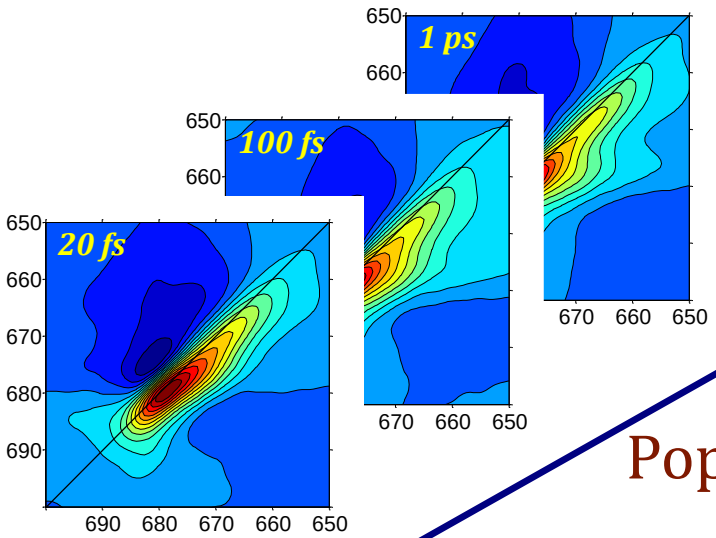

2D spectra
All absorbing and emitting states

Population Time, **T**

2D frequency maps
Only the states oscillating at certain frequency

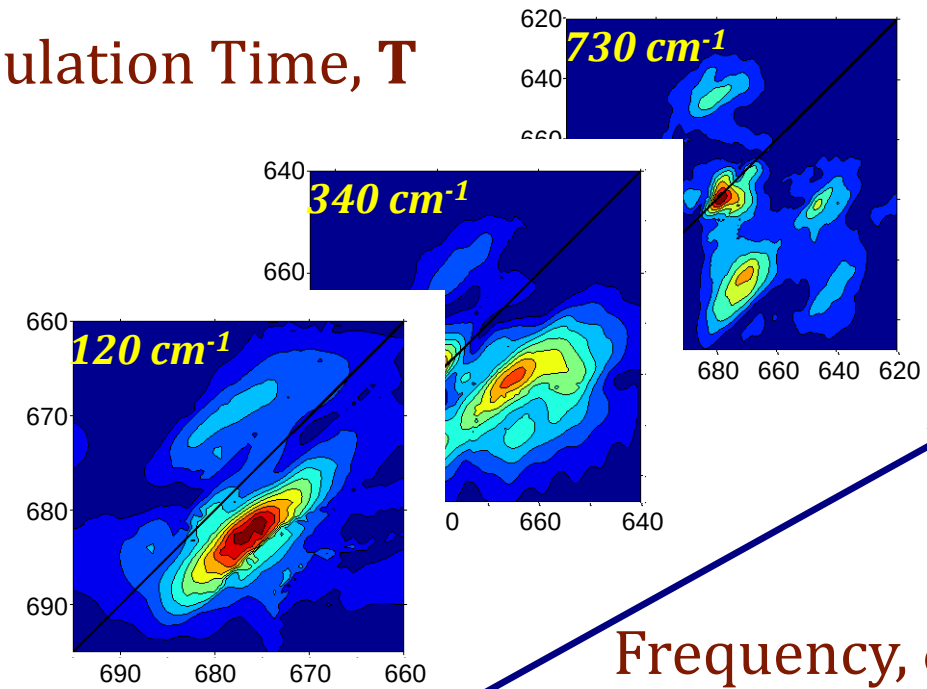

Fourier Transform

Frequency, ω_T

Fourier transform: from population time to frequency

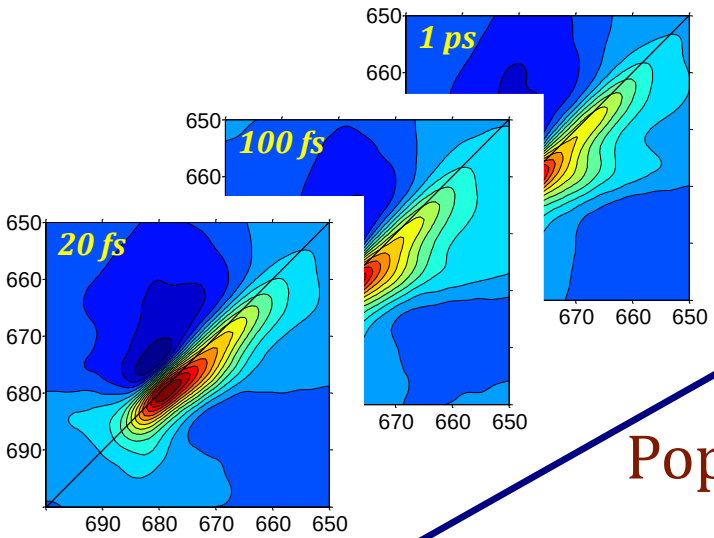

2D spectra

All absorbing and emitting states

Can we have both Frequency and Time information?

YES **Wavelet analysis**

Population Time, **T**

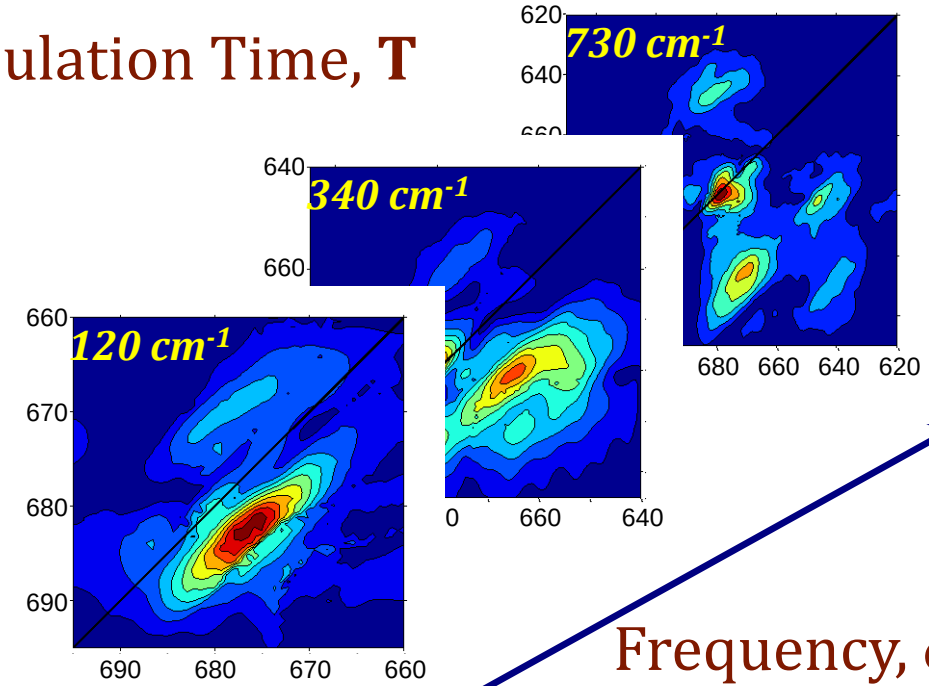

Frequency, ω_T

Fourier Transform

Wavelet analysis

Example I:

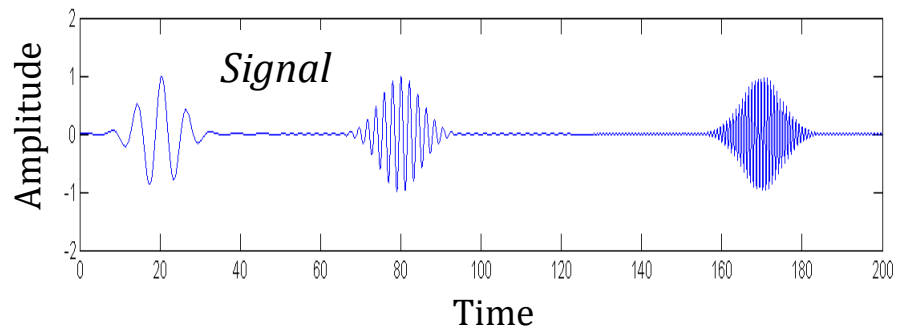

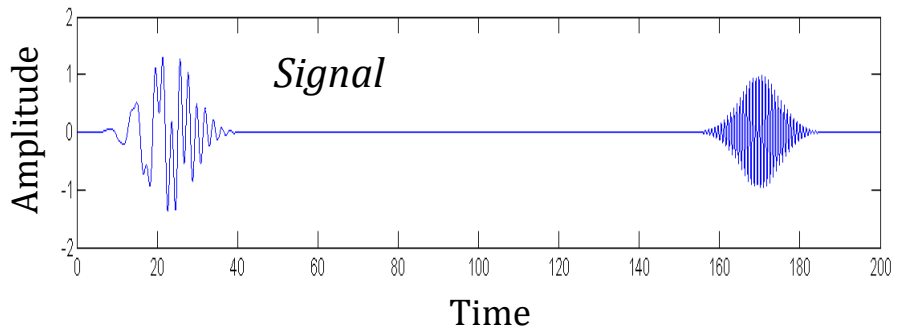

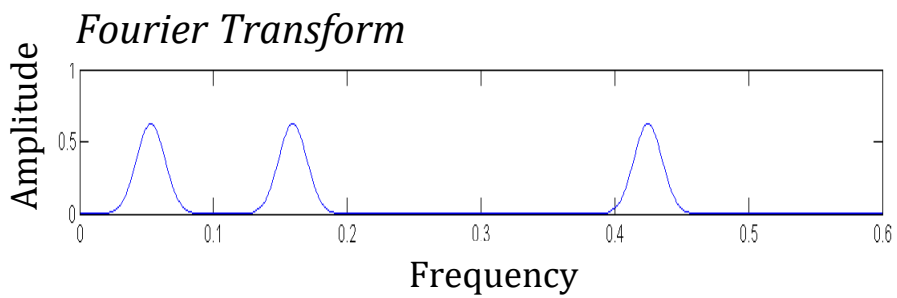

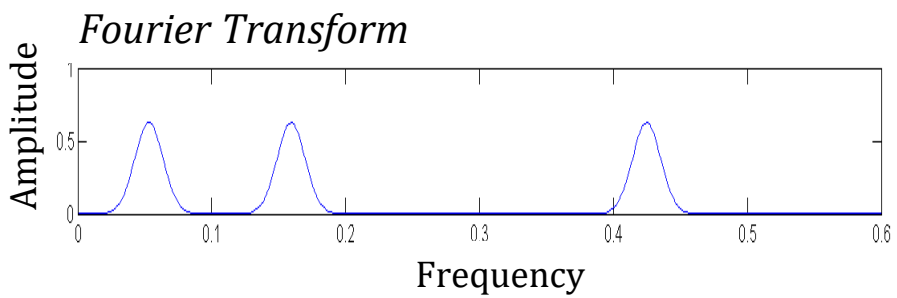

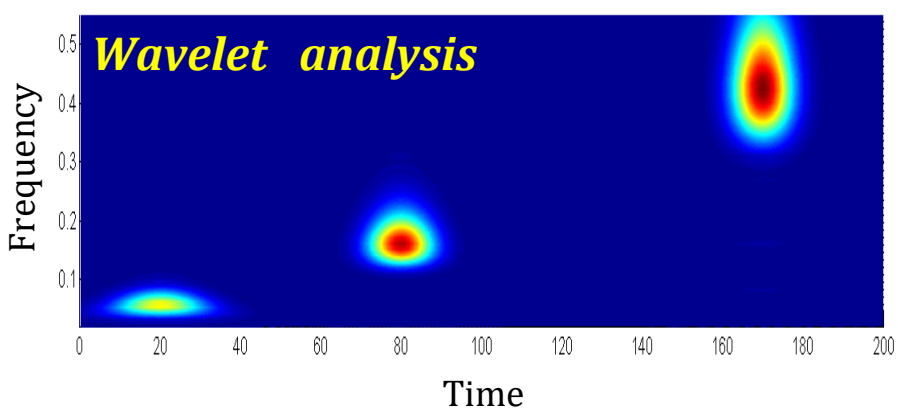

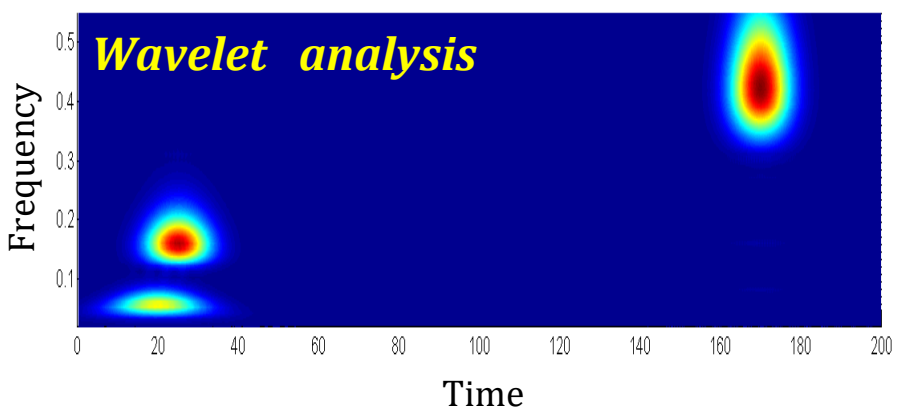

Electronic state in the PSII RC

Quantum Coherence

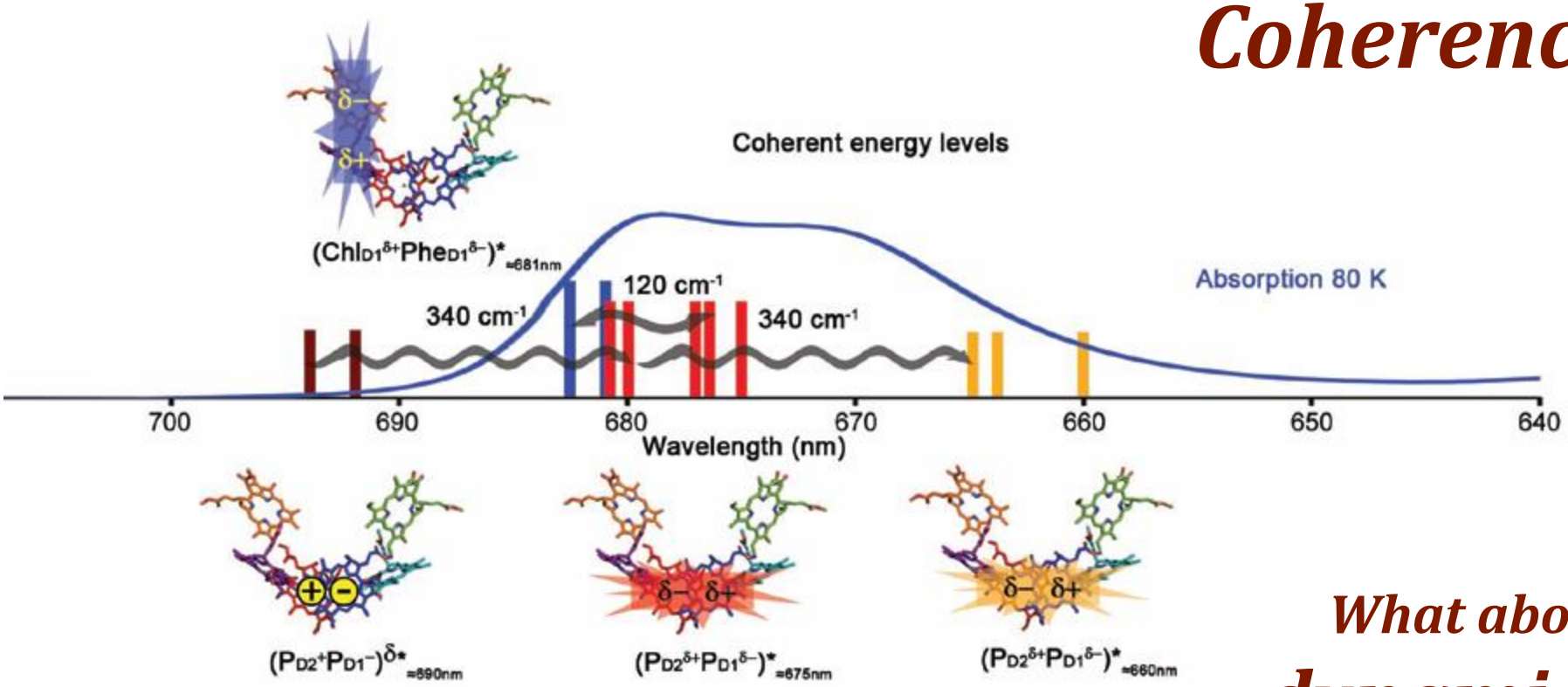

What about the dynamics of Quantum Coherence?

120 cm^{-1} movie

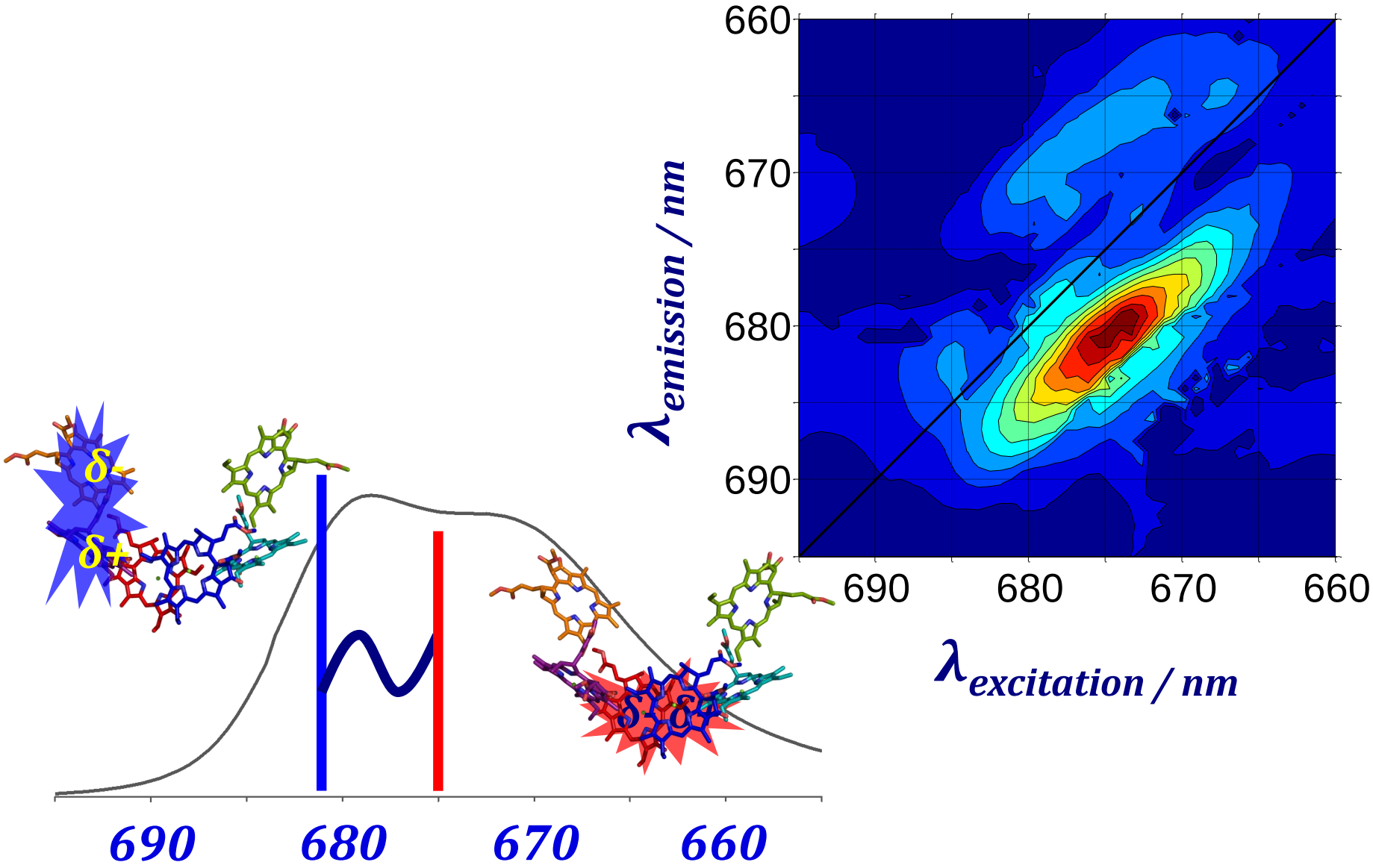

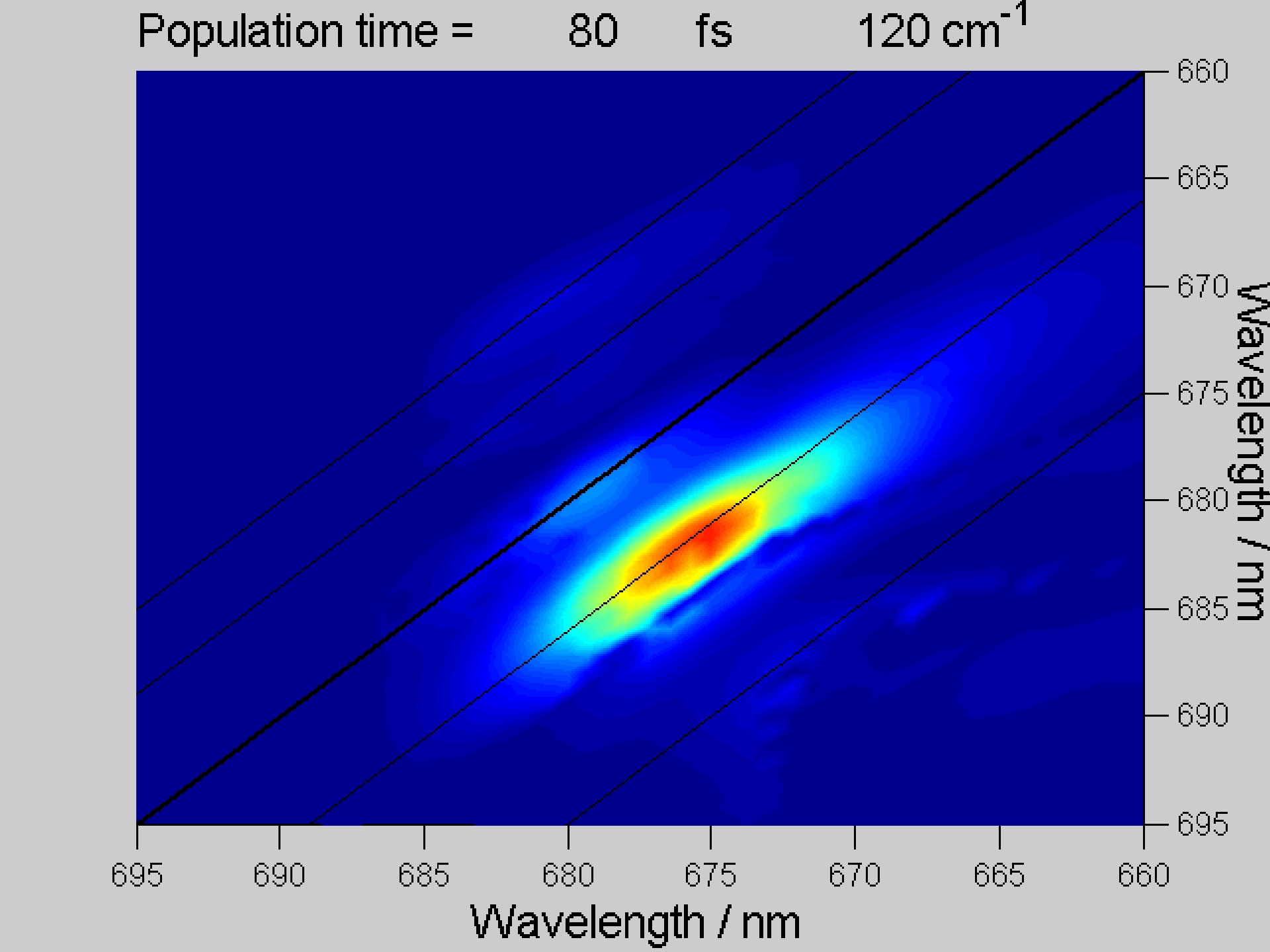
Population time = 80 fs 120 cm-1
660
665
670
675
680
685
690
695
Wavelength / nm
695
690
685
680
675
670
665
660
Wavelength / nm

120 cm^{-1} movie

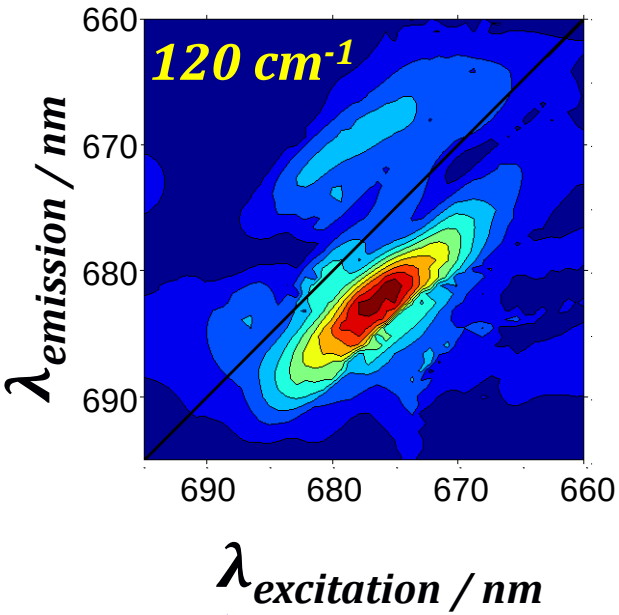

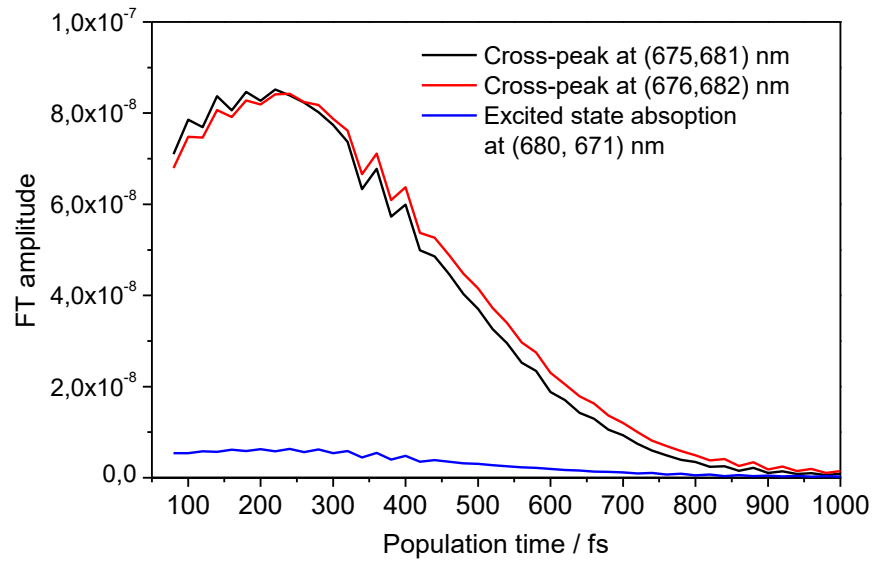

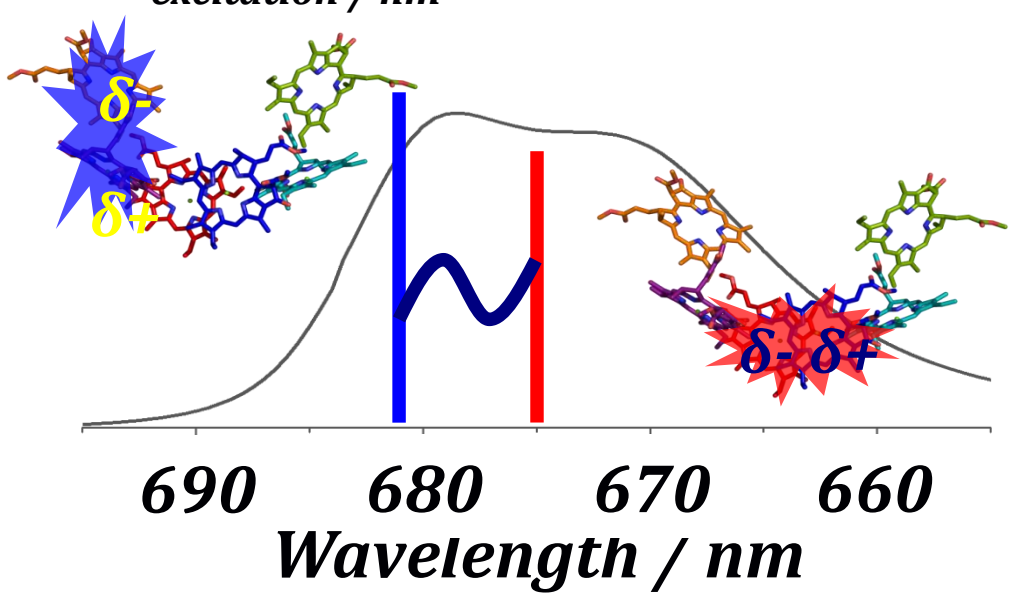

340 cm^{-1} movie

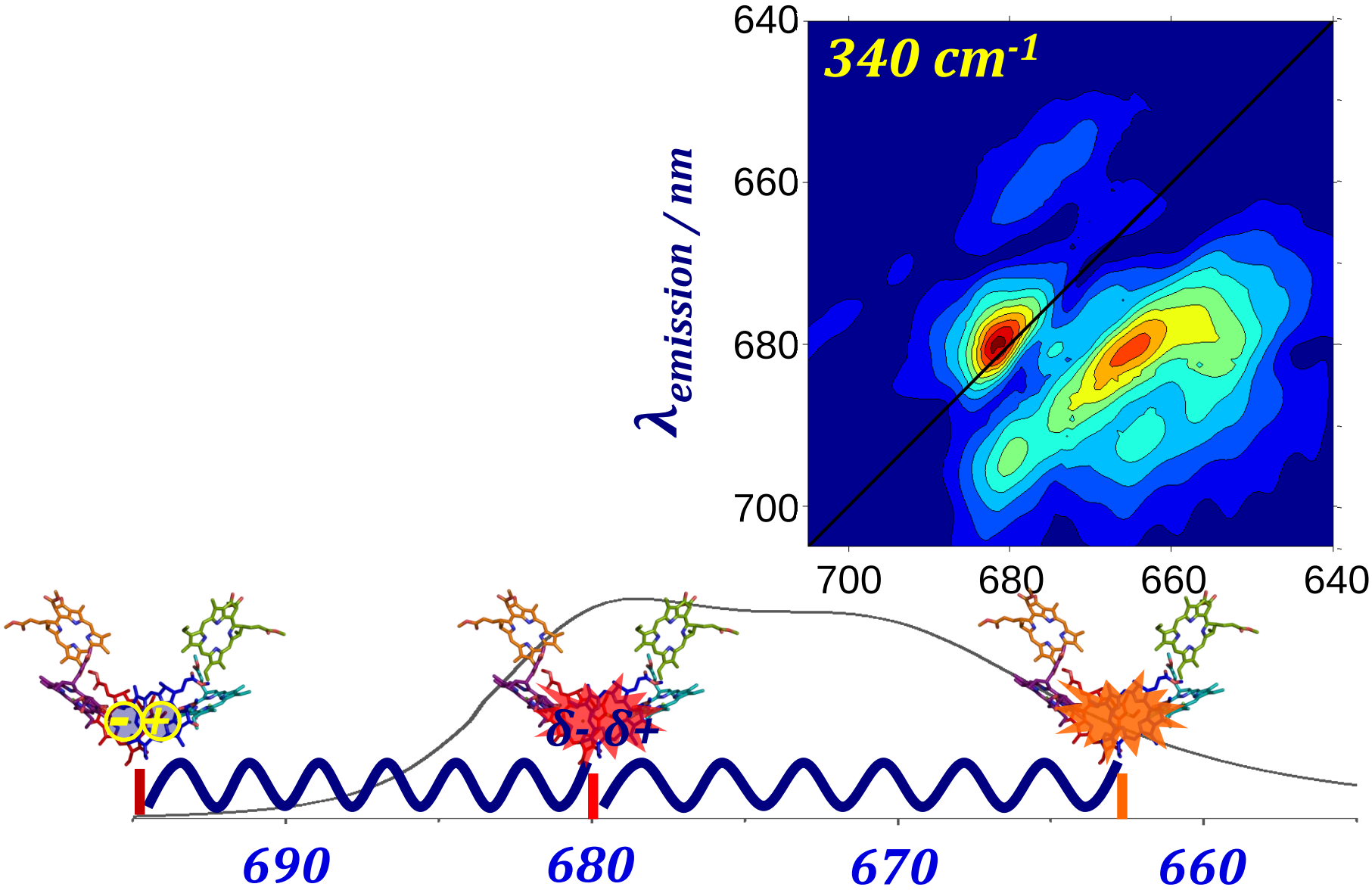

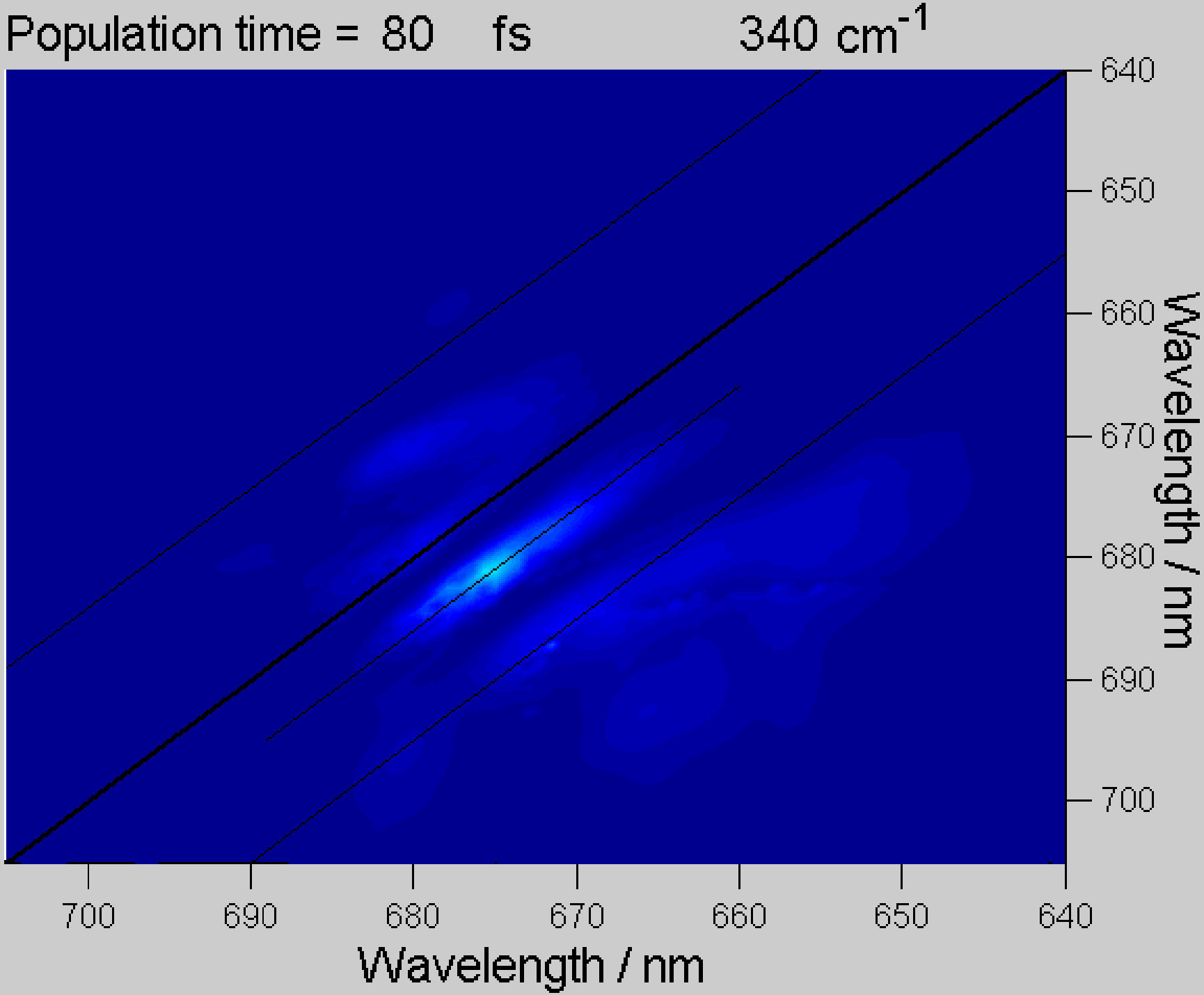
Population time = 80 fs
340 cm-1
640
650
660
670
680
690
700
Wavelength / nm
700
690
680
670
660
650
640
Wavelength / nm

340 cm^{-1} movie

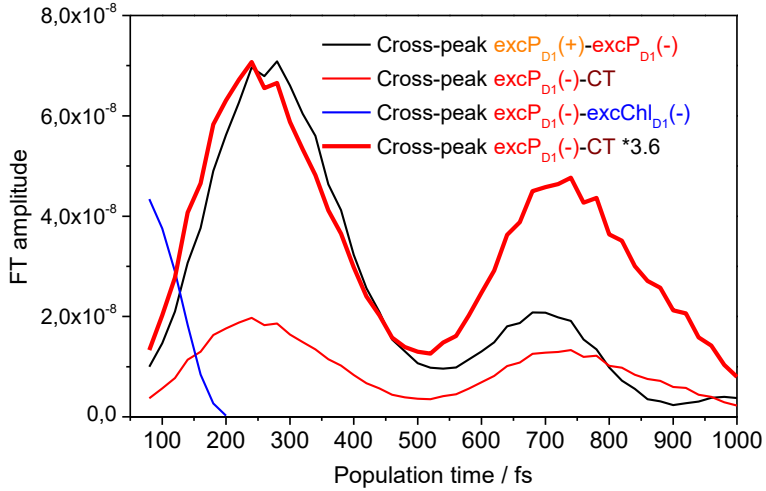

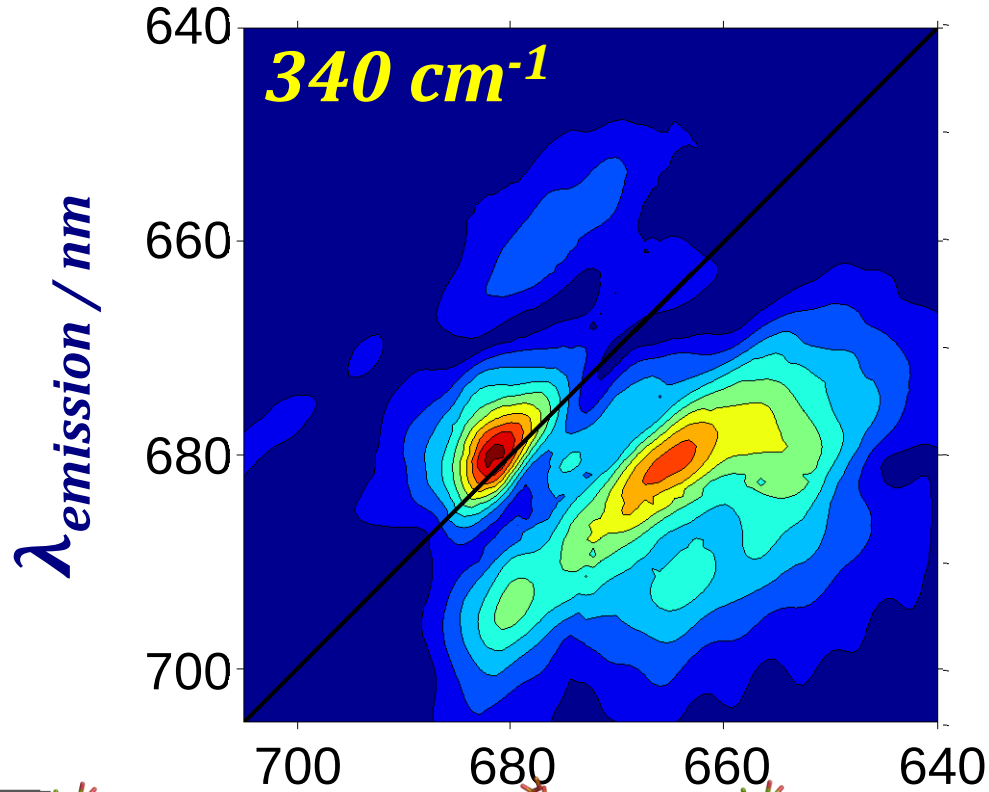

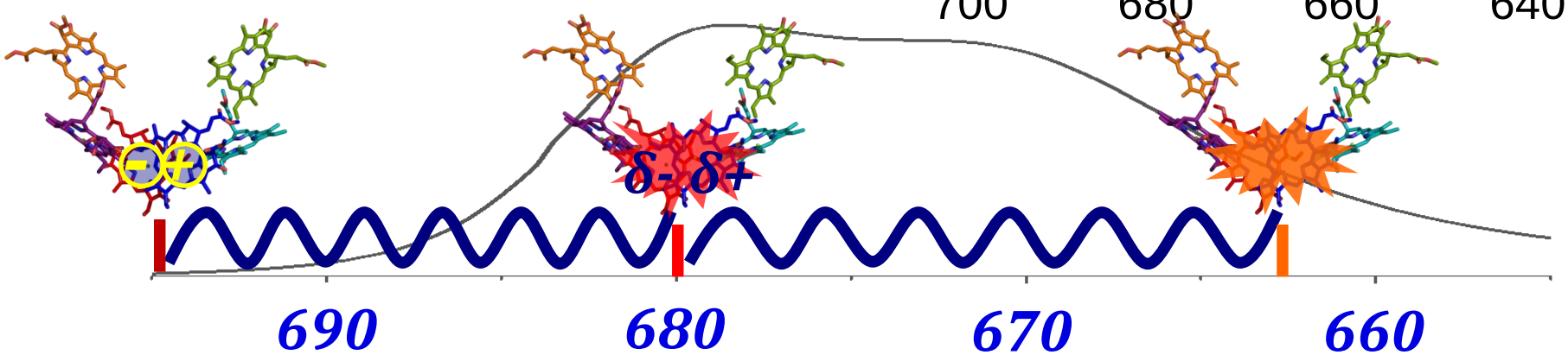

Limits of spectral resolution measurements by quantum probes

Javier Prior

Universidad Politécnica de Cartagena

Instituto Carlos I
Física teórica y computacional

CSRC. Beijing (China), 17th June 2019

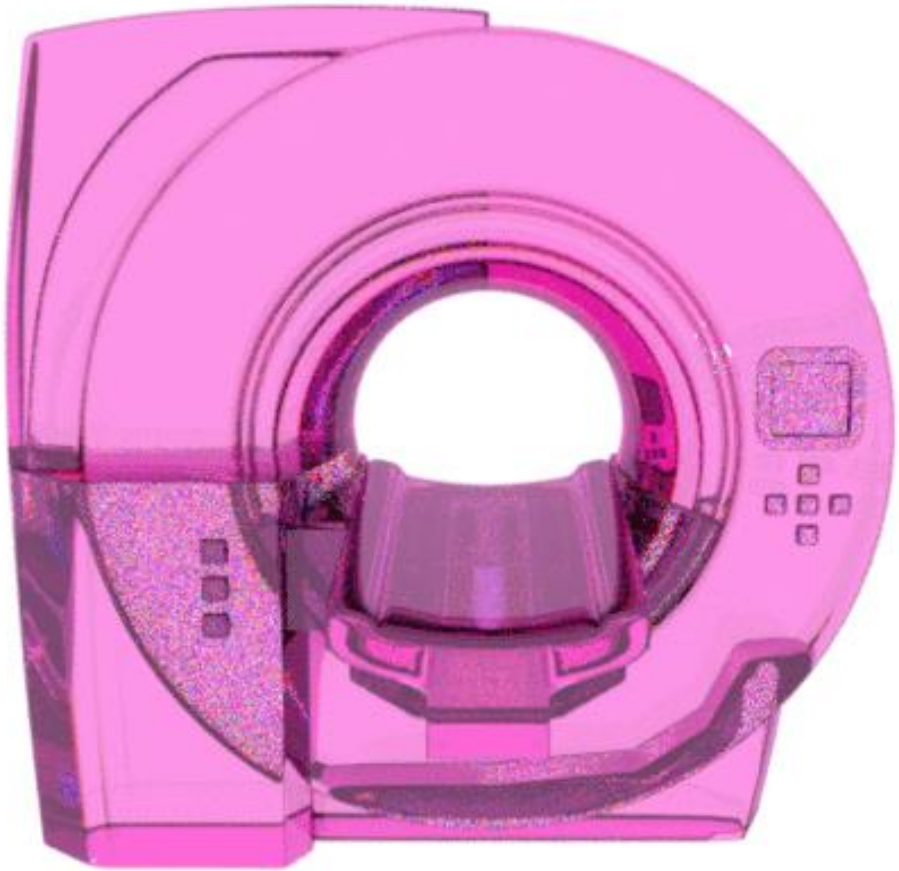

THE NV CENTER

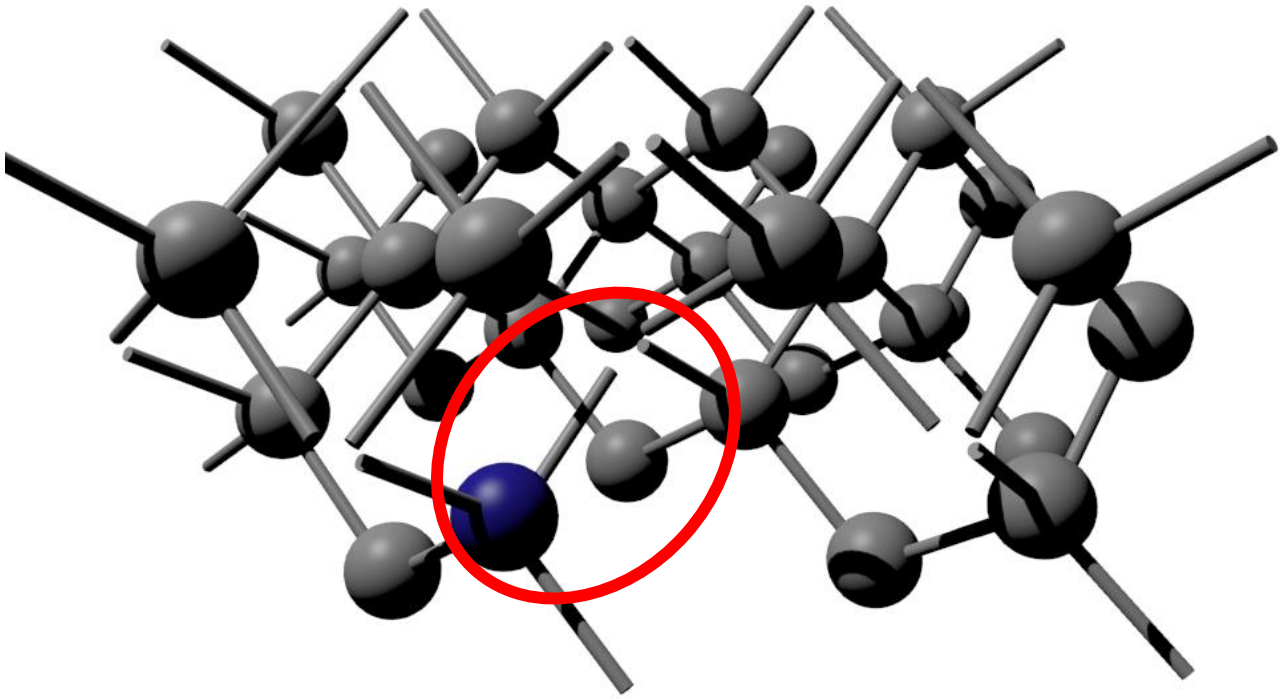

THE NV CENTER

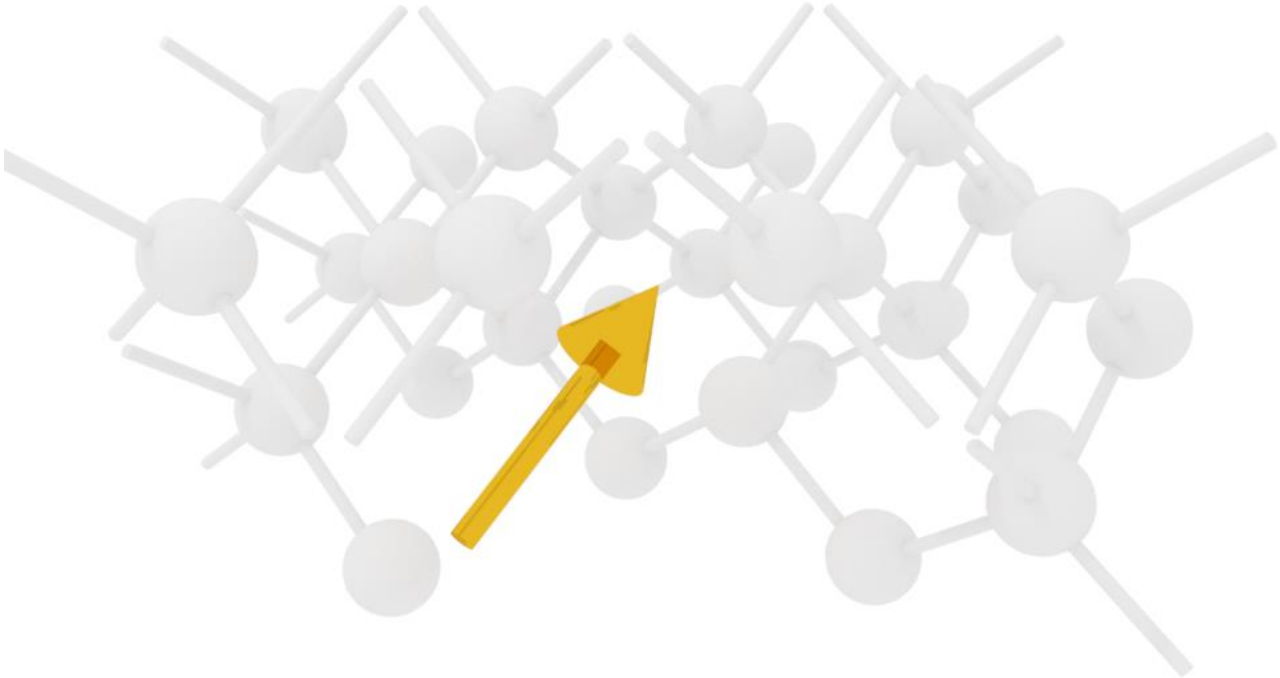

THE NV CENTER

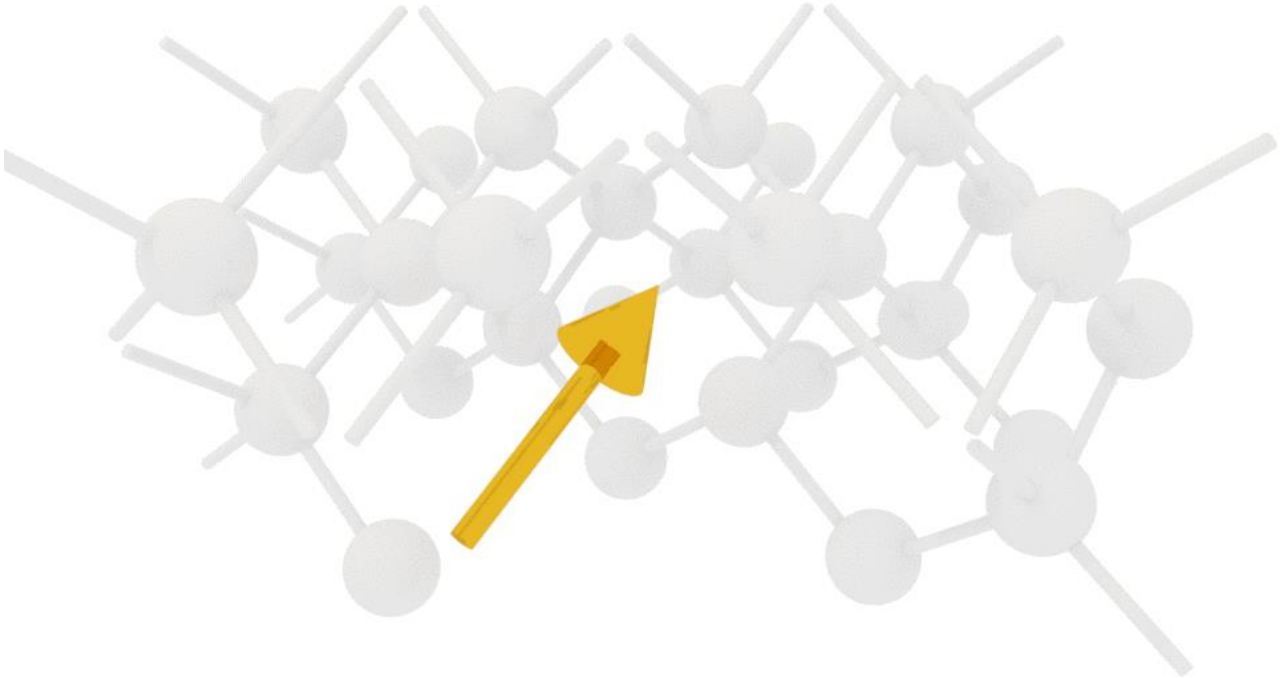

THE NV CENTER

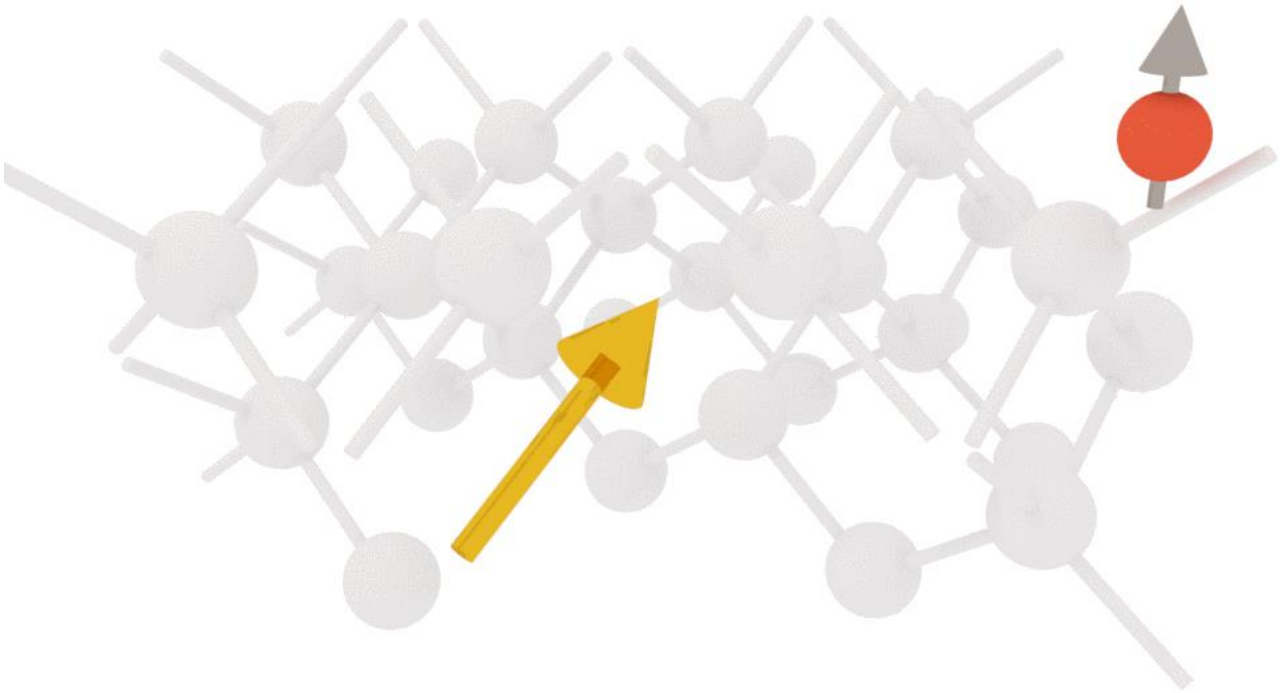

THE NV CENTER

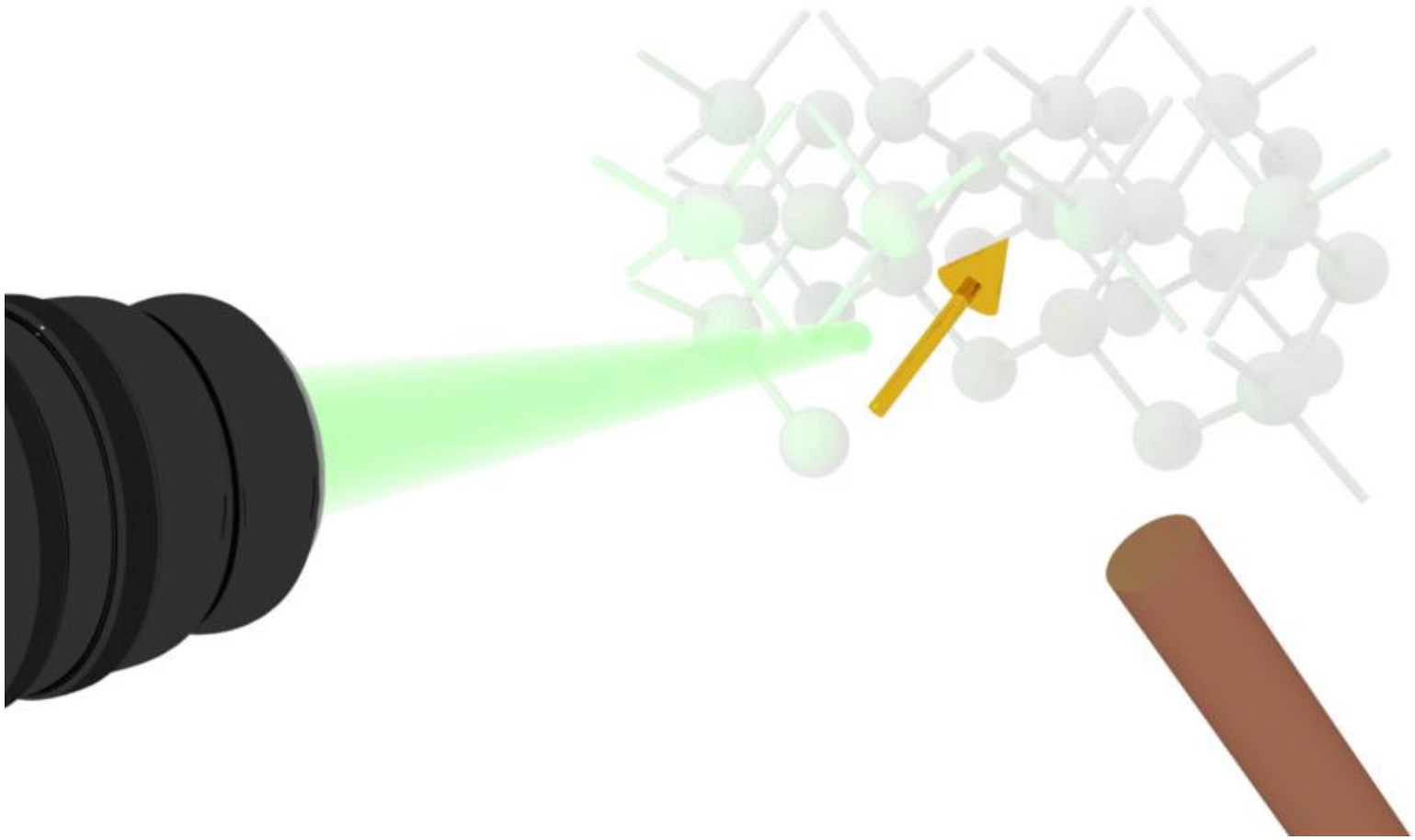

THE NV CENTER

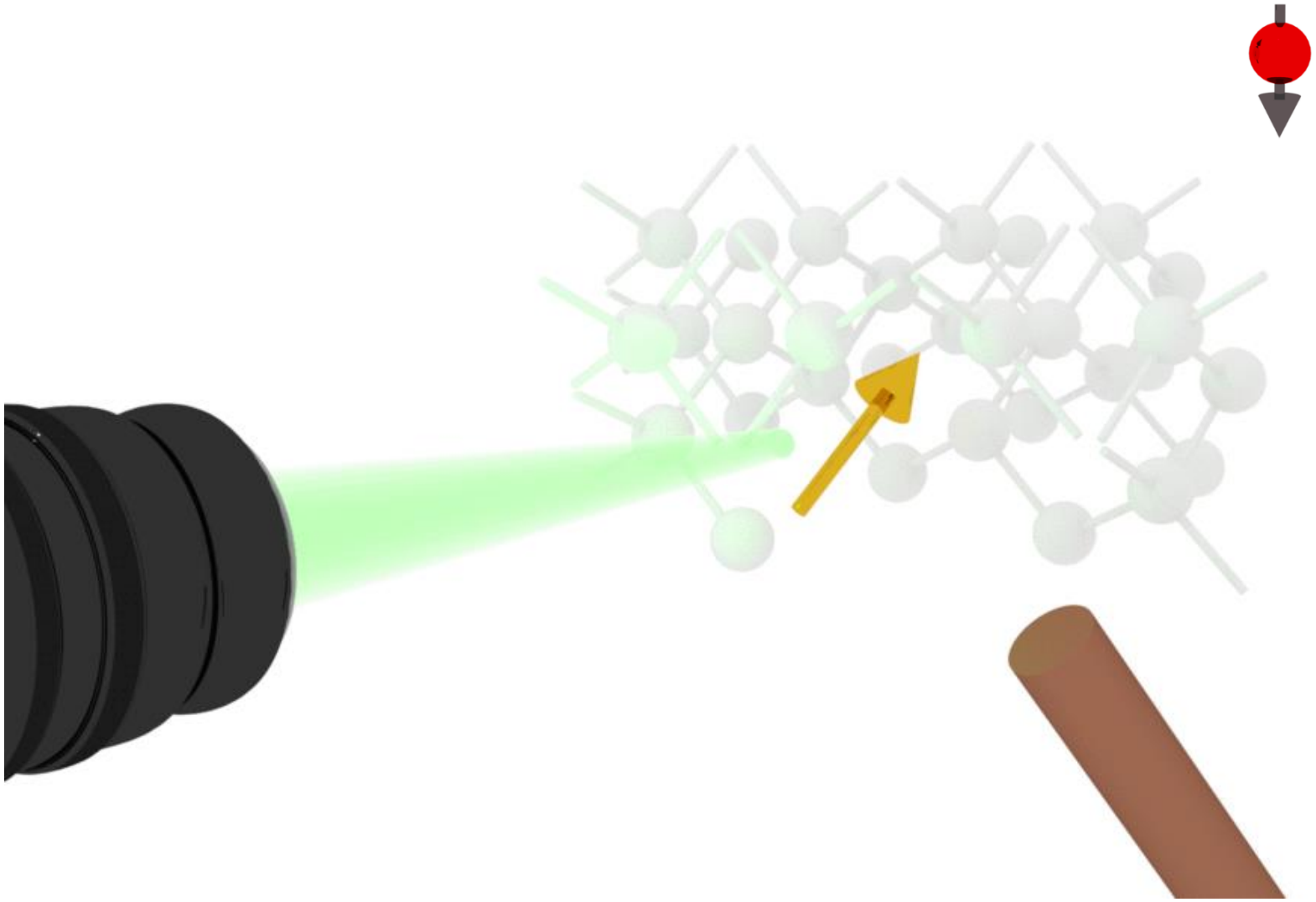

THE NV CENTER

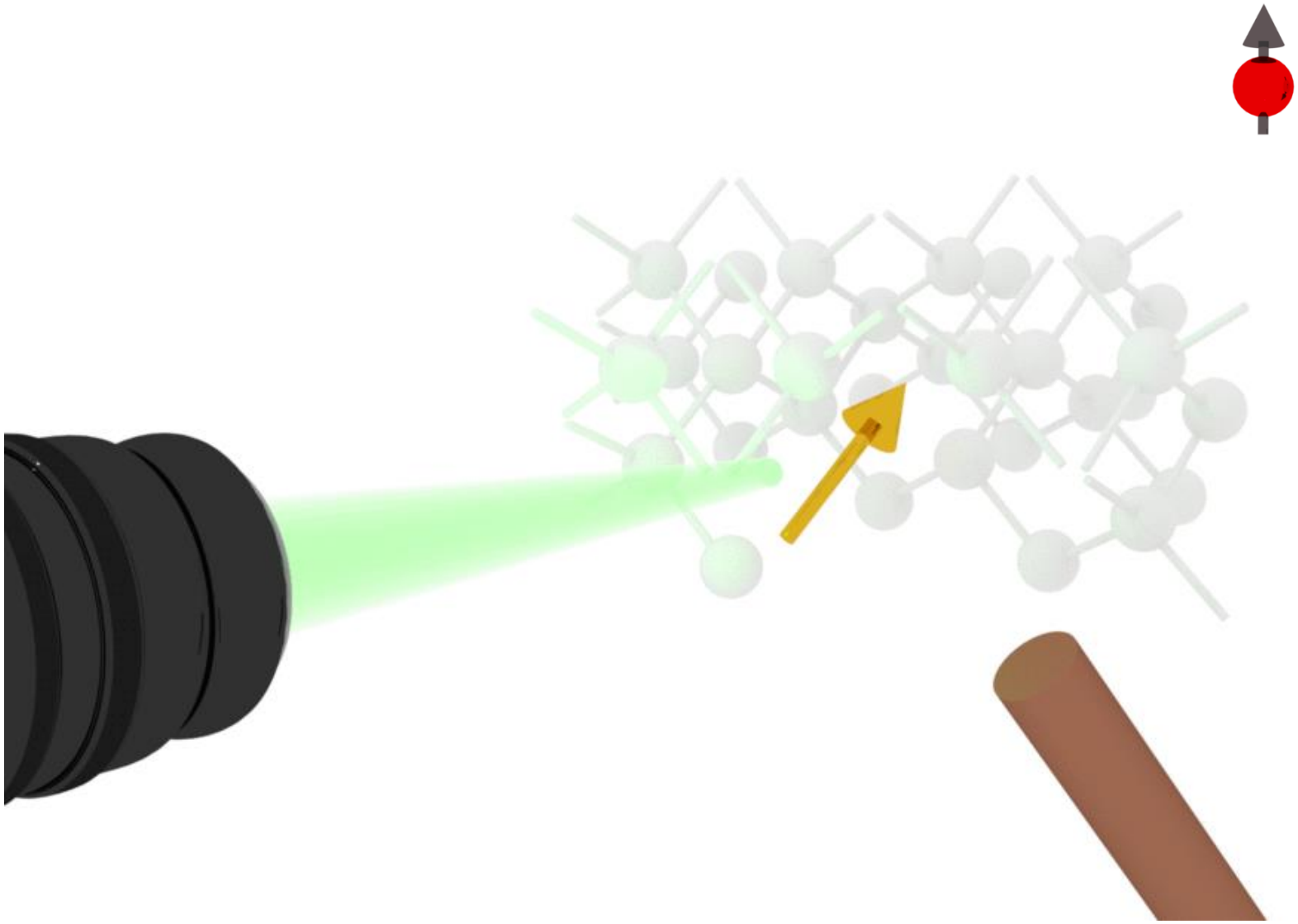

THE NV CENTER

- ✓ Electron spin
- ✓ Good properties conferred by the diamond lattice
  - In particular, long $T_{1\rho}$
- ✓ Easy to manipulate
  - Polarize and Read-out

THE NV CENTER

Electron spin + Characteristic level structure

THE NV CENTER

Electron spin + Characteristic level structure

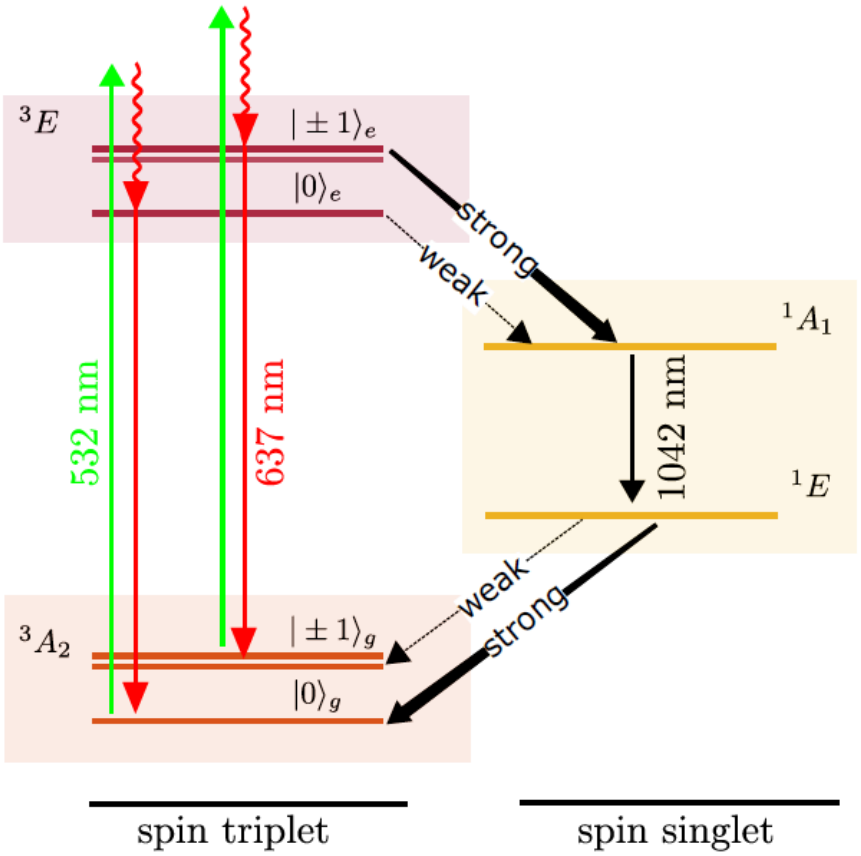

- When illuminated with green light:
  - ➢ Polarization
  - ➢ Read-Out

THE NV CENTER

Electron spin + Characteristic level structure

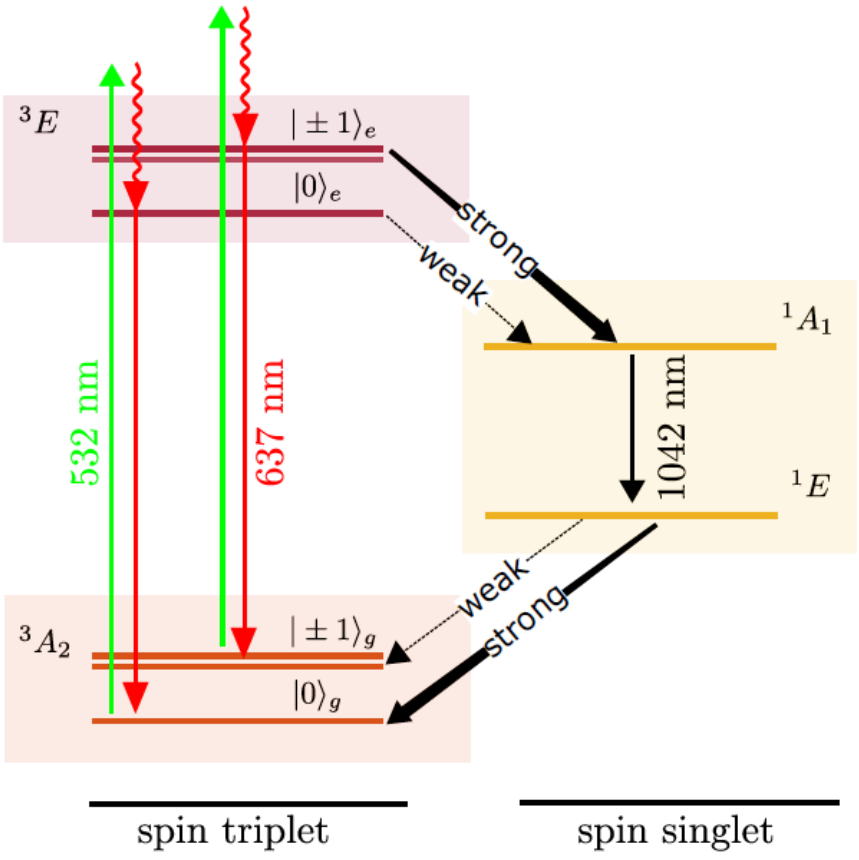

- When illuminated with green light:
  - ➢ Polarization
  - ➢ Read-Out

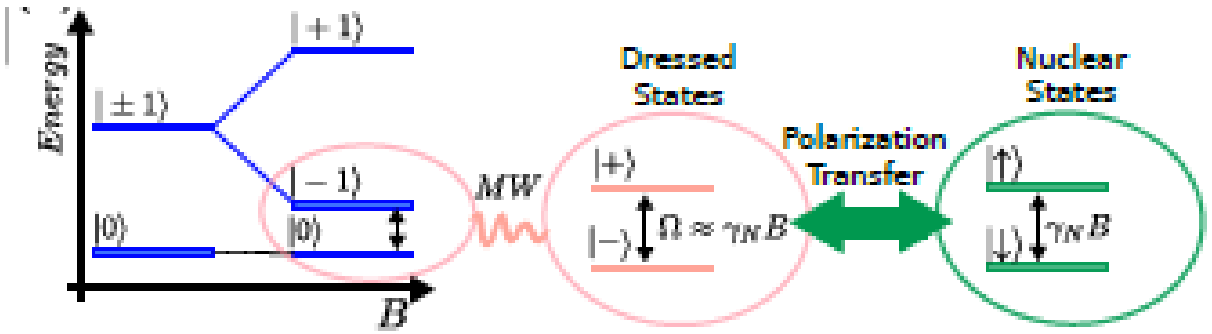

COHERENT CONTROL

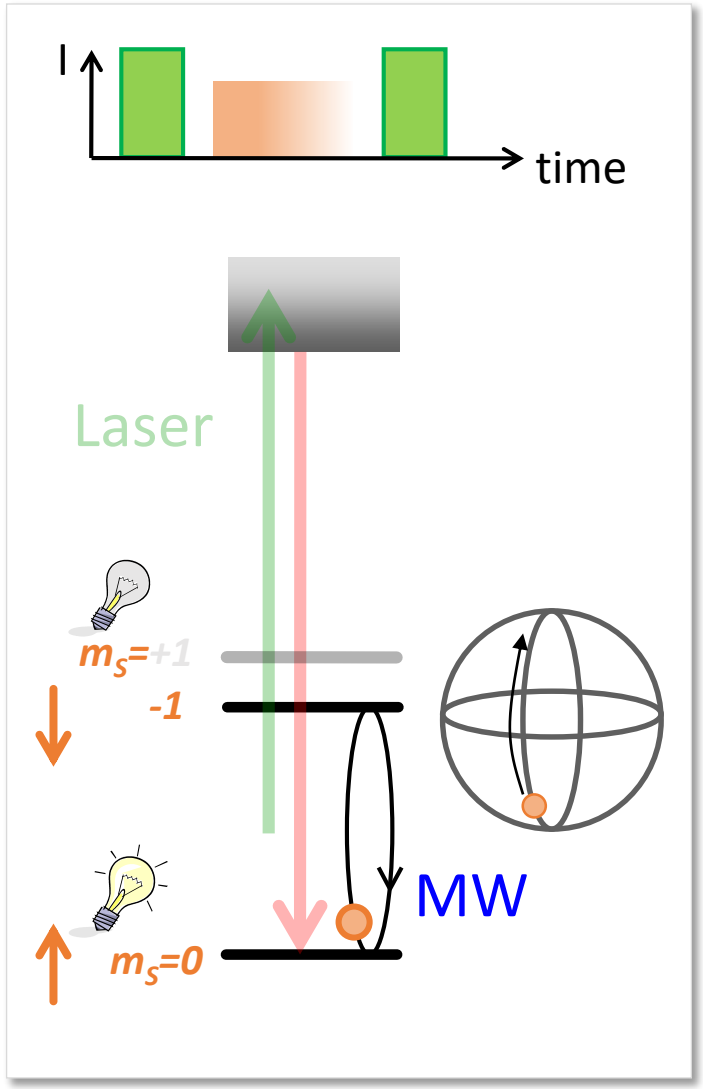

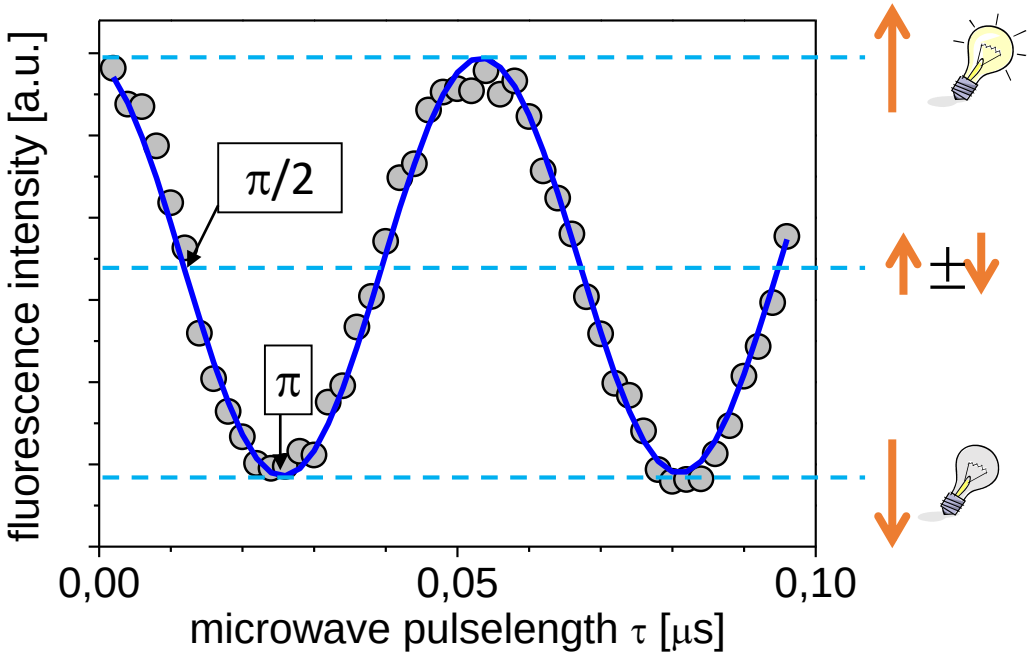

SINGLE SHOT READOUT 1 NUCLEAR SPIN

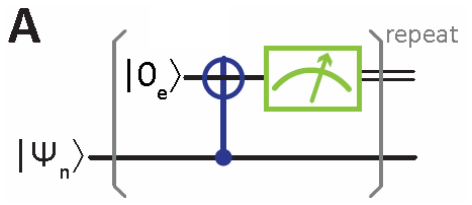

Repetitive QND measurements reveal quantum jumps of a single nuclear spin (in diamond at room temperature)

Neumann et al., Science 2010

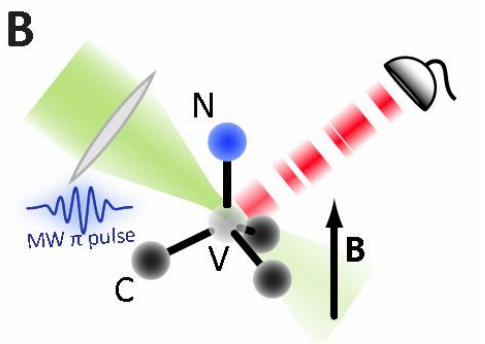

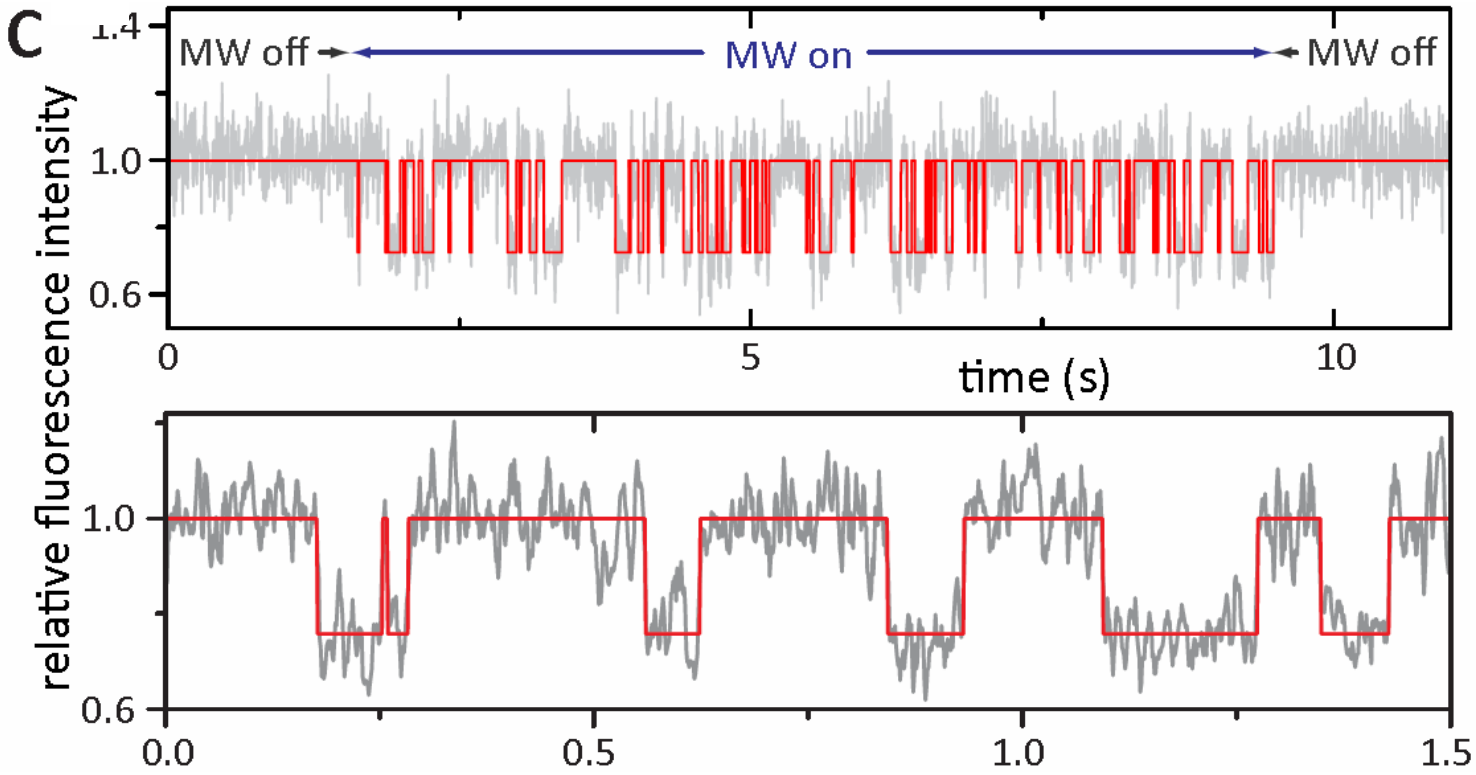

THE NV CENTER

Electron spin + Characteristic level structure

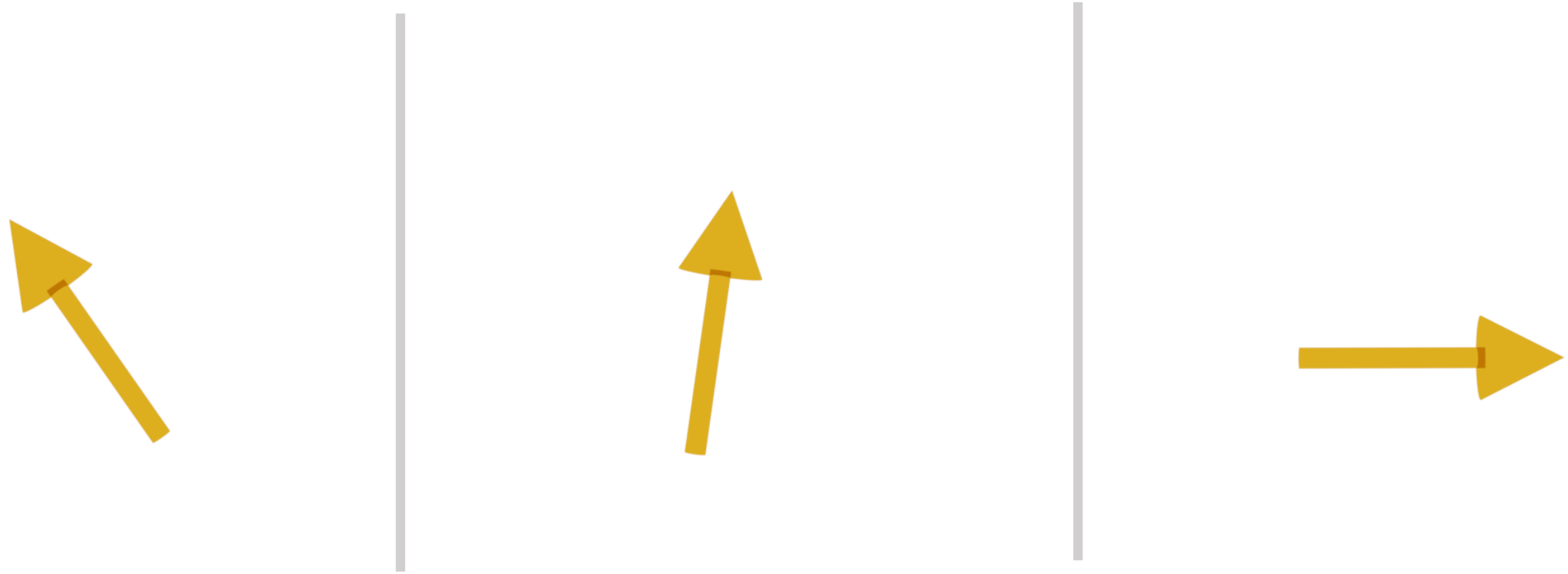

THE NV CENTER

Electron spin + Characteristic level structure

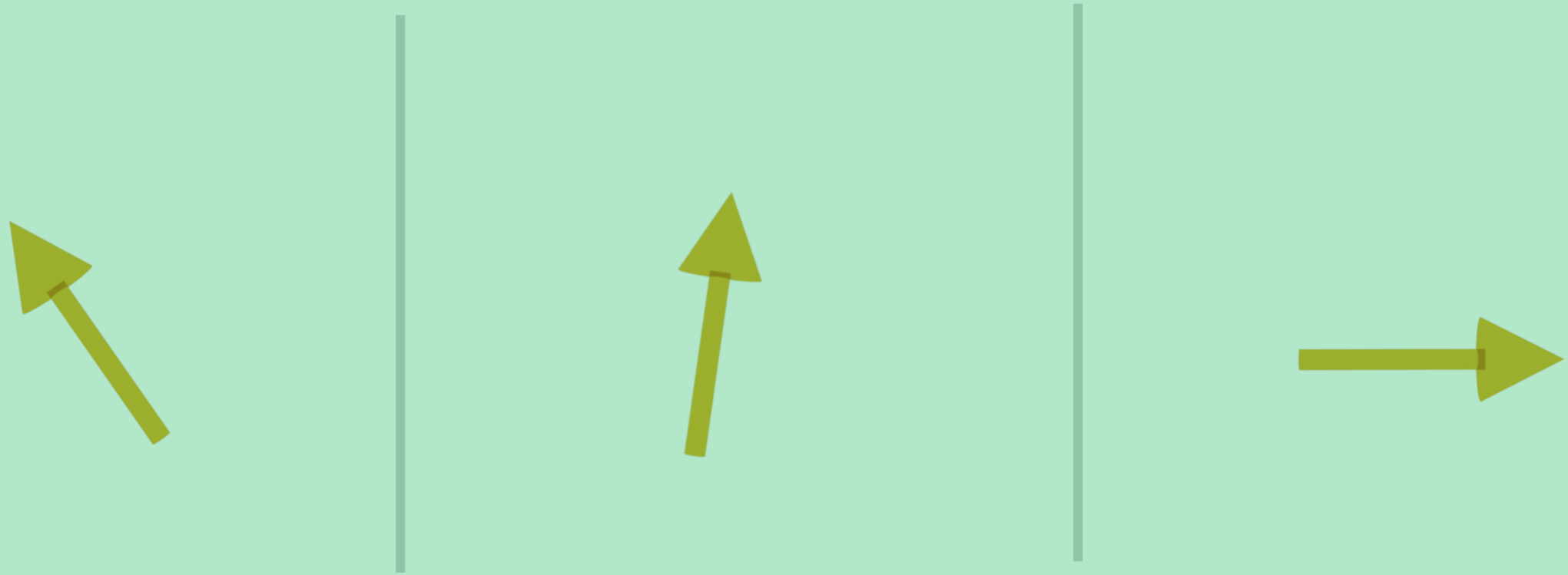

THE NV CENTER

Electron spin + Characteristic level structure

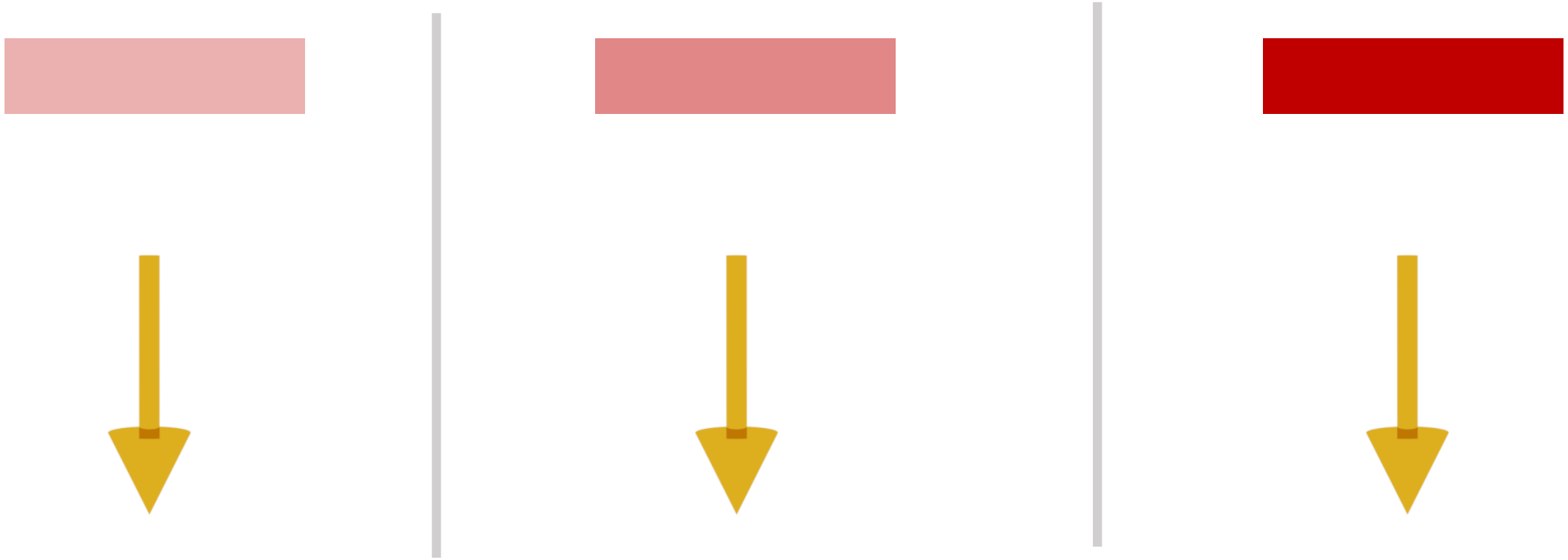

POLARIZATION TRANSFER

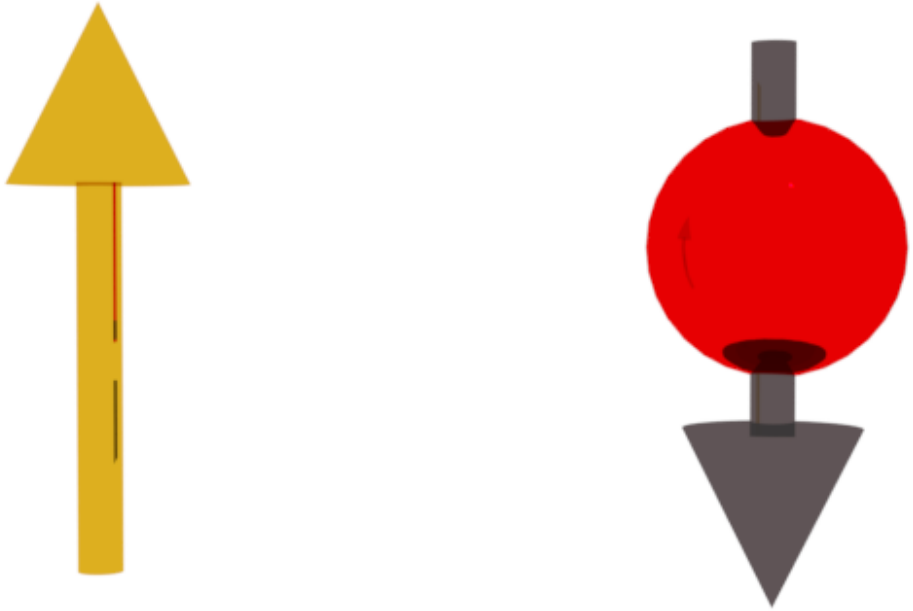

POLARIZATION TRANSFER

POLARIZATION TRANSFER

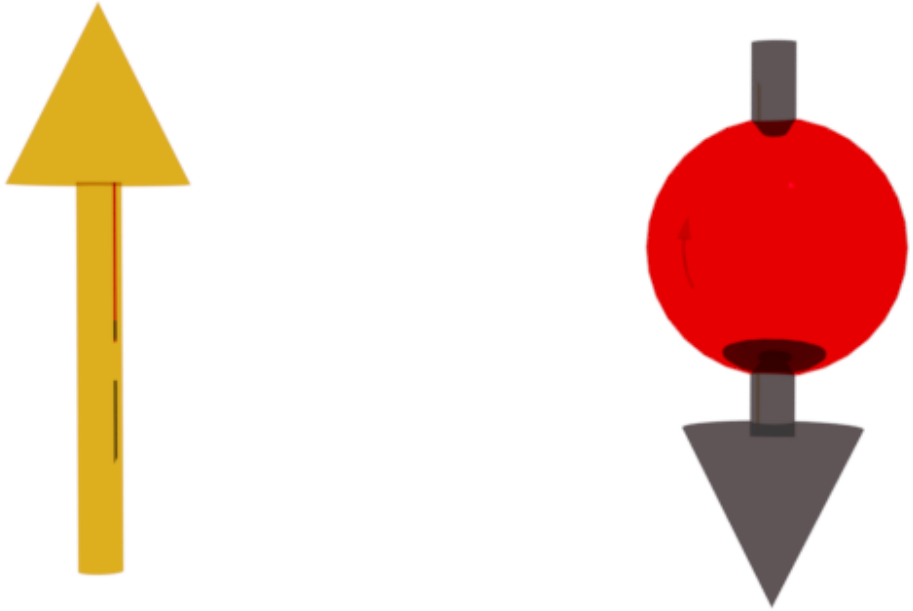

POLARIZATION TRANSFER

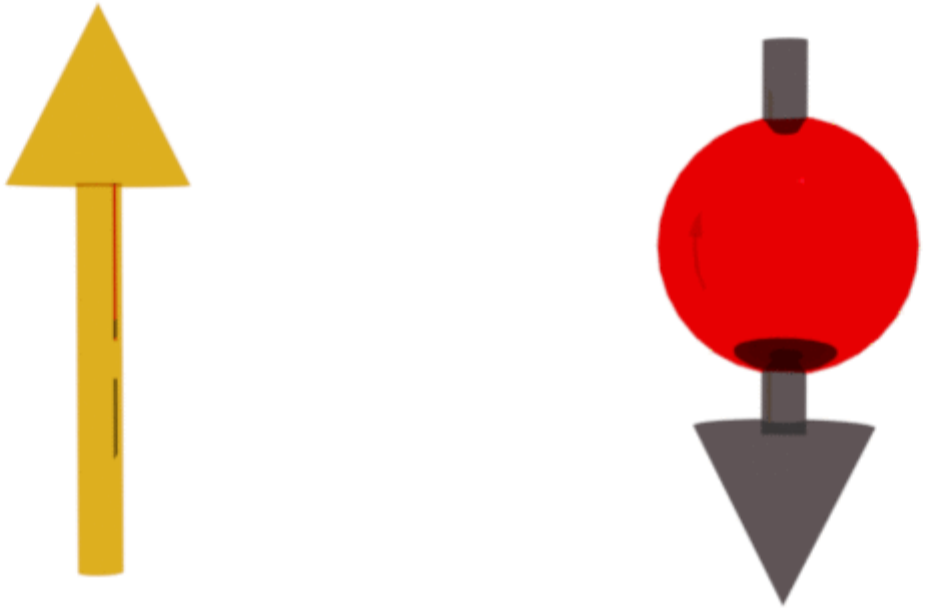

LARGE SPIN SYSTEMS

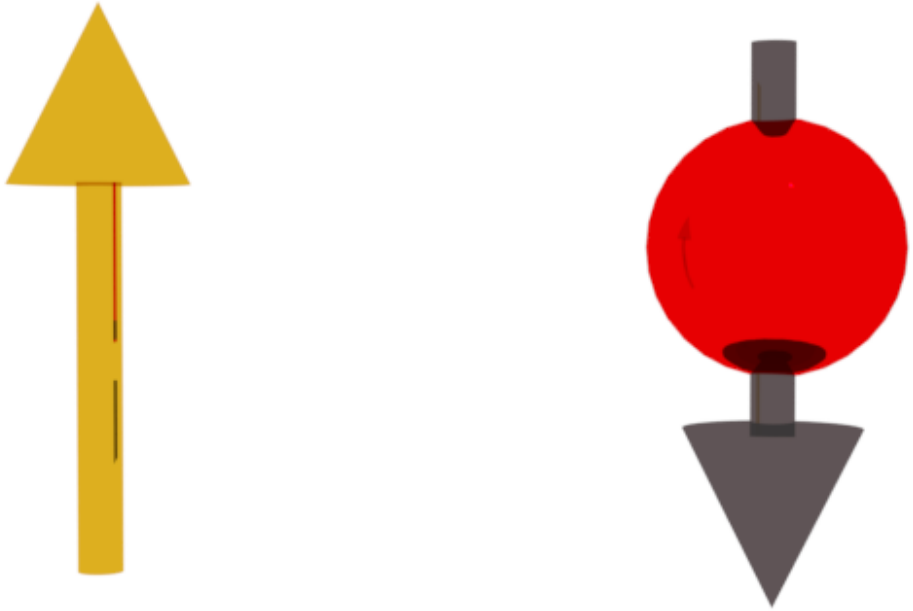

LARGE SPIN SYSTEMS

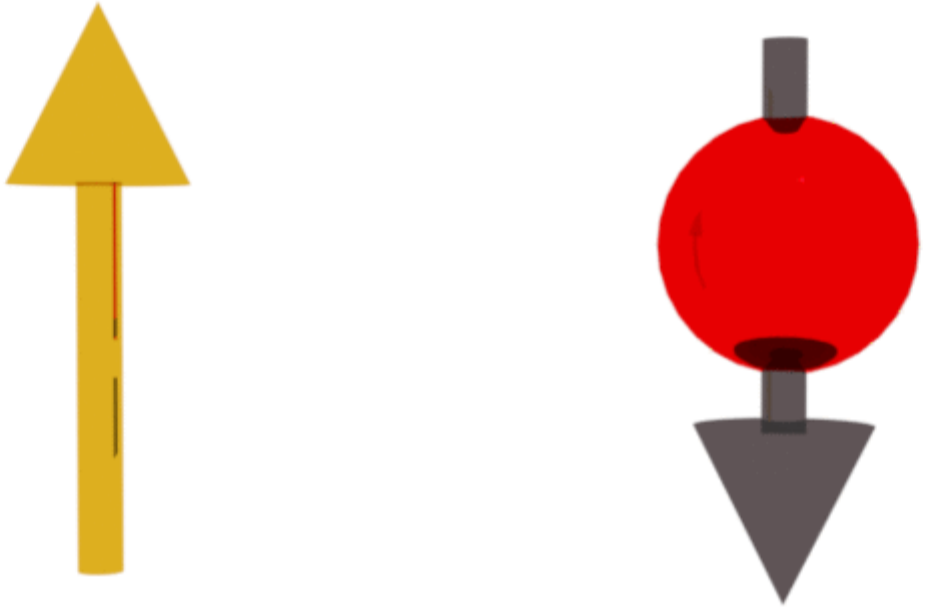

LARGE SPIN SYSTEMS

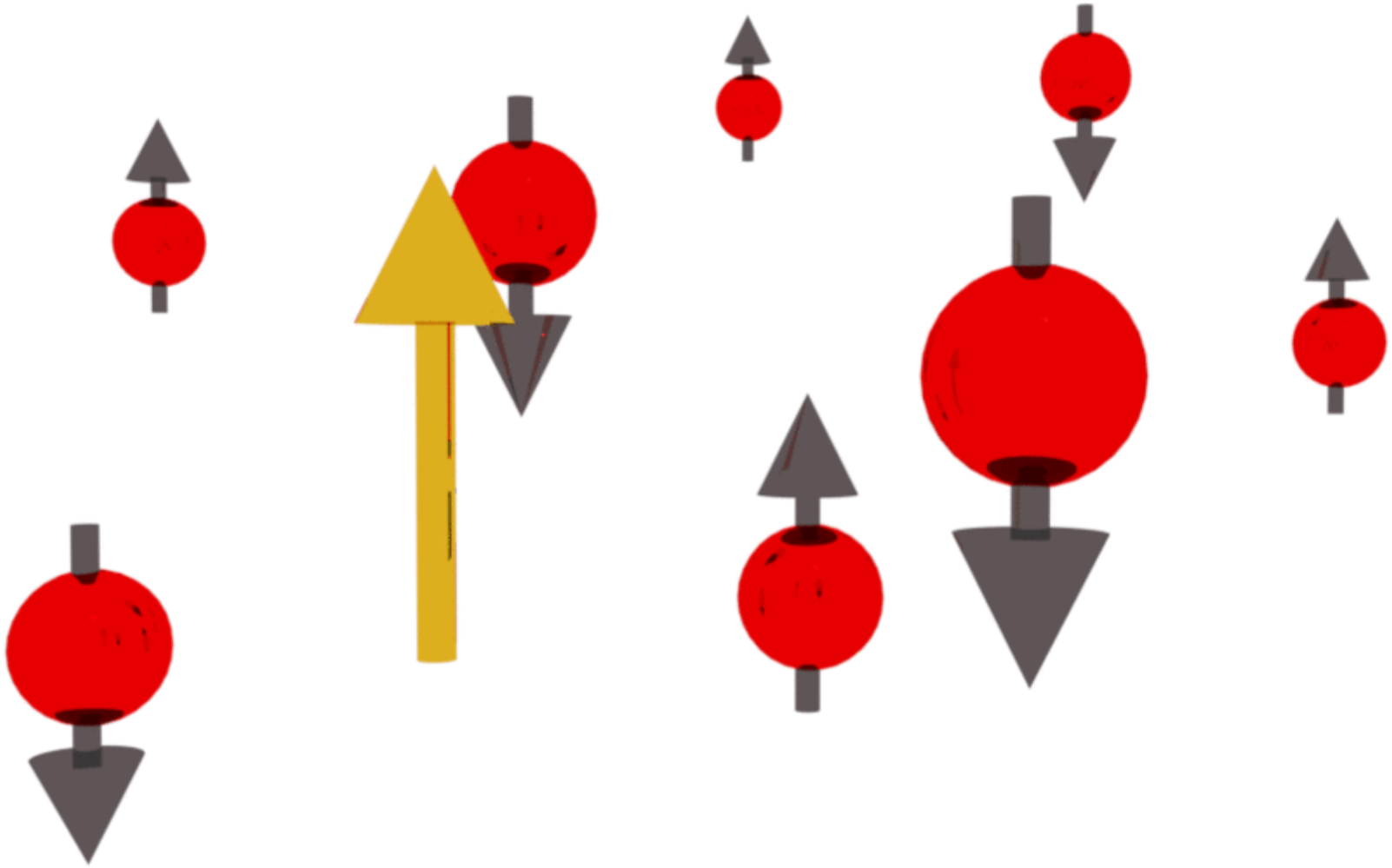

GENERAL NMR SCENARIO

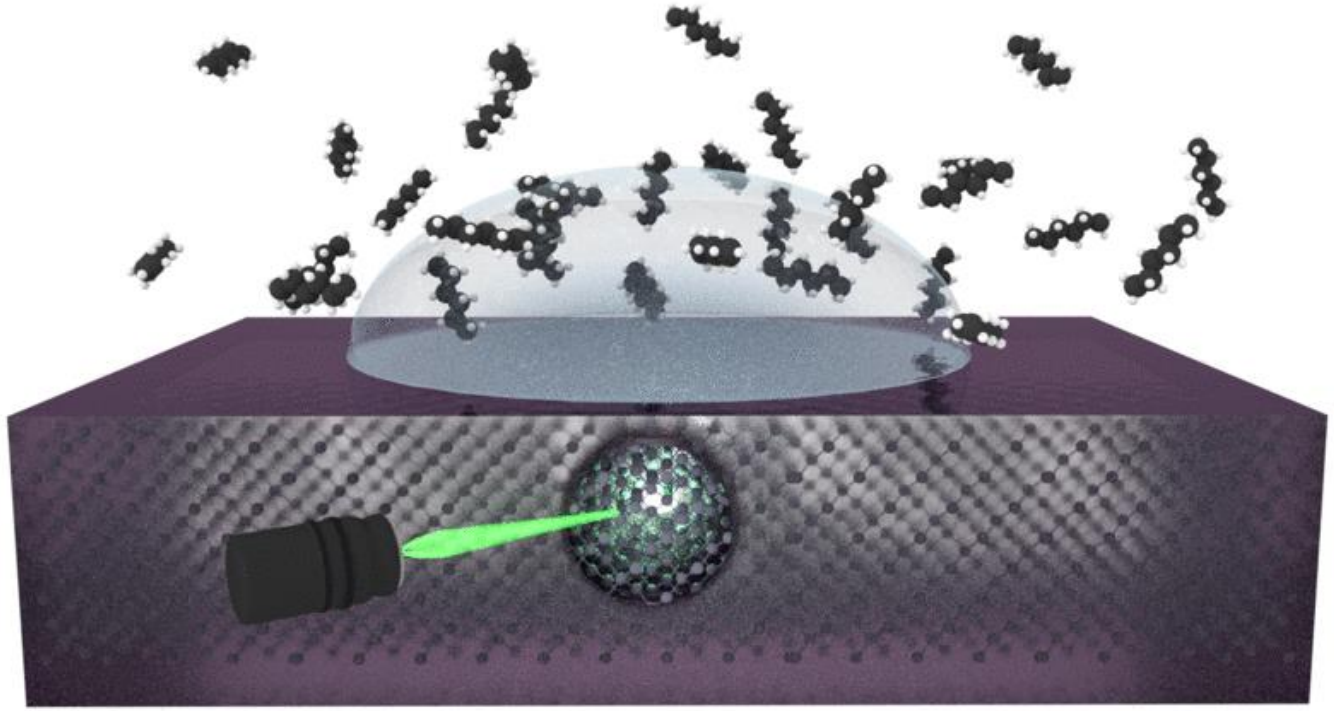

GENERAL NMR SCENARIO

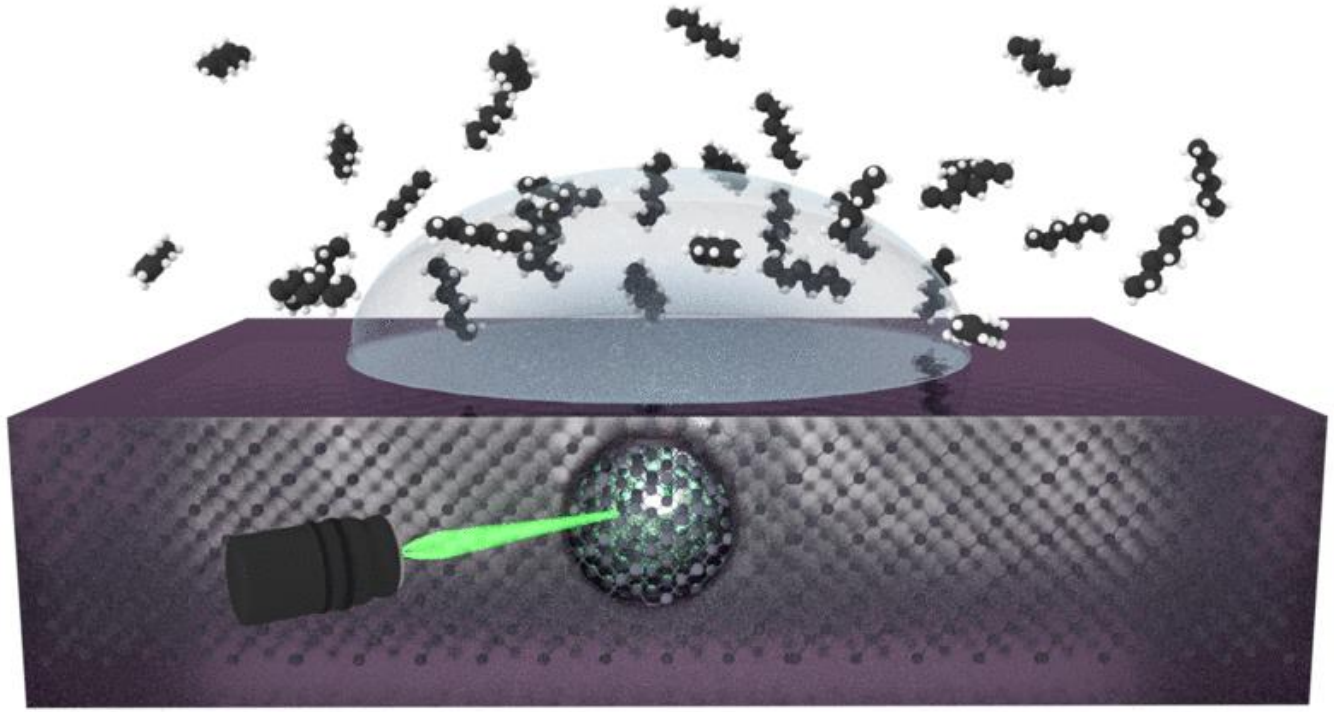

?

$$H_{eff}(t) = B(t)_z$$

CHEMISTRY FREE LAB ON A CHIP

Small amount – targeting statistical polarization

NMR AND SIGNAL PROCESSING

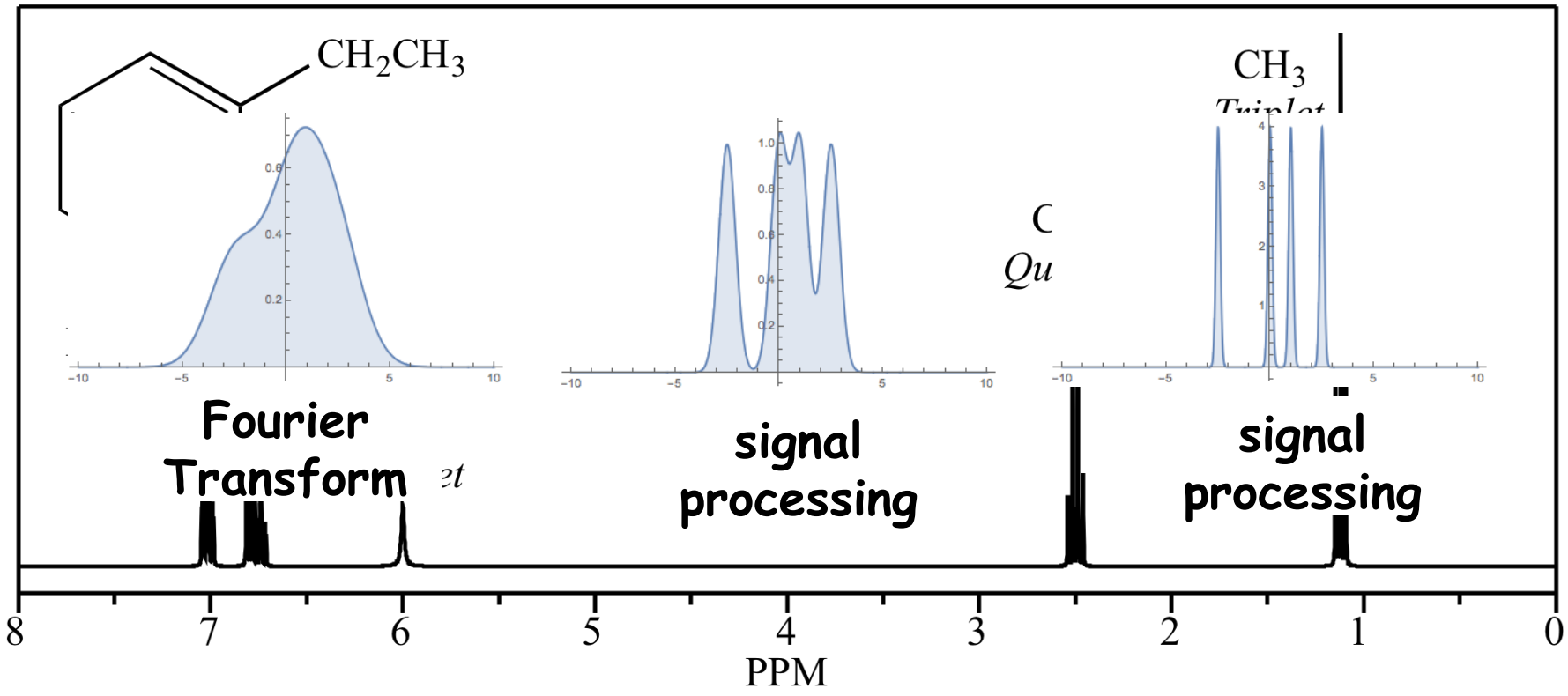

PHASE SENSITIVE MEASUREMENTS

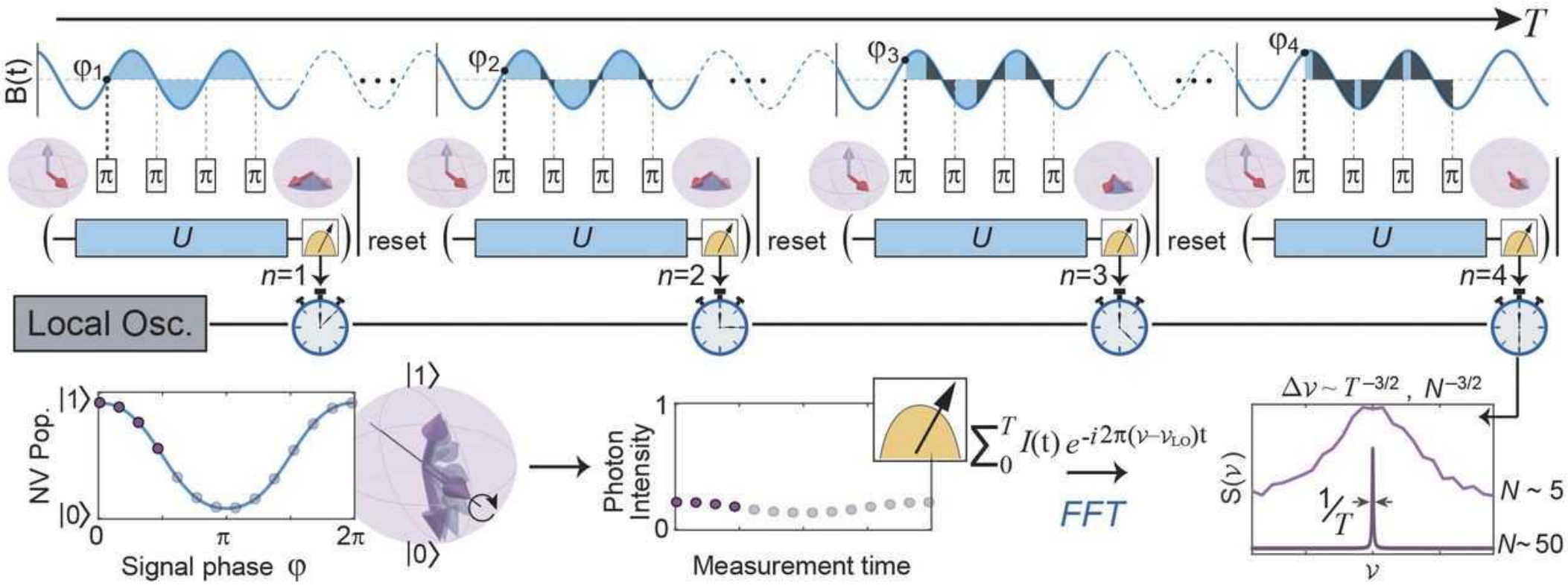

Submillihertz magnetic spectroscopy performed with a nanoscale quantum sensor. Simon Schmitt, Tuvia Gefen, et. al. *Science* 26 May 2017: Vol. 356, Issue 6340, pp. 832-837.

LIMITS OF SPECTRAL RESOLUTION MEASUREMENTS BY QUANTUM PROBES

There is a crucial difference between the ability to resolve a few frequencies and the precision of estimating a single one. Whereas the efficiency of single frequency estimation gradually increases with the square root of the number of measurements, the ability to resolve two frequencies is limited by the specific time scale of the signal and cannot be compensated for by extra measurements.

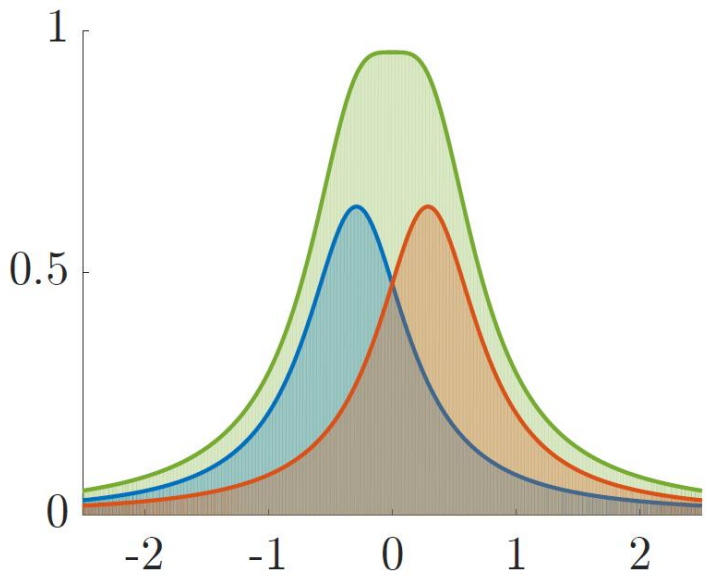

LIMITS OF SPECTRAL RESOLUTION MEASUREMENTS BY QUANTUM PROBES

Phase sensitive measurement

$+$

Adequate post processing

$\Downarrow$

Resolution limit $\neq$ Rayleigh limit

$\Downarrow$

Scales like single frequency estimation

MAXIMUM LIKELIHOOD ESTIMATION

- Given measurement data $x_t \sim p_t(\{\Omega_j, \delta_j, \varphi_j\})$
- Best estimator for δ_j
- Cramer- Rao bound: $\Delta(\delta) \sim {}^{1}/_{\sqrt{I_{\delta,\delta}}}$
- Maximum Likelihood estimation saturates the Cramer-Rao bound

Likelihood function:

$$L(x; t|\{\Omega_k, \delta_k, \varphi_k\}) = \prod_{j=1}^{n} {q_j}^{x_j}(1 - q_j)^{1-x_j}$$

Probability for detecting a photon

$$q_j = r_{\downarrow}(1 - p_j) + r_{\uparrow} p_j$$

QUBIT AS A MAGNETOMETER

$$\Delta w = g m B$$

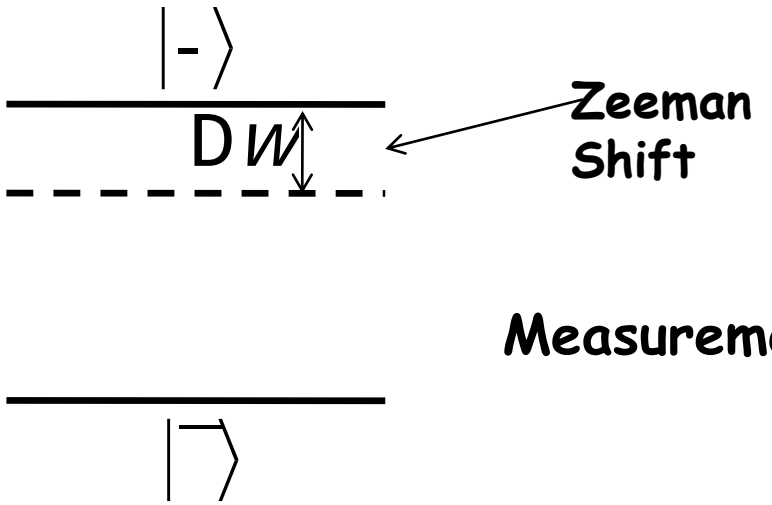

Measurement results: 0,1,1,1,0,0,1,0,1,0,.....

$$p_{\uparrow} = \frac{1 + \cos(\Delta\omega t)}{2}$$

THE PROBLEM: MATHEMATICAL ANALYSIS

NV dynamics: $H(t) = \sigma_z \sum_{k=1}^{2} \Omega_k \cos(\delta_k t + \varphi_k)$

Probability of detecting a photon:

$$p_j = \sin^2\left(\sum_{k=1}^{2} \Omega_k \tau \, \mathrm{sinc}\left(\frac{\delta_k \tau}{2}\right) \cos\left(\delta_k t_j + \varphi_k\right)\right) + \frac{\pi}{4}$$

The Cramér-Rao bound reads $\Delta(\delta_2 - \delta_1) \sim \dfrac{1}{\Omega^2 \, \tau^{\frac{3}{2}} {T_\varphi}^2 \sqrt{T} \, (\delta_2 - \delta_1)}$

Therefore, in the limits of $|\delta_2 - \delta_1| T \ll 1$,
no resolution seems possible.

LIMITS OF SPECTRAL RESOLUTION MEASUREMENTS BY QUANTUM PROBES

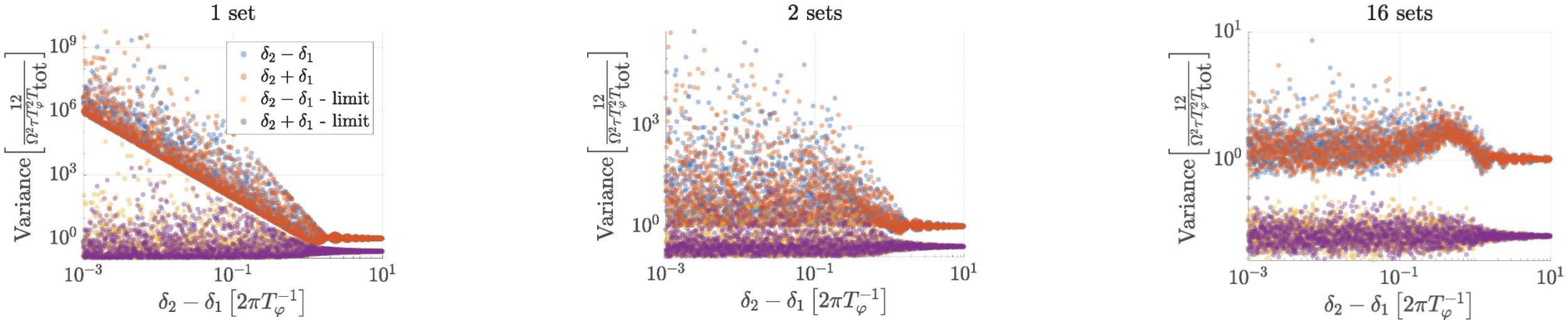

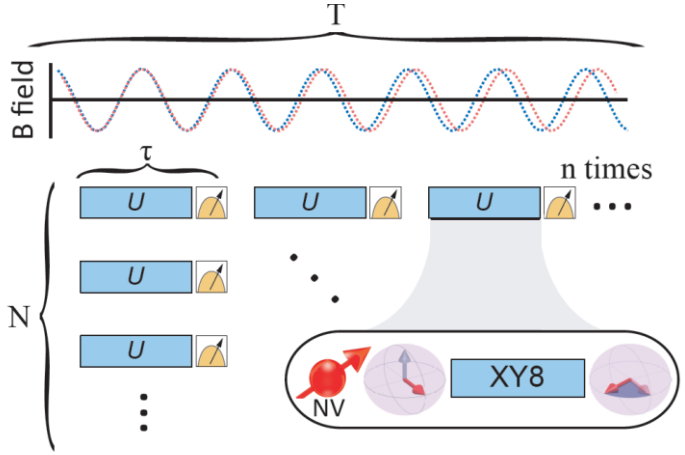

INTUITION

We want to estimate $\delta = |\delta_2 - \delta_1|$. In the limit of $\Omega\tau \ll 1$ and $\delta T_\varphi \ll 1$, the probability is simplified to:

$$p \approx \frac{1}{2} + \Omega\tau(cos(\varphi) - sin(\varphi)\delta t)$$

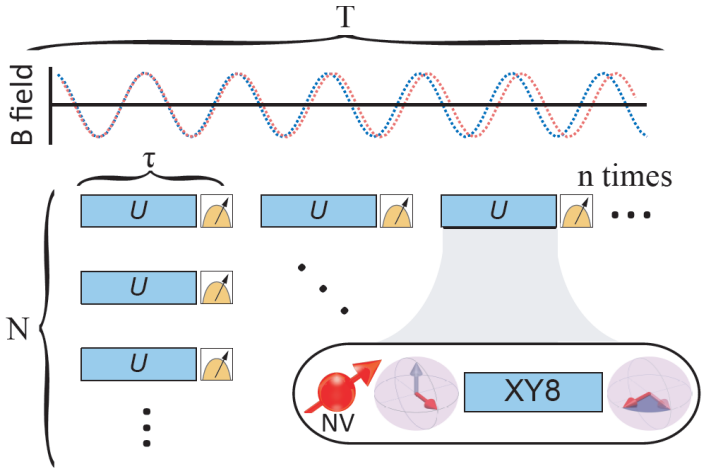

$\Omega\cos\varphi_1$
$\Omega\delta\sin\varphi_1$
$\delta, \Omega, \varphi_1$

INTUITION

We want to estimate $\delta = |\delta_2 - \delta_1|$. In the limit of $\Omega\tau \ll 1$ and $\delta T_\varphi \ll 1$, the probability is simplified to:

$$p \approx \frac{1}{2} + \Omega\tau(cos(\varphi) - sin(\varphi)\delta t)$$

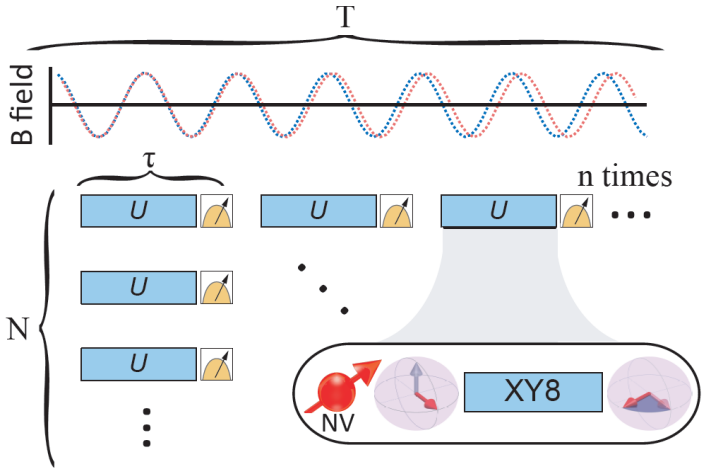

$\Omega\cos\varphi_1$ $\Omega\cos\varphi_2$

$\Omega\delta\sin\varphi_1$ $\Omega\delta\sin\varphi_2$

$\delta, \Omega, \varphi_1$ φ_2

LIMITS OF SPECTRAL RESOLUTION MEASUREMENTS BY QUANTUM PROBES

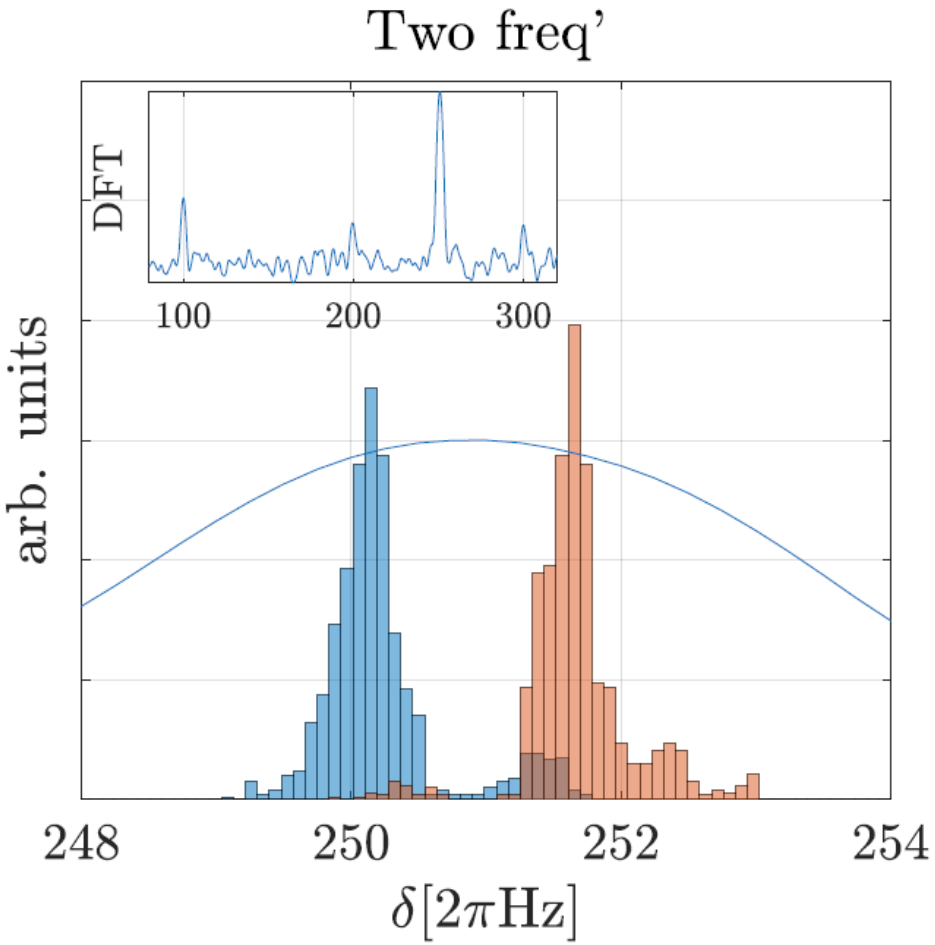

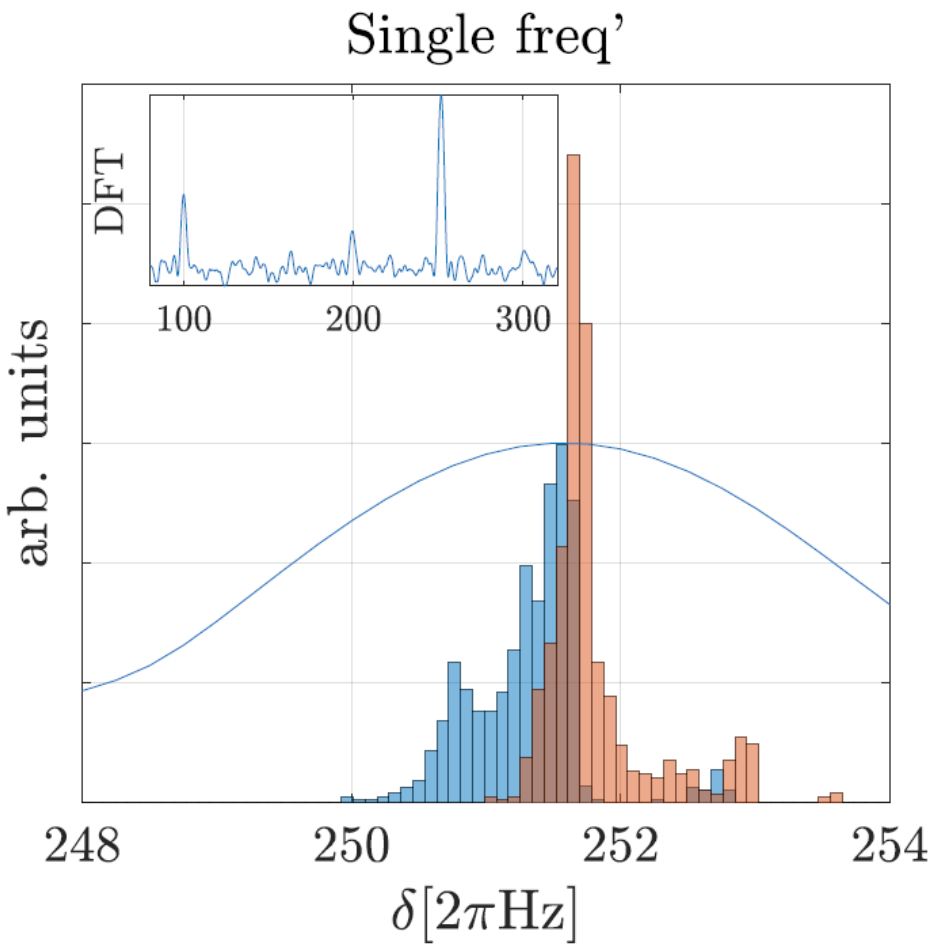

Resolving the experimental data. Fig. Left: Two frequencies with a frequency difference below the DFT limit, δ_1 = 250 [2πHz] and δ_2 = 251.6 [2πHz] (δ_2 - δ_1 = 0.4 [$2\pi/T_\varphi$]), were resolved. The Rabi-frequency of the signal was $\Omega\approx$12 [2πkHz]. The inset, and the blue line over the histogram, show the DFT of 33 measurement sets. The figure depicts a histogram of the estimators from 2^{10} iterations of MLE, each over the 33 measurement sets randomly chosen from the total of 880 data-sets. The average estimators are $<\delta_1>$= 250.22 ± 0.45 [2πHz], and $<\delta_2>$= 251.68 ± 0.40 [2πHz] (the errors represent the SD); i.e., over 2.4σ apart. Fig. Right: The result of the same procedure, for data containing only a single frequency. The average of the difference is $<|\delta_2 - \delta_1|>$= 0.51 ± 0.53 [2πHz].

LIMITS OF SPECTRAL RESOLUTION MEASUREMENTS BY QUANTUM PROBES

Assuming constant amplitudes (more on that in a few slides), adding new measurements increases degrees of freedom by two, but constraints by four! The requirement is phases that change in a random fashion. Which occurs in the case of quantum noises!

$$I^{(t)}_{\theta_i\theta_j} = \frac{1}{p_t(1-p_t)}\frac{dp_t}{d\theta_i}\frac{dp_t}{d\theta_j}$$

Fisher Information matrix

$$\Delta(\theta_j) \geq \sqrt{\frac{1}{I_{\theta_j\theta_j}}}$$

Cramér-Rao bound

$$\Delta(\delta_n) = \sqrt{12}\sqrt{\frac{\frac{r_\uparrow + r_\downarrow}{2}\left(1 - \frac{r_\uparrow + r_\downarrow}{2}\right)}{(r_\uparrow - r_\downarrow)^2}}\frac{1}{\Omega_n\sqrt{\tau}T_\varphi^{3/2}\sqrt{N}}$$

INTUITION; UNPOLARIZED NMR

We want to estimate $\delta = |\delta_2 - \delta_1|$. In the limit of $\Omega\tau \ll 1$ and $\delta T_\varphi \ll 1$, the probability is simplified to:

$$p \approx \frac{1}{2} + \Omega\tau(cos(\varphi) - sin(\varphi)\delta t)$$

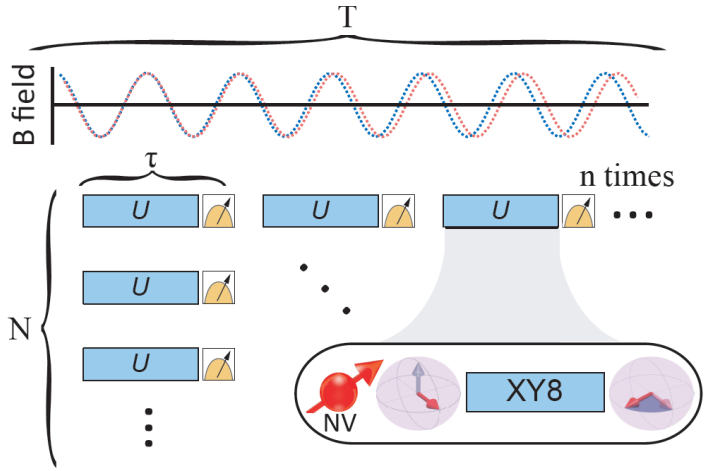

$\Omega_1 \cos\varphi_1$
$\Omega_1 \delta \sin\varphi_1$
$\delta, \Omega_1, \varphi_1$

INTUITION; UNPOLARIZED NMR

We want to estimate $\delta = |\delta_2 - \delta_1|$. In the limit of $\Omega\tau \ll 1$ and $\delta T_\varphi \ll 1$, the probability is simplified to:

$$p \approx \frac{1}{2} + \Omega\tau(cos(\varphi) - sin(\varphi)\delta t)$$

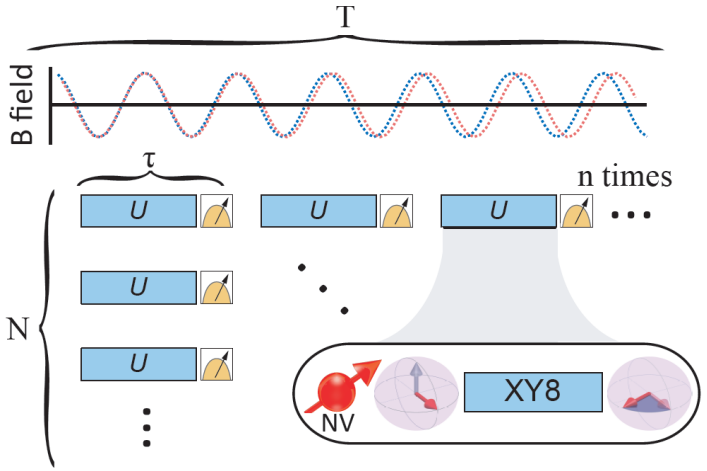

$\Omega_1 \cos\varphi_1$ $\Omega_2 \cos\varphi_2$

$\Omega_1 \delta \sin\varphi_1$ $\Omega_2 \delta \sin\varphi_2$

$\delta, \Omega_1, \varphi_1$ Ω_2, φ_2

INTUITION; UNPOLARIZED NMR

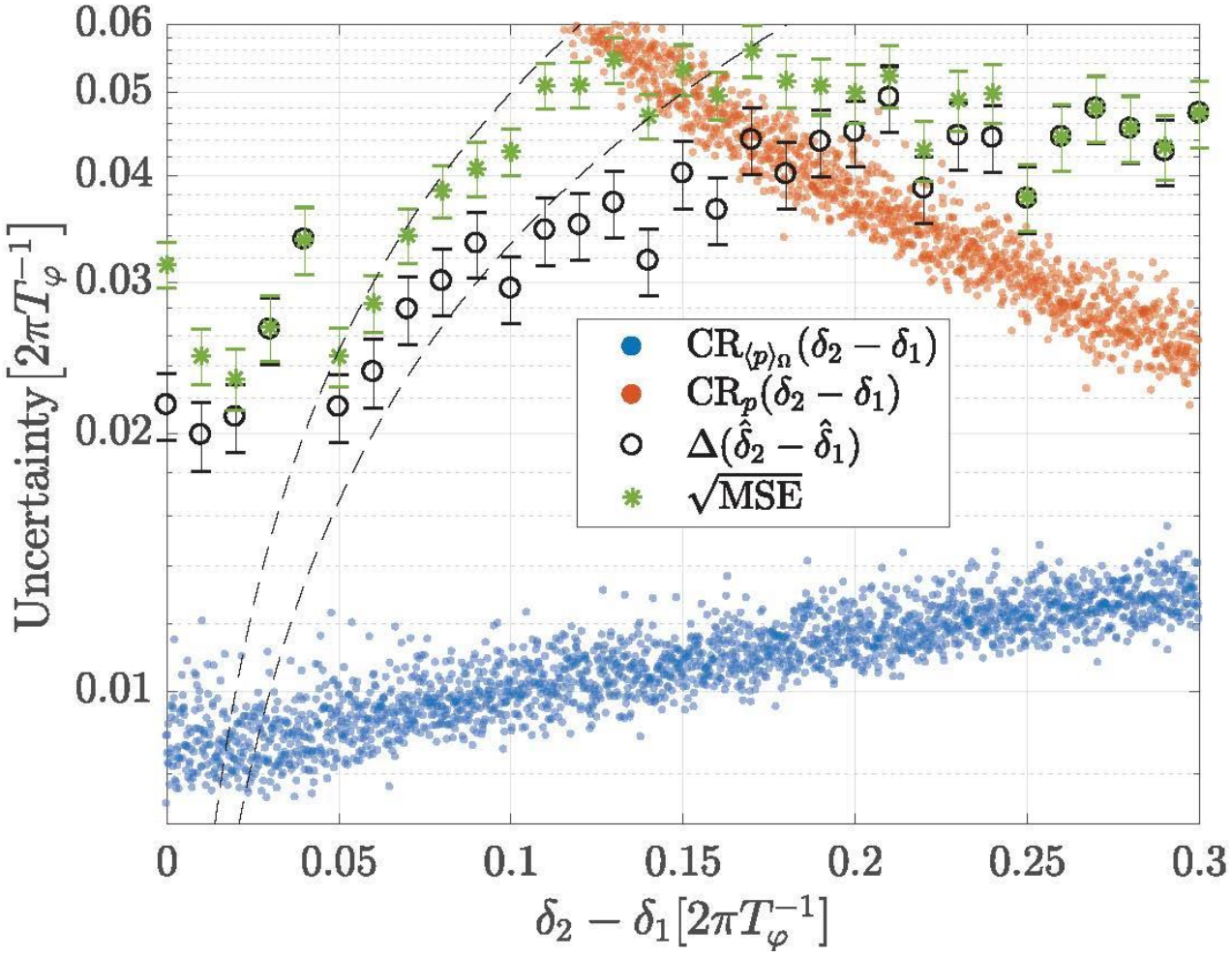

NANO-NMR VELOCITY-METER

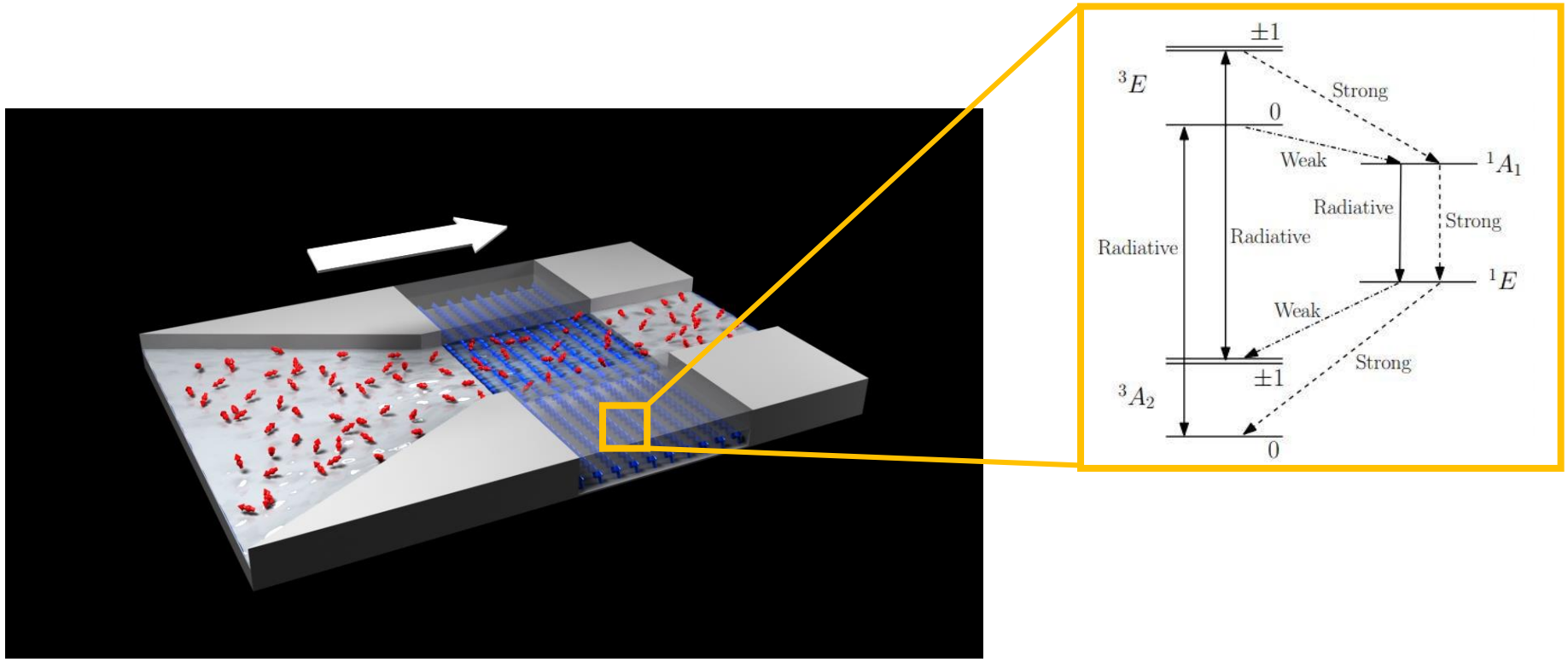

SENSING DYNAMICAL FEATURES OF LIQUIDS

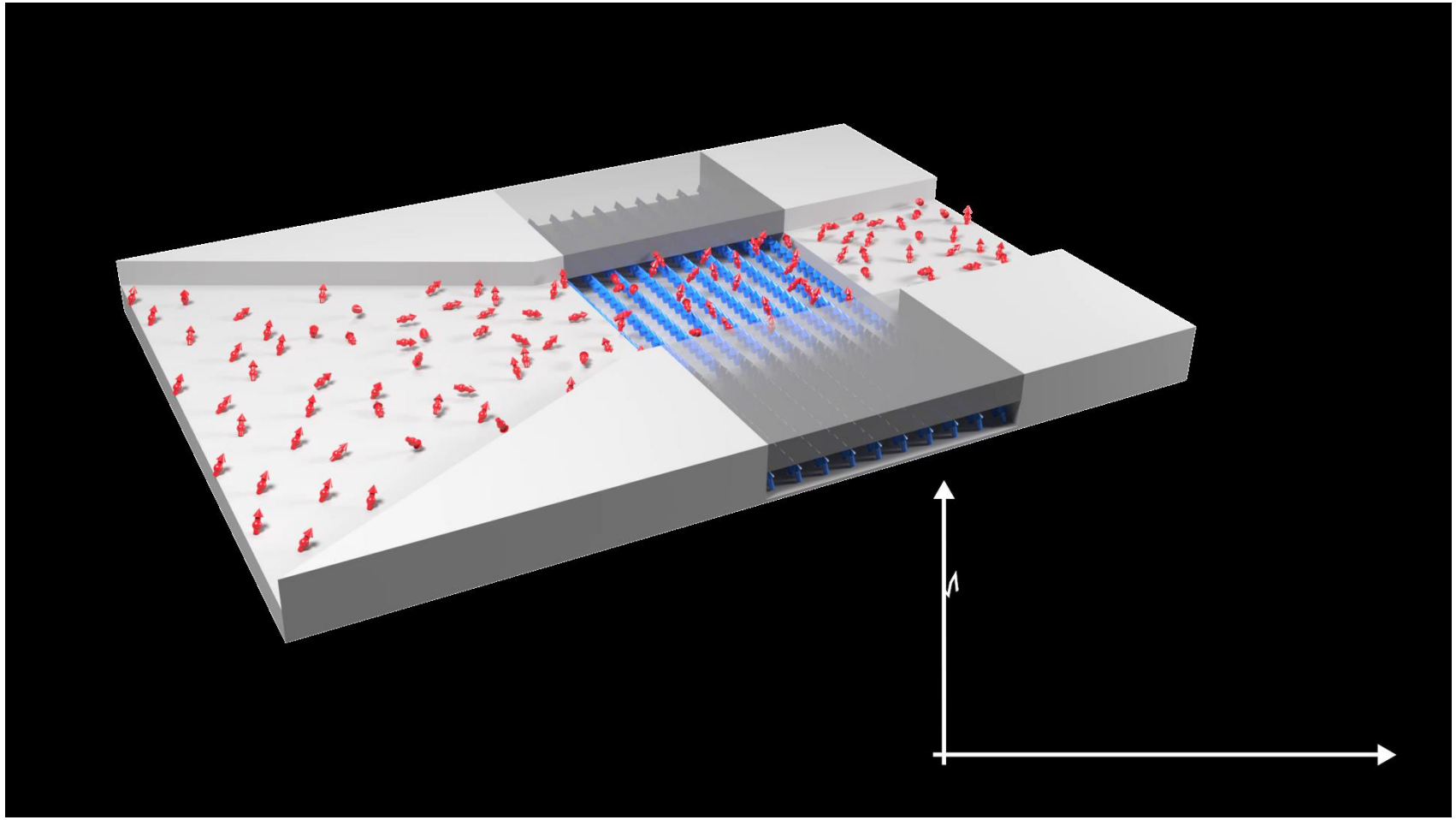

CONCLUSIONS

- We have shown theoretically and verified experimentally that resolution scales like $\approx {}^{1}/_{\sqrt{N}}$
- Utilising phase and amplitude noise it is possible to increase the resolution of nano-NMR experiments beyond the line-width paradigm

THE TEAM


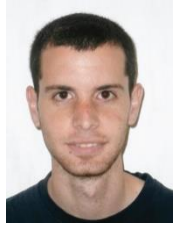




THANKS

Limits of spectral resolution measurements by quantum probes

Funding:

Universidad Politécnica de Cartagena

GOBIERNO DE ESPAÑA MINISTERIO DE ECONOMÍA Y COMPETITIVIDAD

f SéNeCa(+)
Agencia de Ciencia y Tecnología
Región de Murcia

MR IS FUNDAMENTAL TOOL IN BASIC RESEARCH AND CLINICAL IMAGING

Nuclear magnetic resonance (NMR)

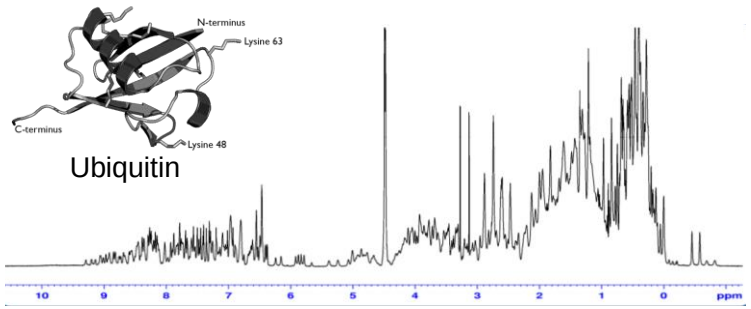

- Used for static and dynamic characterization of molecules (structure, interaction, motion, reactions, etc.)
- Sensitive to atom type and molecular environment

~10,000 units WW

Magnetic resonance imaging (MRI)

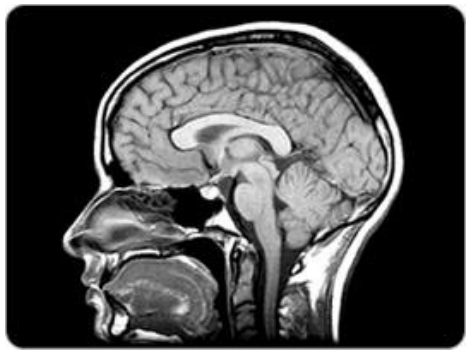

- Used for medical imaging by differentiating MR properties (decoherence, relaxation) of different tissues

~36,000 units WW

MR IS FUNDAMENTAL TOOL IN BASIC RESEARCH AND CLINICAL IMAGING

	NMR Polarizer	MRI Polarizer
		
Overview	External solution for the NMR industry	External solution for MRI medical centers
Impact	• **Sensitivity-enhanced NMR** (from mM-µM to nM) • **x1,000 shorter measurement time**, fits drug discovery cycles • **Cheap and easy to use** benchtop solutions	• **Metabolic imaging** of ^{13}C injected molecules, not just ^{1}H anatomical imaging • **Tumor diagnostics,** indicative to level of aggressiveness • **Real-time assessment**
Market size	$290-670mn	~$3bn

ACCURACY. HYPERPOLARIZED (HP) MRI HAS SHOWN TO BE A PROMISING METHOD COMPARED TO BOTH PET AND STANDARD MRI

Specific: HP MRI vs. PET

Hyperpolarized MRI has shown to be comparable, and in some cases superior to FDG-PET (here PET shows a false-positive result in canine sarcoma model) (2015)[1]

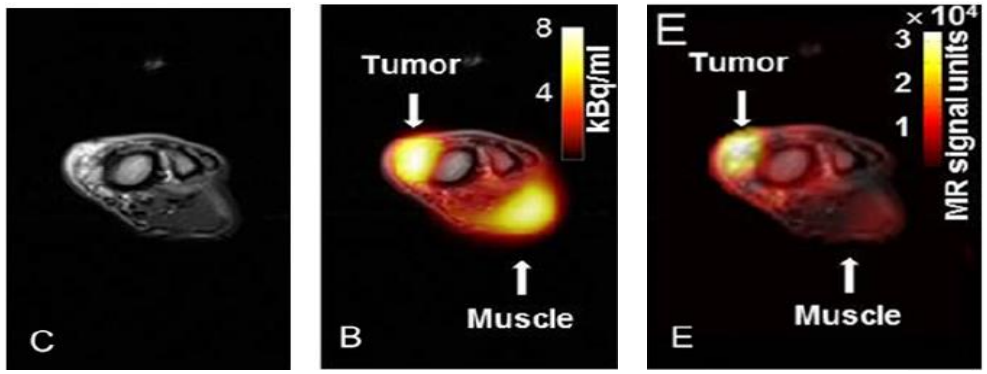

MRI MRI+PET MRI+HP-MRI

Sensitive: HP MRI vs. just MRI

Hyperpolarized MRI has shown to be able to detect bilateral, biopsy proven, prostate tumors, while only one tumor was detected by standard MRI (2013)[2]

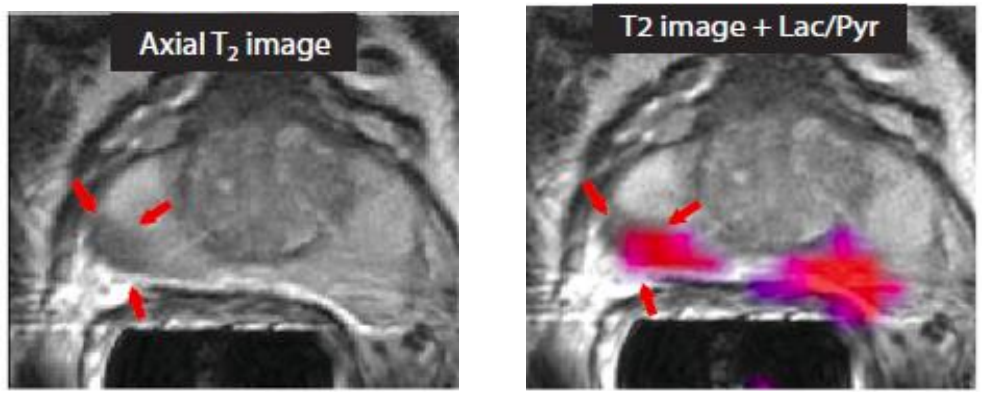

MRI MRI+HP-MRI

1 Gutte, H. et al. Am J Nucl Med Mol Imaging 2015;5(1):38-45
2 Nelson, J., et al. Science translational medicine 2013;5(198).